AD-A045 606 LOCKHEED MISSILES AND SPACE CO INC PALO ALTO CALIF PA--ETC F/G 20/14
ANALYSIS OF SATELLITE DATA ON PRECIPITATING PARTICLES IN COORDI--ETC(U)
JUN 77 W L IMHOF, T R LARSEN, J B REAGAN N00014-75-C-0954
UNCLASSIFIED LMSC-D560323 NL

1 OF 2
AD
A045606

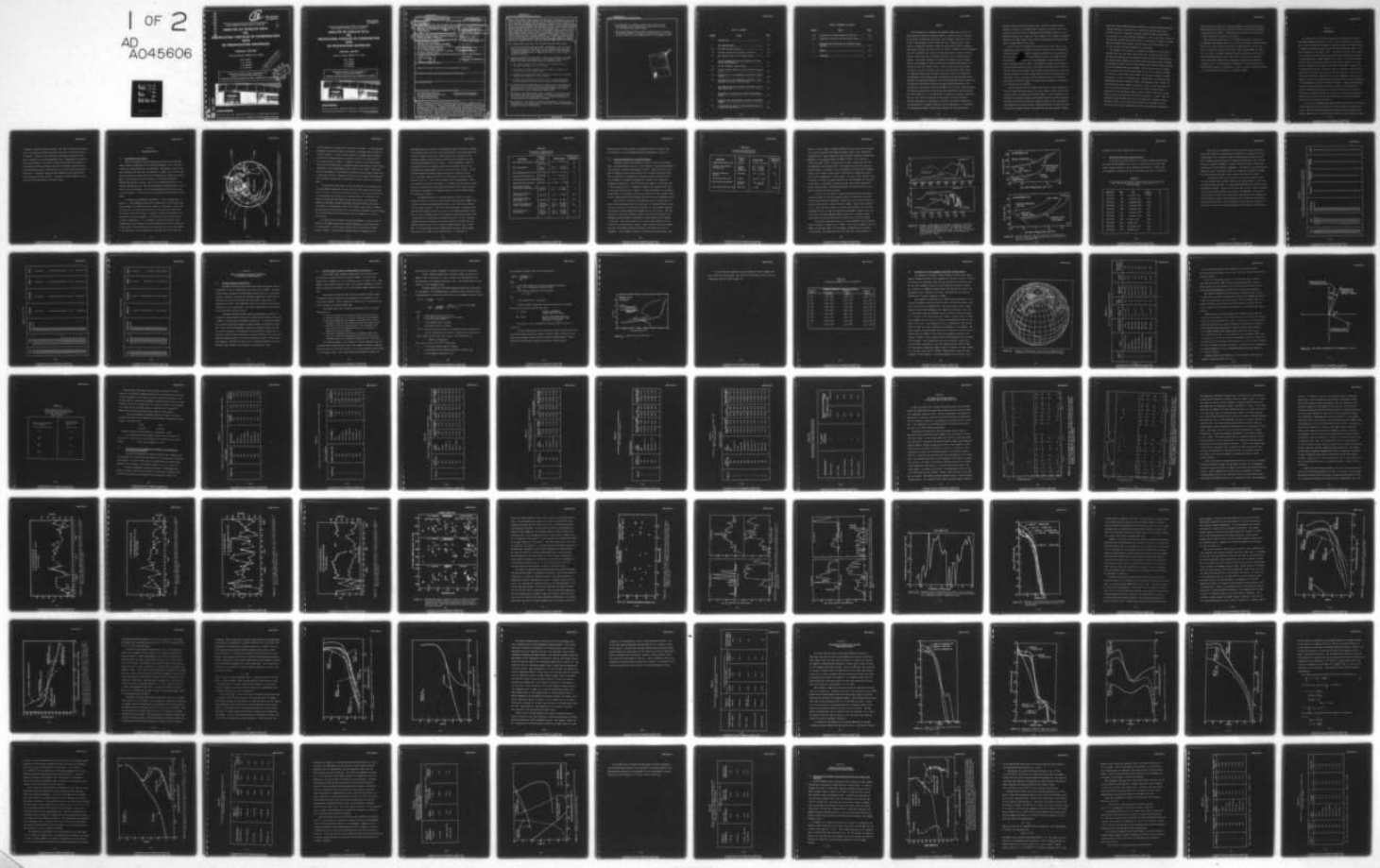

LMSC-D560323
30 JUNE 1977

The research was sponsored by the Office of Naval Research
Contract N00014-75-C-0954, Task No. NR 089-109

ANALYSIS OF SATELLITE DATA ON PRECIPITATING PARTICLES IN COORDINATION WITH ELF PROPAGATION ANOMALIES

ANNUAL REPORT

Contract Number N00014-75-C-0954

W. L. Imhof
T. R. Larsen
J. B. Reagan
E. E. Gaines

LOCKHEED
PALO ALTO RESEARCH LABORATORY
LOCKHEED MISSILES & SPACE COMPANY, INC. • A SUBSIDIARY OF LOCKHEED AIRCRAFT CORPORATION
PALO ALTO, CALIFORNIA

LMSC-D560323
30 JUNE 1977

The research was sponsored by the Office of Naval Research
Contract N00014-75-C-0954, Task No. NR 089-109

ANALYSIS OF SATELLITE DATA ON PRECIPITATING PARTICLES IN COORDINATION WITH ELF PROPAGATION ANOMALIES

ANNUAL REPORT

Contract Number N00014-75-C-0954

W. L. Imhof
T. R. Larsen
J. B. Reagan
E. E. Gaines

LOCKHEED

PALO ALTO RESEARCH LABORATORY

LOCKHEED MISSILES & SPACE COMPANY, INC. • A SUBSIDIARY OF LOCKHEED AIRCRAFT CORPORATION
PALO ALTO, CALIFORNIA

UNCLASSIFIED

SECURITY CLASSIFICATION OF THIS PAGE (When Data Entered)

REPORT DOCUMENTATION PAGE

READ INSTRUCTIONS BEFORE COMPLETING FORM

1. REPORT NUMBER: LMSC/D560323	2. GOVT ACCESSION NO.
3. RECIPIENT'S CATALOG NUMBER	
4. TITLE (and Subtitle): ANALYSIS OF SATELLITE DATA ON PRECIPITATING PARTICLES IN COORDINATION WITH ELF PROPAGATION ANOMALIES.	5. TYPE OF REPORT & PERIOD COVERED: Annual Report for period ending 14 June 1977
	6. PERFORMING ORG. REPORT NUMBER: LMSC/D560323
7. AUTHOR(s): William L. Imhof, Trygve R. Larsen, Joseph B. Reagan, Edward E. Gaines	8. CONTRACT OR GRANT NUMBER(s): N00014-75-C-0954
9. PERFORMING ORGANIZATION NAME AND ADDRESS: Space Sciences Laboratory, LOCKHEED PALO ALTO RESEARCH LABORATORY, 3251 Hanover Street, Palo Alto, CA 94304	10. PROGRAM ELEMENT, PROJECT, TASK AREA & WORK UNIT NUMBERS: NR 089-109
11. CONTROLLING OFFICE NAME AND ADDRESS: Mr. R. Gracen Joiner, Code 461, Office of Naval Research/DEPT. OF THE NAVY, Arlington, Virginia 22217	12. REPORT DATE: 30 June 1977 13. NUMBER OF PAGES: 117
14. MONITORING AGENCY NAME & ADDRESS (if different from Controlling Office): 127p.	15. SECURITY CLASS. (of this report): UNCLASSIFIED 15a. DECLASSIFICATION/DOWNGRADING SCHEDULE

16. DISTRIBUTION STATEMENT (of this Report)

Approved for public release and sale; distribution unlimited.

17. DISTRIBUTION STATEMENT (of the abstract entered in Block 20, if different from Report)

18. SUPPLEMENTARY NOTES

19. KEY WORDS (Continue on reverse side if necessary and identify by block number)

ELF transmission anomalies
Satellite energetic particle data
Precipitating electrons
Ion-pair production rates
Free electron concentrations
D-region electron densities

20. ABSTRACT (Continue on reverse side if necessary and identify by block number)

Based on energetic particle measurements from a satellite, a study has been made of the effects of particle precipitation into the atmosphere on the transmission of ELF signals. Coordinated exercises were conducted between satellite measurements of the precipitating particles and ELF transmissions between the U.S. Navy Wisconsin Test Facility and receiving stations in Maryland, Greenland, Norway, and Italy. Significant fluxes of precipitating electrons were often measured with the Lockheed payload on the polar-orbiting satellite 1972-076B.

DD FORM 1 JAN 73 1473 EDITION OF 1 NOV 65 IS OBSOLETE

UNCLASSIFIED

SECURITY CLASSIFICATION OF THIS PAGE (When Data Entered)

Based on the fluxes, energy spectra, and pitch-angle distributions of the particles, ion-pair production profiles were calculated and electron density profiles subsequently obtained with application of known effective electron loss rates. From the coordinated data, correlative studies between signal strengths and electron density profiles were performed with use of an ELF wave-guide-mode computer program developed at the Naval Ocean Systems Center. With the inclusion of data from several stations, the transmission signal strength could be studied simultaneously under a variety of ionospheric conditions. The wave-guide computer program calculations indicated that energetic particle precipitation events may cause a signal enhancement or degradation, depending upon where the disturbance is occurring along the path. The consistent occurrence during electron precipitation events of signal strength anomalies in either direction is supported by the coordinated satellite/ELF station measurements.

The following major conclusions have followed from this study effort:

- From both the satellite and ELF station measurements it has been found that direct particle precipitation into the atmosphere can cause ELF transmission anomalies. The signal strengths may be either attenuated or enhanced depending upon the geometry and details of the ion pair production profiles.

- Sensitivity studies have been made to assess the dependence of the ELF signal strengths on such parameters as the electron and ion density profiles and their distribution along the propagation path.

  - The signal strengths tend to decrease with increasing electron density at altitudes of $\sim$ 60 km or lower.

  - The effect of a given ionization profile depends strongly on its location along the propagation path.

  - The ELF signal strengths are most sensitive to positive ion density profiles at altitudes of $\sim$ 45 km or lower.

  - The ELF signal strengths are very sensitive to sporadic E-layers, with the altitude of the ledge being a very critical parameter.

- The measured and predicted effects of energetic electron precipitation events can provide a readily available verification of the effects on ELF transmission of more rarely occurring and possibly more severe phenomena such as polar cap absorption (PCA) events.

- Variations in the nighttime ELF signal strengths on a fine time scale are observed which may be due entirely to electron precipitation but cannot be accounted for quantitatively due to present limitations in the measurements and computational techniques.

- The geometry for the effect of electron precipitation on nighttime ELF transmission is very complex and as a result the following recommendations are made for future investigations:

- New techniques for mapping electron precipitation profiles simultaneously over a broad spatial region should be used in a coordinated measurement program.

- Existing ELF waveguide-mode computer programs should be modified to include treatment of variations in the electron and ion density profiles along a direction perpendicular to the propagation path.

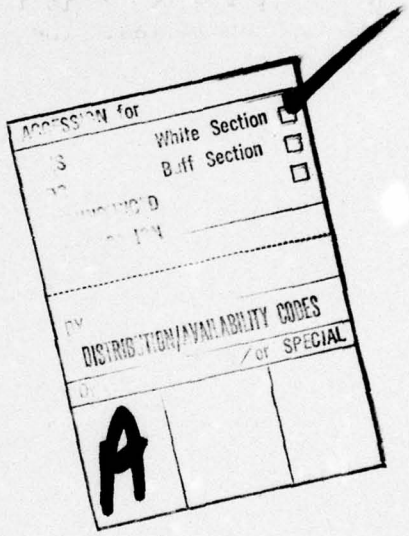

TABLE OF CONTENTS

TABLE OF CONTENTS (continued)

PREFACE

The transmissions of extremely-low-frequency (ELF) waves from the U. S. Navy operated Wisconsin Test Facility (WTF) to a receiving site in Connecticut are known to experience significant signal strength reductions of up to ≈ 3 dB on approximately 60 to 80 nights per year. Transmissions to other stations in Maryland, Greenland, Norway and Italy display similar anomalies. These signal strength reductions, which may result in degraded system performance, have been speculated to be caused by the precipitation of electrons from the radiation belts resulting in enhanced ionization in the D- and E-region ionosphere. In the past, attempts to correlate the anomalous signal strength behavior with geomagnetic indices indicative of disturbed magnetospheric conditions have met with limited success. These inconclusive studies clearly pointed out the need to achieve a convincing cause-and-effect relationship by comparing the ELF signal strengths directly with particle precipitation. The opportunity for performing such a correlative study was provided by data acquired with scientific payloads on the low-altitude polar orbiting satellites 1971-089A and 1972-076B developed by the Space Sciences Laboratory of the Lockheed Palo Alto Research Laboratory (LPARL) for the Office of Naval Research, the Defense Nuclear Agency and the Defense Advanced Research Projects Agency. The latter satellite is still operational and capable of acquiring coordinated data. In the course of achieving the prime goals of the two different satellite experiments, a large body of scientific data had been obtained on the precipitation of energetic particles into the atmosphere. To investigate the relationship between the ELF signal strengths and the precipitating

electron fluxes using these satellite data, the Office of Naval Research supported an effort by the LPARL group to analyze the satellite data in the vicinity of and at the times of measured signal strength reductions in the WTF-to-Connecticut link. Under the initial phase of this program a successful correlation was made between direct particle precipitation and anomalous ELF signal strength (Imhof et al., 1976).

On all of the 11 coordinated cases studied in the first phase of this investigation significant fluxes of energetic electrons having substantially different intensities and spectral shapes were observed to be precipitating into the atmosp[illegible] Resulting ion-production rates in the upper D-region (70-100 km) w[illegible]culated to be often comparable to those produced by intense solar-particle-events (SPE). Corresponding enhanced electron density profiles were at times in excess of $10^5 e^-/cm^3$ at altitudes above $\sim$ 80 km. A positive qualitative correlation was therefore established for the first time between anomalously low nighttime ELF signal levels and the precipitation of significant fluxes of electrons from the radiation belts, but a detailed quantitative correlation between the severity of the anomalies and particle inputs remained to be performed.

From the previous effort it became clear that for a given transmission site the signal amplitudes received at various stations around the world may vary with time in an appreciably different manner. If the fluctuations are associated with energetic particle precipitation then the station-to-station variations may reflect latitude and longitude changes in the total precipitating particles and energy spectra. Stimulated by these considerations and the previous findings a special coordinated exercise was conducted in March-

April 1976 between LPARL satellite measurements of the precipitating particles and ELF transmission between the U. S. Navy Wisconsin Test Facility and receiving stations in Maryland, Greenland, Norway and Italy coordinated by Dr. John Davis of the Naval Research Laboratory. Also a large body of satellite data has been acquired during 1974 and 1975 in the general vicinity of the ELF paths to receivers at the various stations during times of operation, and analysis of these data would clearly be of great value.

The purpose of this report is to present the findings of a study using available satellite data taken during nights when the ELF receivers were in operation and experiencing both normal and anomalous signal strength behavior. For selected cases comparisons were made between the measured signal strengths and theoretical results using the ELF waveguide-mode computer program developed at the Naval Ocean Systems Center (NOSC). This study has shown for example, that an intense Solar Particle Event (SPE) such as the one measured by LPARL at 1144 UT on 4 August 1972 would decrease the ELF signal strengths from WTF to Norway by 2-5 dB for a nighttime path. Unfortunately, no cooperative ELF measurements were made during this highly disturbed period that effected the entire polar cap down to magnetic latitudes of $\sim 60^{\circ}$. On the other hand, for various hypothesized electron and positive ion density profiles based on variations of the measurements made at 1254 UT 5 August 1972, when the solar particle intensities were much lower than at the peak on 4 August 1972, the calculated signal strengths are found to decrease with increasing electron density at 60 km, but the signal levels may be above the ambient levels. For relativistic electron precipitation events the coordinated measurements

and calculations indicate that signal enhancements or decreases may result, depending upon the details of the density profiles and where the disturbance is occurring along the path. The experimental results and the calculations of these effects are discussed in this report.

Many individuals contributed to this successful program. Special acknowledgments are extended to Mr. R. G. Joiner of the Office of Naval Research and to Dr. T. Quinn, while at the Office of Naval Research, for their important cooperation, support and direction under Contract N00014-75-C-0954. Dr. J. R. Davis of the Naval Research Laboratory generously provided all of the experimental ELF data used in this study. Mr. W. Moler of the Naval Ocean System Center (NOSC) kindly cooperated in providing the NOSC wave propagation code. We acknowledge the cooperation of the Norwegian Defence Research Establishment in granting Dr. T. Larsen a leave of absence to engage in this ELF study activity while in residence at LPARL.

Section 1

INTRODUCTION

In recent years it has been recognized that at least some of the observed ELF propagation anomalies in the U. S. Navy experimental transmission link are due to anomalous ionospheric ionization caused by the precipitation of energetic electrons and protons into the earth's atmosphere (Davis, 1974; Davis and Meyers, 1975; Larsen, 1974). For the first time in 1976 a successful correlation was made between direct particle precipitation and anomalous nighttime ELF signal strengths (Imhof et al., 1976). In the latter study, energetic particle data were obtained with scientific payloads on the low-altitude polar-orbiting satellites 1971-089A and 1972-076B. During all 11 coordinated cases studied, significant fluxes of energetic electrons having substantially different intensities and spectral shapes were observed to be precipitating from the radiation belts into the atmosphere. Resulting ion-production rates in the upper D-region were calculated to be often comparable to those produced by intense solar-particle-events. Corresponding enhanced electron density profiles were at times in excess of 10^5 electrons/cm^3. A positive qualitative correlation was therefore stablished, but a detailed quantitative correlation between the severity of the anomalies and particle characteristics such as intensity and spectra was not firmly established because of the limited data base used.

In this effort performed under Contract N00014-75-C-0954 with the Office of Naval Research the satellite data taken during special coordinated exercises in 1975 and 1976 were analyzed and compared with measured ELF transmission between the U. S. Navy Wisconsin Test Facility and receiving stations

in Maryland, Greenland, Norway and Italy. The times of the satellite passes used in the study are listed in Section 2 along with a brief description of the payload. In Section 3 the waveguide mode program is described along with a discussion of the path segmentation used. Subsequently the satellite data and the results of the signal strength calculations are presented for the March-April 1976 coordinations (Section 4), for other relativistic electron precipitation cases in 1975 (Section 5), and for Solar Particle Events (Section 6). In Section 7 waveguide mode calculations are presented for selected sporadic E-layer profiles. In Section 8 a short summary is given along with the conclusions of the present study.

Section 2

THE SATELLITE DATA

2.1 The LPARL Particle Payload

Under this program, direct correlations have been made between ELF signal strength observations and coordinated measurements from a satellite of particles precipitating into the atmosphere. The energetic particle data were obtained by the Space Sciences Laboratory at LPARL in two different ONR sponsored satellite programs having the designations 1971-089A and 1972-076B. Each of these satellites has the advantage of being at low altitudes (750-800 km) and polar orbiting. Most of the coordinated data used in the analyses reported here were taken with the satellite 1972-076B which is spinning and the instrumentation can therefore provide good pitch angle distribution measurements. This satellite is still operational at the time of this report.

An example of a coordinated measurement is shown schematically in Figure 2-1. The propagation path from the transmitter at the Wisconsin Test Facility (WTF) to a receiver at Tromso, Norway is illustrated. At the time of interest the satellite passed through the outer radiation belt/auroral zone region where intense fluxes of energetic electrons were observed to be precipitating into the atmosphere. The fluxes of electrons above 160 keV are shown schematically. It is important to measure the particle fluxes simultaneously with conduction of the ELF transmissions since the fluxes and energy spectra of precipitating electrons are known often to be very dynamic in time and space. Since variations with longitude also occur, data from

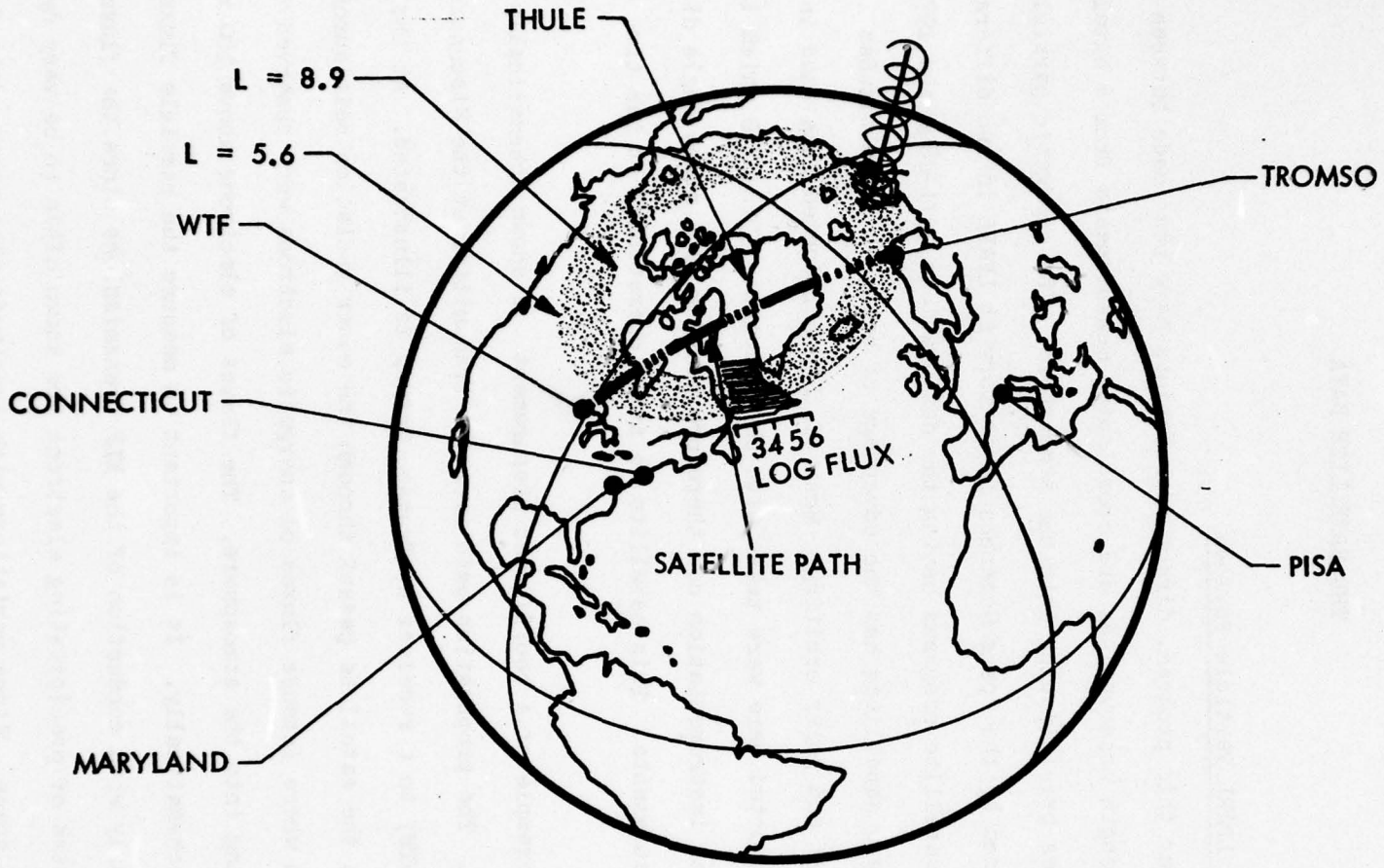

Figure 2-1. Schematic illustration of a coordinated set of particle measurements from a satellite and ELF propagation measurements over the WTF to Tromso path.

multiple satellite crossings were used whenever available. In both satellite experiments high data coverage was achieved on a worldwide basis through use of tape recorders. On each of these satellites the LPARL payload contains an array of instruments measuring electrons, protons, and alpha particles over a broad range of energies. A gamma ray detector in the 1972-076B payload has also provided data on widespread electron precipitation events through observation of the bremsstrahlung x-rays (Imhof et al., 1974a). These data provide measurements of the spatially integrated electron fluxes incident over a large area, but due to depletion in May 1973 of the cryogen associated with that instrument the data are not applicable to most of the event of interest here.

Of particular concern here are the data taken with the energetic electron spectrometers measuring the intensities and energy spectra of electrons from ~ 130 keV to 2.5 MeV with 256-channel analysis. Two such identical electron spectrometers are located on the oriented satellite 1971-089A at look angles of 90° and 20° with respect to the local zenith. On the spinning satellite, 1972-076B, a single spectrometer provides detailed pitch angle distributions on the same time scale as the satellite spin period, 5 seconds. The Lockheed group has obtained data on precipitating electrons from one of these two low altitude satellites continuously since 1971 (Imhof et al., 1973; 1974b, 1974c).

In addition to the energetic electron measurements, on each of the two satellites the LPARL payload also provided measurements of the intensities and energy spectra of lower energy electrons and of protons over a broad range of energies. The low-energy (auroral) particle complement on the

1971-089A spacecraft consisted of 34 individual detectors measuring electrons in the energy range from 6 eV to 40 keV and protons in the energy range from 0.6 keV to greater than 40 keV. These detectors were arranged into six instrument packages including three multiple particle analyzers and three scintillator-photomultiplier instruments. A mass spectrometer capable of distinguishing protons, energetic helium ions and heavier ions over the energy-per-unit-charge range 0.7 keV to 12.1 keV was also included. On the 1971-089A spacecraft detailed fluxes and spectra of energetic protons (1.2 to 100 keV), alpha particles (6.0 to 60 keV) and to a lesser extent electrons, (0.76 to > 2 keV), were obtained with two spectrometers. These were essentially identical instruments, one oriented to view along the zenith direction continually while the other was oriented at 90° to this direction. The particle instruments in the ONR-001 payload on the 1971-089A satellite are summarized in Table 2-1.

The LPARL payload on the spinning satellite contains an array of particle detectors in addition to the Energetic Electron Monitor (EEM) using a plastic-scintillator-photomultiplier detector and a 256-channel analyzer for fine energy resolution. The lower energy environment is measured with a multi-particle analyzer containing a total of nine channel-multiplier detectors. In this instrument three of the detectors are devoted to protons from 1 to 200 keV and six detectors to electrons from 0.06 to 50 keV. Two spectrometers measure the intensities and energy spectra of protons from 1 to 100 MeV, electrons from 0.8 to 2.1 MeV and alpha particles from 6 to 400 MeV. A low energy proton detector (LEP) measures protons over the energy range from 0.2 to 1 MeV in four energy channels. In addition, an

Table 2-1

Instruments in LPARL Payload
on the 1971-089A Satellite

Instrument	Particle Type	Energy Range	Resolution (Channels)
Multi-Particle Analyzers (3)	Protons	1.5 → 400 keV	4
	Electrons		10
Mass Spectrometer	Protons	0.7 → 12 keV	9
	Alphas	1.4 → 24 keV	9
Total Energy Detectors (2)	Electrons	> 10 keV > 21 keV	2
Angular Distribution Inst	Electrons	6 → → 398 keV	7
Total Energy Proton Detector	Protons	0.25 → 1.2 MeV	4
Omnidirectional Detectors	Electrons	> 0.5 MeV, > 1.0 MeV	2
High Energy Angular Distribution Instruments (4)	Protons	1.0 → 2.7 MeV	1
	Alphas	4.0 → 14.0 MeV	1
Relativistic Electron Spectrometer (1)	Electrons	0.13 → 2.5 MeV	256
High Energy Electron Spectrometer (1)	Electrons	0.13 → 2.5 MeV	256
High Energy Alpha and Proton Spectrometer	Protons	1.0 → 100 MeV	
	Electrons	0.80 → 2.1 MeV	512
	Alphas	6.0 60 MeV	
High Energy Proton Spectrometer	Proton	1.0 → 100 MeV	
	Electrons	0.80 → 2.1 MeV	512
	Alphas	6.0 → 60 MeV	

omnidirectional detector measures the integral electron flux above 1 MeV. The instruments on the 1972-076B satellite are summarized in Table 2-2.

2.2 Electron Precipitation at Middle Latitudes

Energetic electron precipitation is known to occur on a worldwide basis. The precipitation patterns are very complex, being strongly dependent upon longitude, latitude and geomagnetic activity. Many studies have been made of energetic electron precipitation, but in general concerted efforts have not been made to coordinate the energetic electron observations with the ionospheric or atmospheric phenomena of interest, such as ELF wave propagation observations. Since the fluxes can change on a very short time or small spatial scale it is important to measure the electrons very close to the times and positions of interest. For many atmospheric and ionospheric applications it is not merely sufficient to measure the total electron fluxes, but the energy spectra and pitch angle distributions must be measured as well.

The electrons at satellite altitudes that are of interest here are those having pitch angles within the loss cone. At middle latitudes a large fraction of the electrons observed at altitudes of a few hundred kilometers are generally locally trapped and therefore of no direct concern. But, the distortion of the earth's magnetic field is such that the altitude of the mirroring electrons changes significantly as the electrons drift eastward in longitude. The mirroring points dip to their lowest altitudes in the vicinity of the South Atlantic Anomaly. Those electrons having pitch angles such that the mirroring altitude dips below ~ 100 km are lost into the atmosphere. Since trapped electrons are continually being perturbed, some

Table 2-2

Instrument in LPARL Payload
on the 1972-076B Satellite

Instrument	Particle Type	Energy Range	Resolution (Channel)
Gamma Spectrometers (2)	Photons	40 keV - 2.8 MeV	4096
Penetrating Radiation Monitors (2)	Protons Alphas Electrons	1.0 - 100 MeV 6.0 - 60 MeV 0.8 - 2.1 MeV	256
Energetic Electron Monitor	Electrons	0.16 - 2.5 MeV	256
Low Energy Proton Det.	Protons	120 keV - 1 MeV	4
Multi-Particle Analyzer	Electrons Protons	.06 - 50 keV 1 - 200 keV	6 3
Omni-directional Detector	Electrons	> 1 MeV	Integral

fraction of those trapped at higher altitudes are continually being scattered into lower mirroring altitudes (Imhof and Smith, 1965). This buildup with longitude drift of quasi-trapped electrons and their subsequent precipitation generally in the longitude range from 68°E to 90°W is often called the "windshield wiper" effect. Although many of these electrons are lost into the atmosphere on the western edge of the Anomaly the losses do occur on a worldwide basis. In addition to the precipitation associated with a gradual change in pitch angle, electrons may be scattered more dramatically and be lost into the atmosphere on a single bounce. For any of these classes of precipitation, to obtain the energy deposited into the atmosphere as a function of altitude it is necessary to measure both the pitch angle distributions and the energy spectra. From such measurements the altitude profile of enhanced ionization can then be derived.

As a result of the Office of Naval Research/Defense Nuclear Agency sponsored program for deriving D-region effective recombination rate coefficients (Contract N00014-70C-0203), valuable data on the general subject of electron precipitation at middle latitudes emerged. These findings (Larsen et al., 1976a) show that energetic electrons may precipitate into the lower ionosphere for up to 10 days following certain magnetic storms and thus very likely may be the most important cause of the so-called "magnetic storm after-effects" (or "post-storm effects") which occur at middle latitudes.

The electron precipitation may be strongly dependent upon latitude as shown in Figure 2-2 (Larsen et al., 1976b). For the two ionospheric stations Ottawa and University Park, Pa. the D-region ionization may on occasions very different, see Figures 2-3a and 2-3b, albeit the close proximity in

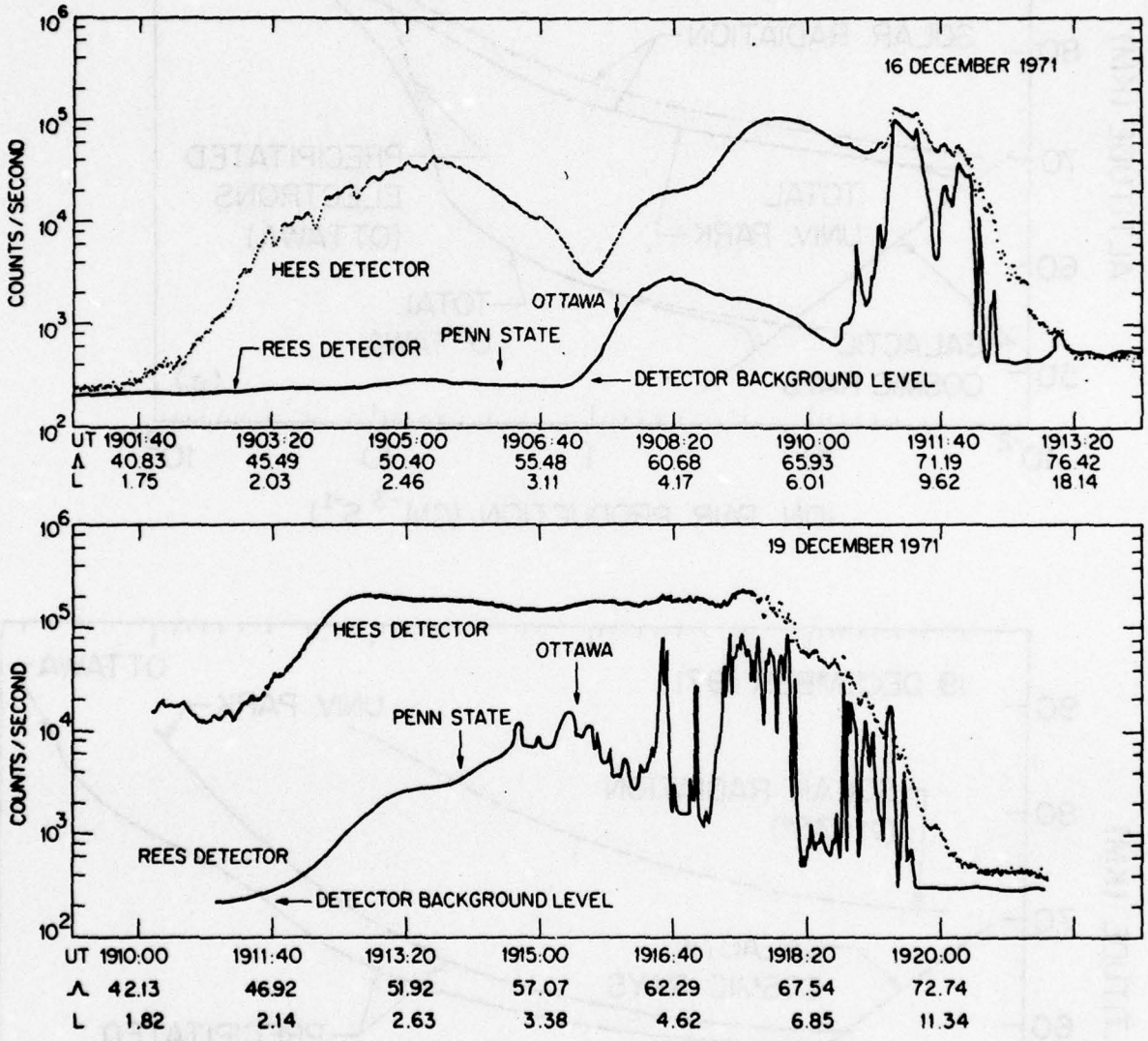

Figure 2-2. Integral counting rates for energies > 130 keV as a function of latitude at 90° (HEES detector) and 25° (REES detector) pitch angles with the geomagnetic field. The University Park and Ottawa positions are marked by arrows. Panel (a) is for a pass on 16 December 1971 and (b) for a pass on 19 December 1971 (Larsen et al., 1976b).

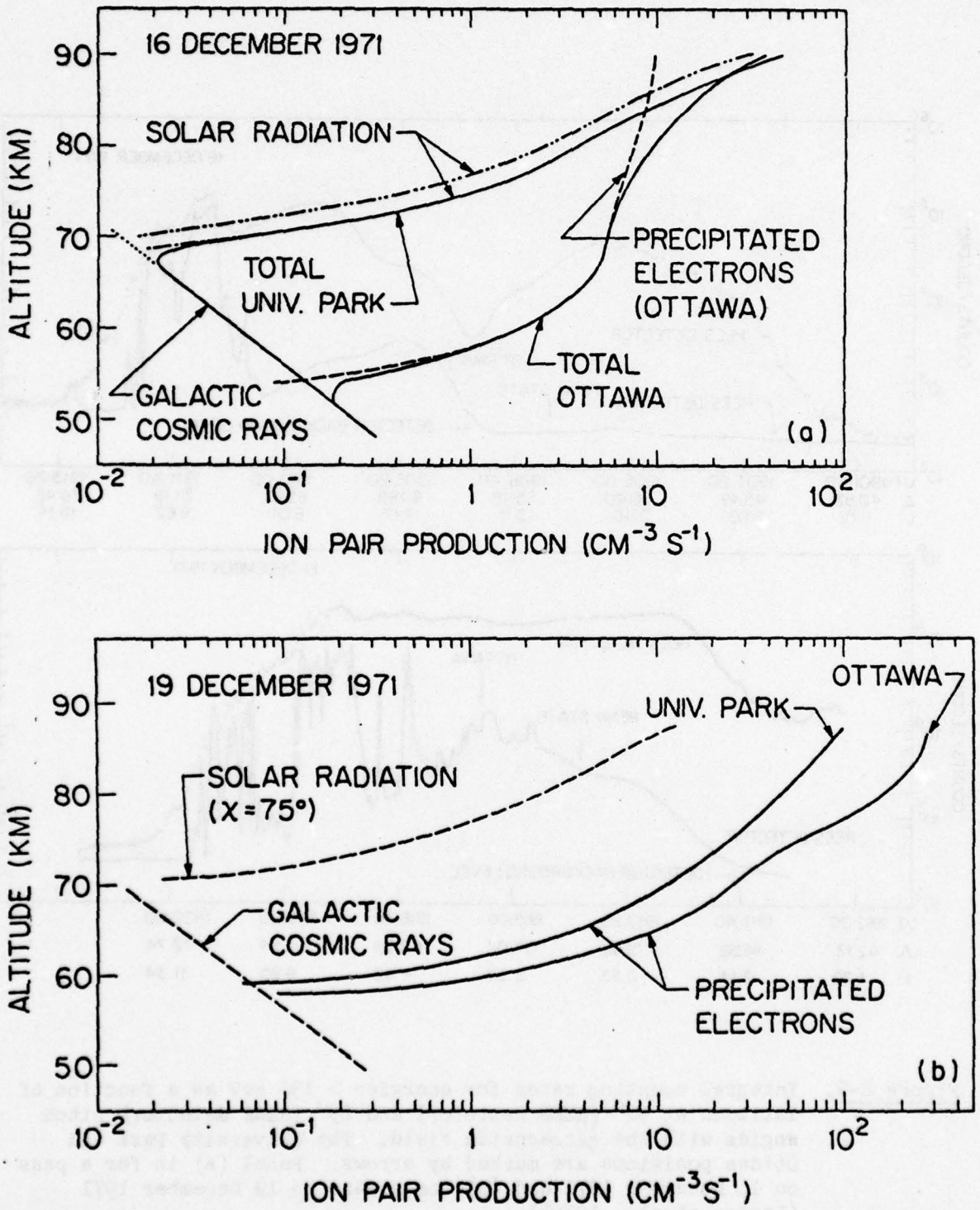

Figure 2-3. Ion pair production rates as a function of height for the University Park and Ottawa positions, a) on 16 December 1971 and b) on 19 December 1971.

latitude (45° and 41°N, respectively) of the sites.

2.3 The Satellite Data for Coordinated Cases

In the previous report (Imhof et al., 1976) the LPARL satellite data were presented and analyzed for 11 cases in conjunction with observed ELF signal strength anomalies over the path WTF to Connecticut. The UT times and geomagnetic conditions for these coordinations are listed in Table 2-3.

Table 2-3

List of Cases for which Satellite Data were coordinated with ELF Signal Strength Measurements (WTF to Connecticut) in the Previous Effort

Satellite	Rev.	Date	UT (Approx.)	K_p
1972-076B	421	31 October 1972	2310	5^-
1972-076B	422	1 November 1972	0049	8^-
1972-076B	423	1 November 1972	0226	8^-
1972-076B	424	1 November 1972	0405	8
1971-089A	5446	1 November 1972	0405	8
1972-076B	425	1 November 1972	0544	8
1971-089A	5447	1 November 1972	0545	8
1972-076B	2880	20 April 1973	0326	5
1972-076B	3242	15 May 1973	0441	5^-
1972-076B	6941	26 January 1974	0422	4^+
1972-076B	7779	26 March 1974	0411	4^-

Since the time of acquisition of the last data covered in the previous report extensive coordinations were performed in July-August 1975 and in March-April 1976. During the latter coordinated exercise with Dr. John Davis, of NRL, excellent satellite coverage was obtained over all of the ELF stations in operation (Maryland, Greenland, Norway and Italy). These data were acquired from the satellite 1972-076B. A tabulation of the satellite data acquisition times is provided in Table 2-4, along with a listing of the ELF receiving stations from which signal strength data have been acquired.

The satellite particle data from all of the passes listed in Table 2-4, were surveyed with a special alert for any unusual behavior in the electron precipitation profiles, i.e. high fluxes associated with relatively broad precipitation regions. Special attention was also devoted to passes occurring at times when unusual behavior was observed in the ELF data. For the more important passes the detailed energy spectra were processed and averaged over broad latitude intervals, energy deposition profiles obtained, and electron density profiles derived. Selected portions of these data are presented in the various sections of this report dealing with the different coordinations.

Table 2-4

List of Cases for which Satellite Data were coordinated with ELF Signal Strength Measurements since March 1975

Rev.	Date	System Time	Data from ELF Receiving Stations			
			Maryland	Greenland	Norway	Italy
12851	11 March 75	0401 HR UT	X	X	X	X
12852	11 March	0542	X	X	X	X
12865	12 March	0317	X	X	X	X
12867	12 March	0636	X	X	X	X
14470	1 July	0454	X	X	X	X
14484	2 July	0409	X	X	X	X
14513	4 July	0419	X	X	X	X
14514	4 July	0559	X	X	X	X
14528	5 July	0513	X	X	X	X
14542	6 July	0429	X	X	X	X
14543	6 July	0609	X	X	X	X
14557	7 July	0523	X	X	X	X
14571	8 July	0436	X	X	X	X
14572	8 July	0618	X	X	X	X
14585	9 July	0353	X	X	X	X
14586	9 July	0532	X	X	X	X
14599	10 July	0309	X	X	X	X
14600	10 July	0449	X	X	X	X
14615	11 July	0542	X	X	X	X
14629	12 July	0500	X	X	X	X
14643	13 July	0413	X	X	X	X
14644	13 July	0554	X	X	X	X
14658	14 July	0508	X	X	X	X
14672	15 July	0422	X	X	X	X
14687	16 July	0518	X	X	X	X
14702	17 July	0612	X	X	X	X
14716	18 July	0527	X	X	X	X
14730	19 July	0442	X	X	X	X

Table 2-4 (continued)

Rev.	Date	System Time	Maryland	Greenland	Norway	Italy
14744	20 July 75	0358 HR UT				
14745	20 July	0537				
14760	21 July	0632	X	X	X	X
14773	22 July	0408	X	X	X	X
14788	23 July	0502	X	X	X	X
14802	24 July	0418	X	X	X	X
14816	25 July	0332	X	X	X	X
14831	26 July	0427				
14845	27 July	0343				
14846	27 July	0522				
14860	28 July	0437	X	X	X	X
14861	28 July	0618	X	X	X	X
14875	29 July	0532	X	X	X	X
14889	30 July	0448	X	X	X	X
14890	30 July	0618	X	X	X	X
14903	31 July	0402	X	X	X	X
14904	31 July	0542	X	X	X	X
18311	23 March 76	0005	X	X	X	X
18326	24 March	0100	X	X	X	X
18343	25 March	0508	X	X	X	X
18344	25 March	0648	X	X	X	X
18350	25 March	1708				
18355	26 March	0108	X	X	X	X
18358	26 March	0602	X	X	X	X
18364	26 March	1624				
18365	26 March	1804				
18369	27 March	0028	X	X	X	X
18372	27 March	0518	X	X	X	X
18410	29 March	2350	X	X	X	X
18416	30 March	0624	X	X	X	X
18427	31 March	0042	X	X	X	X
18429	31 March	0400	X	X	X	X

Table 2-4 (concluded)

Rev.	Date	System Time	Maryland	Greenland	Norway	Italy
18430	31 March 76	0539 HR UT	X	X	X	X
18440	31 March	2219				
18456	1 April	2313	X	X	X	X
18457	2 April	0052	X	X	X	X
18459	2 April	0548	X	X	X	X
18469	2 April	2229				
18472	3 April	0326	X	X		
18473	3 April	0503	X	X		
18514	6 April	0111	X	X	X	
18517	6 April	0607	X	X	X	
18528	7 April	0028	X	X	X	X
18542	7 April	2342	X	X	X	X
18543	8 April	0122	X	X	X	X
18545	8 April	0438	X	X	X	X
18556	8 April	2258				
18560	9 April	0533	X	X	X	X
18571	9 April	2352	X	X	X	X
18572	10 April	0129	X	X	X	X
18574	10 April	0448	X	X	X	X
18575	10 April	0627	X	X	X	X
18615	13 April	0057	X	X	X	X
18632	14 April	0508	X	X	X	X

Section 3

THE ELF PROPAGATION DATA AND CALCULATION OF PROPAGATION CHARACTERISTICS

3.1 The ELF Propagation Measurements

The ELF field strength measurements were made using signals from the transmitter at the U. S. Navy ELF Wisconsin Test Facility (WTF). The transmission source, located in the Cheqeamegon National Forest in north-central Wisconsin, consists of two 22.5 km north-south antennas (one buried and one elevated) and one 22.5 km elevated east-west antenna. Each antenna is grounded at both ends. The transmission station is located at the mid-point intersection of the two antennas. The antenna array pattern can be steered to any particular receiving location.

A separate experimental ELF recording program under the auspices of the Office of Naval Research has provided measured field strength values from a number of receiving sites using WTF transmissions. In this report emphasis will be given to the path from WTF to Tromso, Norway; but transmission from WTF to other stations at Maryland, Connecticut, Greenland, Norway and Italy will also be discussed. The ELF data for the polar path to Norway were obtained by the Naval Research Laboratory under the direction of Dr. John Davis. Narrow band ELF receivers with effective integration times of $\sim$ 4000 second were employed. The data were taken at 42 or 76 Hz and represent the actual measured field strengths for two periods in 1975 and one in 1976.

3.2 The ELF Computer Program for Model Waveguide Calculations

The waveguide model computer program used in the present studies was developed at Naval Electronics Laboratory (NELC) [now Naval Ocean Systems Center (NOSC)] and is well documented (see e.g. Sheddy et al., 1968; Pappert, 1970; Pappert and Moler, 1974). Mr. W. Moler of NOSC has kindly assisted in adapting the program to run at the Lockheed (LMSC) computer facilities.

The program is based upon the formalism developed by Budden (1961) and Budden and Daniell (1965) for electromagnetic wave propagation in the terrestrial waveguide. Special emphasis has been given to its applicability in the extremely low frequency (ELF) range.

The program allows for a terrestrial waveguide with the following characteristics:

- Arbitrary electron and ion density distributions with height.
- Variable electron and ion collision frequency height profiles.
- The lower boundary of the waveguide is assumed to be a smooth homogeneous earth with arbitrary conductivity and permittivity.
- Allowance is made for the anisotropy of the ionosphere; arbitrary values for the strength and direction of the earth's magnetic field may be applied.
- Horizontal inhomogeneties (along the propagation path) may be taken into account by segmenting the path into regions having different values for the waveguide characteristics listed above.

The computer program is thus capable of treating waveguides that are reasonable model representations of the actual complex terrestrial waveguide. The program does not allow for variation of the guide parameters perpendicular to the propagation path. This simplification, acknowledged by Pappert and

Moler (1974) as the major assumption in the model, should be recognized.

Another computer program (also developed at NELC and supplied to LMSC) is used to calculate the signal strength at the ELF receiver using data provided by the waveguide program as input. The program allows for segmentation of the propagation path.

For ELF propagation in the earth-ionosphere waveguide the expression for the magnetic field component H_ϕ at a distance ζ from a horizontal dipole launching end-on is derived from expressions given by Pappert and Moler (1974).

$$H_\phi(\zeta) = -\frac{1}{Z_o S(\zeta)} E_Z(\zeta)$$

$$= -\frac{1}{Z_o S} \frac{Q\cos\phi}{\sqrt{\sin\zeta/a}} \sqrt{\lambda^T \lambda^R} e_x^T(o) e_z^R(o) \times \exp(-ik\bar{S}\zeta)$$

where

E_Z is the vertical electric wave field
S is the sine of the complex angle of incidence
Z_o is the free-space impedance
ϕ is the azimuth angle in degrees
a is the earth's radius in meters
λ^T, λ^R are the excitation factors for a horizontal dipole launching end-on at the transmitter and receiver, respectively, at ground level
$e_x^T(o)$, $e_Z^R(o)$ are the height gain factors at the transmitter and receiver, respectively.

The factor $Q = 9.01 \times 10^{-8}\ ILf^{3/2}$ [μV/m] where

I is the input antenna current in amperes
L is the length of the transmitting antenna in meters, and
f is the frequency transmitted in Hz.

For an antenna at ground level it can be shown that:

$$e_x^T(o) \simeq \frac{2}{\sqrt{\sigma_T / i\omega\varepsilon_o}}$$

where

σ_T is the earth conductivity under the transmitting antenna ($\sigma_{EW} = 3.2 \times 10^{-4}$ mho/m for the EW antenna)

ω is the angular frequency of the radiowaves ($\omega = 2\pi f$)

and

ε_o is the permittivity of free space.

In order to model the ambient nighttime conditions the following electron and ion density profiles were used:

0 - 100 km	GE Tempo, RPT66TMP-82 1 March 1966 by W. Knapp
100 - 200 km	Satellite Environment Handbook, Stanford University Press, 1965, edited by F. S. Johnson

The profiles, taken from Pappert and Moler (1974), are shown in Figure 3-1.

For the disturbed conditions the ambient electron density profile has been modified above 30-50 km in order to provide a smooth transition to the N(h) profile deduced from the satellite data for greater heights. The N^+ profile has likewise been modified as discussed in later sections.

(h) km

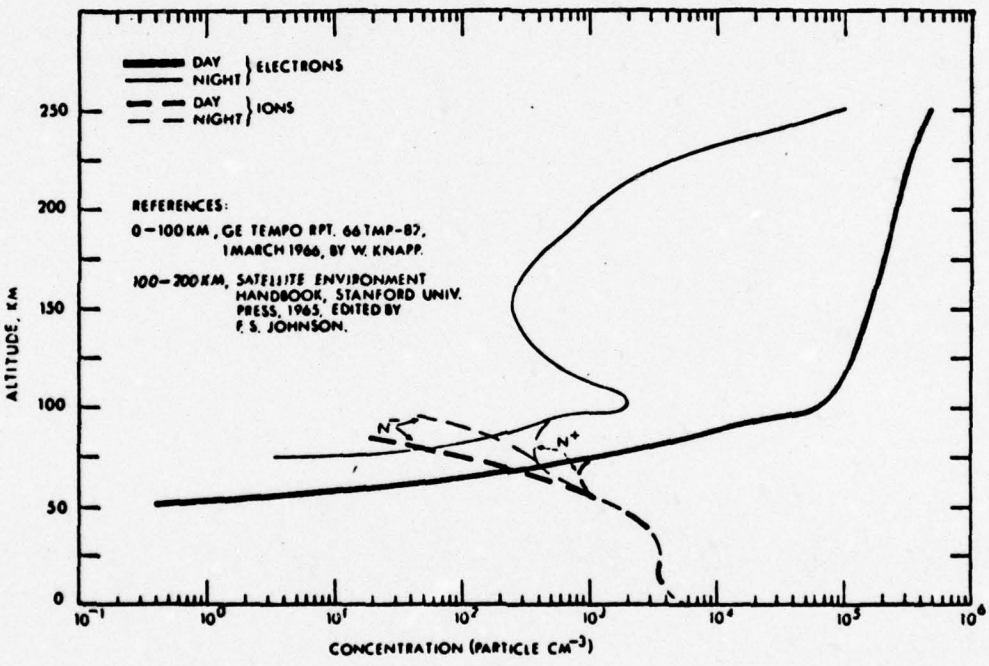

Figure 3-1. Ambient Constituent Profiles.

In this study the nighttime collision frequencies used by Pappert and Moler (1974) have been applied. The values for the electron and ion collision frequencies used are listed in Table 3-1.

Table 3-1

Nighttime Ionospheric Collision Frequency

Altitude (km)	Nighttime Ionospheric Collision Frequency		
	Electrons (sec^{-1})	Positive Ions (sec^{-1})	Negative Ions (sec^{-1})
250	1.05×10^{2}	4.50×10^{-1}	4.50×10^{-1}
225	3.50×10^{1}	9.00×10^{-1}	9.00×10^{-1}
220	3.00×10^{1}	1.00×10^{0}	1.00×10^{0}
210	3.30×10^{1}	1.30×10^{0}	1.30×10^{0}
200	4.50×10^{1}	2.00×10^{0}	2.00×10^{0}
150	1.60×10^{3}	4.50×10^{1}	4.50×10^{1}
120	1.00×10^{4}	3.00×10^{2}	3.00×10^{2}
100	3.90×10^{4}	8.00×10^{3}	8.00×10^{3}
0	4.30×10^{11}	1.07×10^{10}	1.07×10^{10}

3.3 Calculations for the Propagation Path WTF to Tromso, Norway

For propagation from WTF to Tromso, Norway with path length approximately 6 Megameters (Mm), we have computed the radiowave fields as a function of distance due to the direct wave only and rejected the contribution from the wave that propagates around the world through the antipode to Tromso. The difference in propagation length between the long and short path is approximately 34 Mm. Therefore, only small inaccuracies are introduced by neglecting the long path component to Tromso.

The propagation characteristics of ELF waves are dependent not only upon the ionospheric conditions along the path, but also upon changes in the earth's conductivity and permittivity. The path to Norway exhibits large changes in these ground parameters with segments of sea water as well as a $\approx$ 1.1 Mm segment over the Greenland ice cap, as shown in the map in Figure 3-2. In order to take these changes into account, we have divided the path into 8 segments which we feel is a realistic, yet practicable number of segments to deal with. This segmentation is also indicated in Figure 3-2, and Table 3-2 shows the various characteristic parameters of the segments. The earth's magnetic field strengths are given for ground level and these values together with the magnetic co-dip angles and propagation azimuths (with respect to magnetic north) represent values for approximately the mid-points of each segment. The corresponding values for the earth's conductivity (σ) and relative permittivity (ϵ/ϵ_o) are supplied from Mr. Moler of NOSC. For some segments, especially segment number 4, referred to as North Canada, the σ and ϵ/ϵ_o values are not constant. Representative values have been selected for these segments. In the ELF computations the changes in the σ

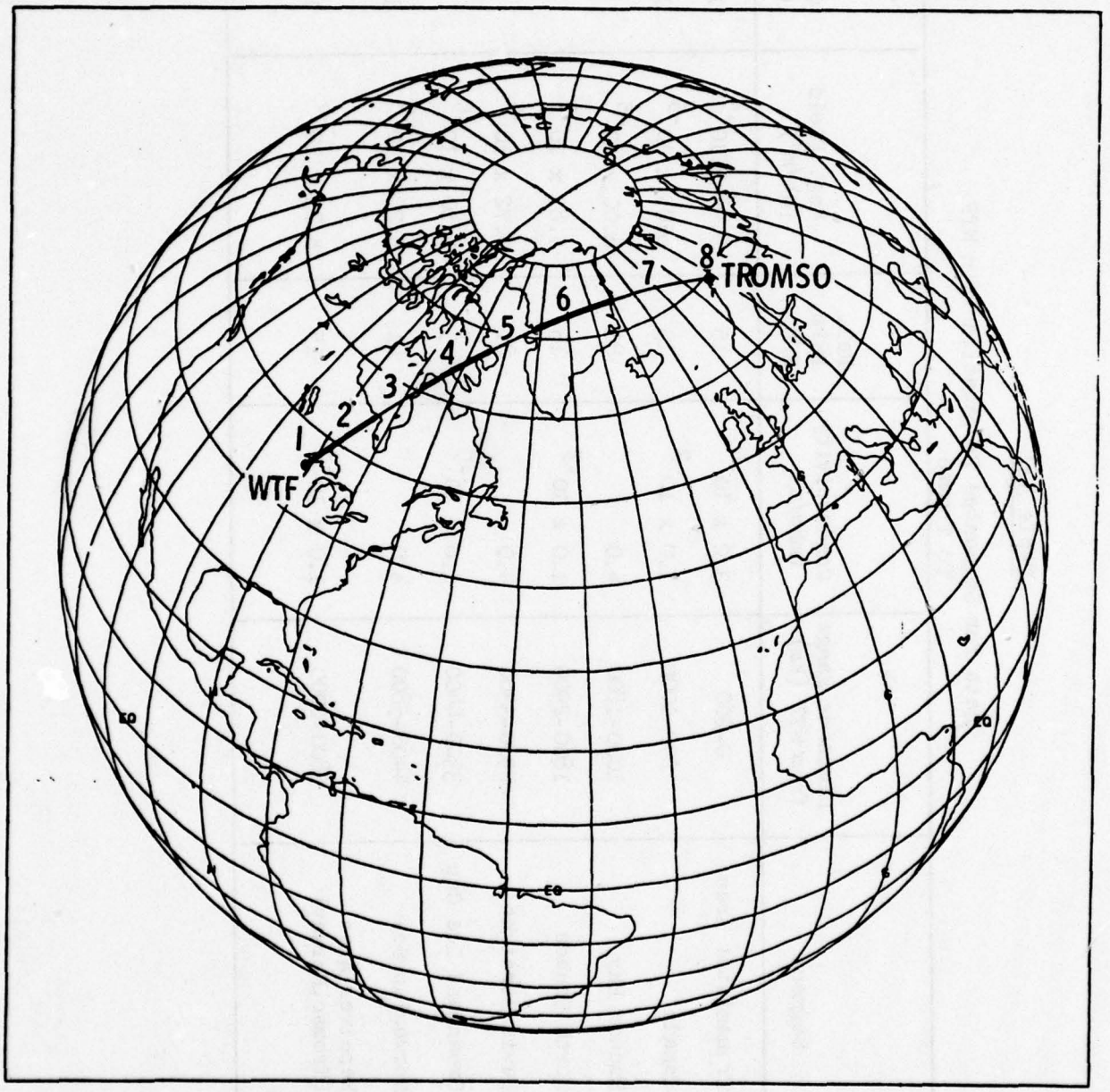

Figure 3-2. Schematic representation of the path and segmentation for calculations of the transmission from Wisconsin to Norway.

Table 3-2

Data for Segmented Propagation Path WTF
To Tromso

Segment No.	Segment	Distance Range from WTF (km)	Conductivity (mho/m)	Rel. Perm. E/E_o	Mag. Field (Wb/m^2)	Co-dip (deg.)	Prop Direct. (azimuth in degrees)
1	Transmitter Area	0-200	3.2×10^{-4}	15	5.94×10^{-5}	15.5°	20°
2	Canada	200-1000	1.0×10^{-3}	15	6.05×10^{-5}	11.6°	27°
3	Hudson Bay	1000-1800	4.0	81	6.00×10^{-5}	7.7	52°
4	North Canada	1800-2900	1.0×10^{-3}	15	5.83×10^{-5}	6.4°	89°
5	Davis Straight	2900-3300	4.0	81	5.72×10^{-5}	6.6°	102°
6	Greenland Ice Cap	3300-4400	1.0×10^{-5}	5	5.50×10^{-5}	8.0°	115°
7	Norwegian Sea	4400-5800	4.0	81	5.26×10^{-5}	10.6°	122°
8	Receiver Area (Tromso,Norway)	5800-6000	1.0×10^{-3}	15	5.23×10^{-5}	12.2°	128°

Field strength calculations have been made for the path to Tromso and ϵ/ϵ_o values were modeled to take place over a 100 km path length between different segments.

During the observational periods of interest here both the north-south (NS) and east-west (EW) antennas were activated at WTF. Relative phasing between the two antennas were 0^o, and transmitted frequency was 76 Hz except during March/April 1975 when 42 Hz signals were transmitted.

The antenna configuration for propagation to Tromso, Norway is shown in Figure 3-3, which also illustrates the fact that the propagation direction to Tromso is perpendicular to the electrical axis for the EW antenna. At Tromso, therefore, only signals from the NS antenna are received and the signal strength should therefore be independent of the NS-EW antenna current phasing.

Measurements at several recording sites indicate, however, that the effective dipole moment of the antenna changes with different phasing angles (Bannister, private communication, 1976). In Table 3-3, for selected phase values the corrections are listed (in dB) @ 75 Hz that should be added to field strength predictions when the normalized antenna dipole moment of 6.75×10^6Am (antenna current 300A, antenna length 22.5 km) and $\sigma_{EW} = 3.2 \times 10^{-4}$mho/m are used. In our presentation both uncorrected values take into account the 10^o offset between the propagation direction to Tromso and the direction of the NS antenna electrical axis (-0.1 dB in signal strength). All field strengths throughout this report, except those for the hypothetical E_s layer, are based on $\sigma = 3.0 \times 10^{-4}$mho/m and would be 0.3 dB lower for $\sigma = 3.24 \times 10^{-4}$mho/m.

No data are presently available as to the corrections that should be applied to predictions made for 42 Hz.

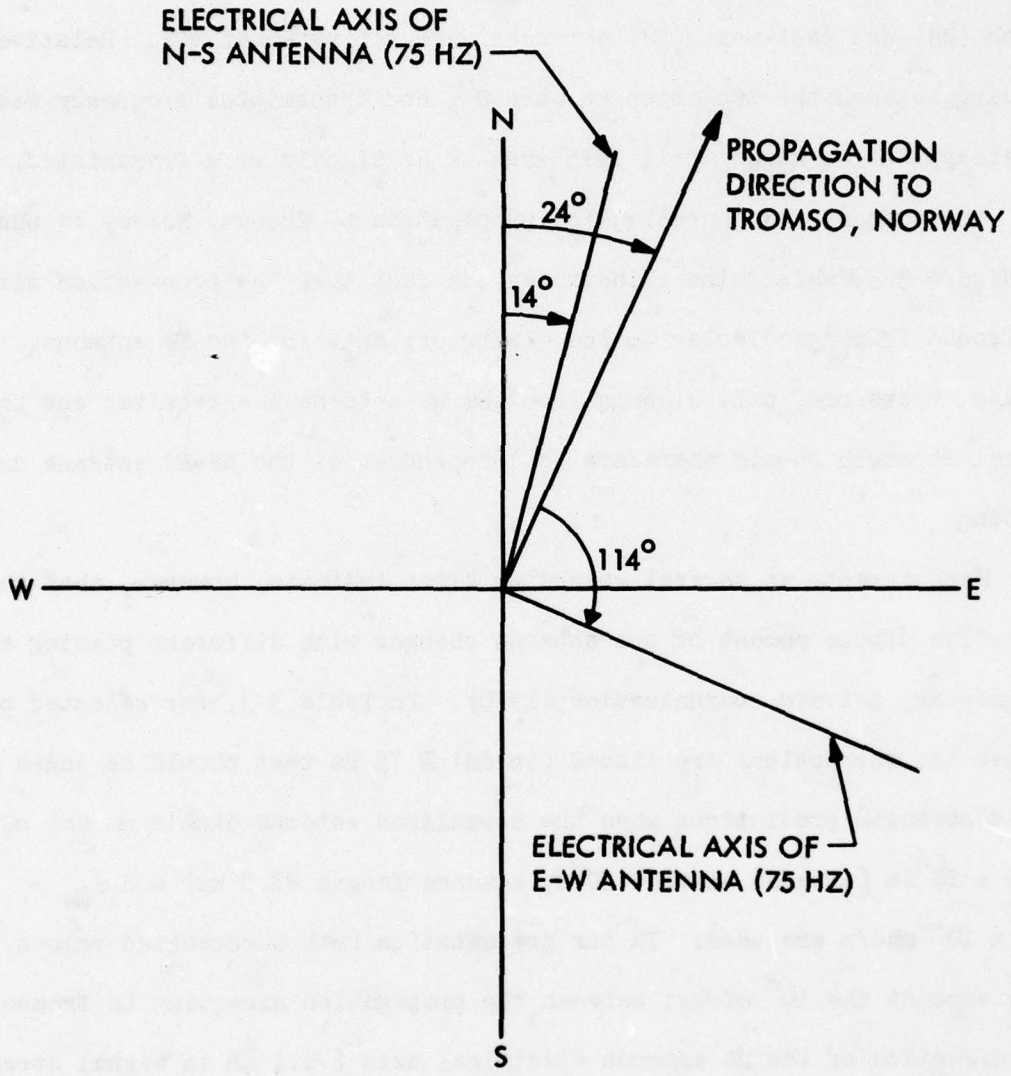

Figure 3-3. WTF antenna configuration for propagation to Norway.

Table 3-3

WTF Antenna Correction Factors
for Propagation to Tromso, Norway
(@ 75 Hz) vs EW-NS antenna
Phasing Angles

Nominal Antenna Phasing (in degrees)	Antenna Factor $\frac{F(\phi)}{B}$ in dB
0°	+ 1.2
120°	+ 2.5
180°	+ 1.8
300°	+ 0.5

Field strength calculations have been made for the path to Tromso using the set of ambient nighttime electron and ion density profiles as well as electron-neutral and ion-neutral collision frequencies described in the previous section. The derived propagation constants @ 42 and 75 Hz are shown in Tables 3-4 and 3-5, respectively. The values are listed for each segment. It is noted that the Greenland segment, as expected shows a higher attenuation rate and wave excitation factor than the other segments.

Using the propagation constants presented in Tables 3-4 and 3-5, the ambient nighttime field strength for the path WTF to Tromso has been calculated. The results are:

42 Hz	75 Hz
-159.3 dB	-155.6 dB

Signal strengths are with respect to 1 ampere/meter. (A/m)

No corrections for antenna phasing pattern have been applied to these values. With correction for 0° phasing the corrected value at 75 Hz becomes: -154.7 dB with respect to 1 A/m

3.4 Calculations for the Propagation Path WTF to Italy, Maryland, Connecticut and Greenland

With similar procedures the ambient nighttime field strengths have been calculated for the ELF receiving stations at Italy, Maryland, Connecticut and Greenland. For each of these paths the segmentation and characteristic parameters of the segments are provided in Tables 3-6, 3-7, 3-8 and 3-9.

Using the propagation constants presented in the aforementioned tables the ambient nighttime field strengths for the paths from WTF to the various stations have been calculated and are summarized in Table 3-10.

Table 3-4

Propagation Characteristics @ 42 Hz for the Segmented Path for WTF to Tromso, Norway

Ambient Night

Segment No.	Segment Length (km)	Path Segment	Att. Rate (dB/Mm)	v/c	Wait Mag (dB)
1	200	WTF	0.93	0.88	-5.64
2	800	Canada	0.91	0.89	-5.77
3	800	Hudson Bay	0.86	0.89	-5.88
4	1100	North Canada	0.89	0.88	-5.73
5	400	Davis Straight	0.81	0.89	-5.80
6	1100	Greenland	1.32	0.82	-4.74
7	1400	Norwegian Sea	0.74	0.88	-5.65
8	200	Tromso Area	0.80	0.87	-5.53

Table 3-5

Propagation Characteristics @ 75 Hz for Segmented Path WTF to Tromso, Norway

Ambient Nighttime

Segment No.	Segment Length (km)	Path Segment	Att. Rate (dB/Mm)	v/c	Wait Mag (dB)
1	200	WTF	1.09	0.85	-5.46
2	800	Canada	1.04	0.85	-5.52
3	800	Hudson Bay	0.97	0.86	-5.59
4	1100	North Canada	1.03	0.85	-5.51
5	400	Davis Straight	0.95	0.86	-5.58
6	1100	Greenland	1.64	0.82	-4.91
7	1400	Norwegian Sea	0.90	0.86	-5.55
8	200	Tromso Area	0.96	0.85	-5.49

Table 3-6

Propagation Characteristics for the segmented Path
WTF to Pisa, Italy
Ambient Nighttime

Seg. No.	Segment Length (km)	Path Segment	Att. Rate (dB/Mm)		v/c		Wait's Mag (dB)	
			42 Hz	75 Hz	42 Hz	75 Hz	42 Hz	75 Hz
1	200	WTF	0.889	1.066	.8706	.8499	-5.557	-5.448
2	800	Canada	0.851	1.012	.8771	.8533	-5.657	-5.502
3	1400	N. Canada	0.980	1.175	.8641	.8446	-5.442	-5.355
4	3800	Atlantic Oc.	0.754	0.910	.8778	.8567	-5.679	-5.558
5	1000	France	0.675	0.822	.8551	.8501	-5.359	-5.472
6	200	Mediterranean	0.650	0.788	.8535	.8503	-5.345	-5.484
7	100	Italy	0.705	0.859	.8477	.8463	-5.252	-5.421

Table 3-7

Propagation Characteristics for the segmented Path
WTF to Stumpneck, Maryland

Ambient Nighttime

Seg. No.	Segment Length (km)	Path Segment	Att. Rate (dB/Mm)		v/c		Wait's Mag (dB)	
			42 Hz	75 Hz	42 Hz	75 Hz	42 Hz	75 Hz
1	100	WTF	0.894	1.069	.8709	.8498	-5.559	-5.443
2	200	Wisconsin	0.816	0.973	.8783	.8548	-5.679	-5.527
3	600	Michigan	0.793	0.948	.8789	.8558	-5.692	-5.544
4	200	Pennsylvania	0.758	0.915	.8758	.8560	-5.654	-5.551
5	300	Maryland	0.795	0.966	.8691	.8524	-5.551	-5.495

Table 3-8

Propagation Characteristics for the segmented Path
WTF to Madison, Connecticut

Ambient Nighttime

Seg. No.	Segment Length (km)	Path Segment	Att. Rate (dB/Mm)		v/c		Wait's Mag (dB)	
			42 Hz	75 Hz	42Hz	75 Hz	42 Hz	75 Hz
1	300	WTF	0.895	1.069	.8709	.8497	-5.557	-5.440
2	600	Michigan & Ont.	0.800	0.952	.8796	.8558	-5.699	-5.540
3	400	New York	0.773	0.928	.8778	.8561	-5.679	-5.549
4	200	New York - Conn.	0.803	0.973	.8701	.8525	-5.562	-5.492
5	100	Connecticut	0.736	0.890	.8747	.8563	-5.640	-5.556

Table 3-9

Propagation Characteristics for the segmented Path
WTF to Thule, Greenland

Ambient Nighttime

Seg. No.	Segment Length (km)	Path Segment	Att. Rate (dB/Mm)		v/c		Wait's Mag (dB)	
			42 Hz	75 Hz	42 Hz	75 Hz	42 Hz	75 Hz
1	100	WTF	0.888	1.068	.8716	.8508	-5.582	-5.471
2	200	N. Wisconsin	0.812	0.964	.8828	.8570	-5.757	-5.571
3	800	Canada	0.861	1.021	.8795	.8543	-5.700	-5.524
4	800	Hudson Bay	0.822	0.958	.8882	.8583	-5.829	-5.585
5	200	Southampton Is.	0.919	1.088	.8751	.8507	-5.620	-5.459
6	200	Foxe Channel	0.807	0.951	.8862	.8581	-5.800	-5.579
7	200	Melville, Pen.	0.906	1.081	.8736	.8506	-5.599	-5.457
8	200	Foxe Basin	0.795	0.943	.8845	.8579	-5.776	-5.577
9	400	Baffin Is.	0.970	1.171	.8636	.8450	-5.440	-5.365
10	300	Baffin Bay	0.775	0.929	.8816	.8576	-5.736	-5.573
11	200	Greenland	1.311	1.635	.8214	.8185	-4.734	-4.915

Table 3-10

Ambient Nighttime Field Strengths Calculated
for the Path WTF to various receiving Stations

Receiving Stations	No. Segments used in Calculation	Calculated Field Strength at (with respect to 1 A/M)	
		42 Hz	75 Hz
Tromso, Norway	8	-159.3 dB	-155.6 dB
Pisa, Italy	7	-162.1	-158.5
Stumpneck, Maryland	5	-149.2	-144.6
Madison, Connecticut	5	-149.8	-145.2
Thule, Greenland	11	-155.4	-151.1

Section 4

THE SATELLITE AND MULTI-STATION COORDINATED CASES IN MARCH-APRIL 1976

In March and April 1976 a special coordinated exercise was performed between the LPARL satellite payload and the ELF receiving stations at Maryland, Greenland, Norway and Italy. For this coordination the payload was operated at all practical times when the satellite passed through regions near the transmission path and the transmitter and receivers were in operation. The coordination with the ELF receivers was performed through Dr. John Davis of the Naval Research Laboratory.

Precipitating electron data from the satellite passes during the March-April 1976 coordinations were surveyed, plots were made of the precipitating fluxes, and the energy spectra from the more interesting passes were obtained and subsequently processed through the LMSC energy deposition program, AURORA. Maximum precipitating electron fluxes measured on each satellite pass are plotted in Figures 4-1 and 4-2 as a function of time superposed on the ELF field strengths measured at the various receiving stations. The ELF transmission data were taken predominately on the nightside. For reference, the time of local midnight at each station is marked with an arrow. The fluxes of electrons > 160 keV are shown in the former figure whereas the lower energy (> 1.03 keV) fluxes are plotted in the latter graph. To provide an indication of the geomagnetic activity plots of the Dst index are also included. Certain obvious features in the plots are to be noted. The various receiving stations display a similar nightly average pattern, i.e. a general trend toward increasing signal strength as

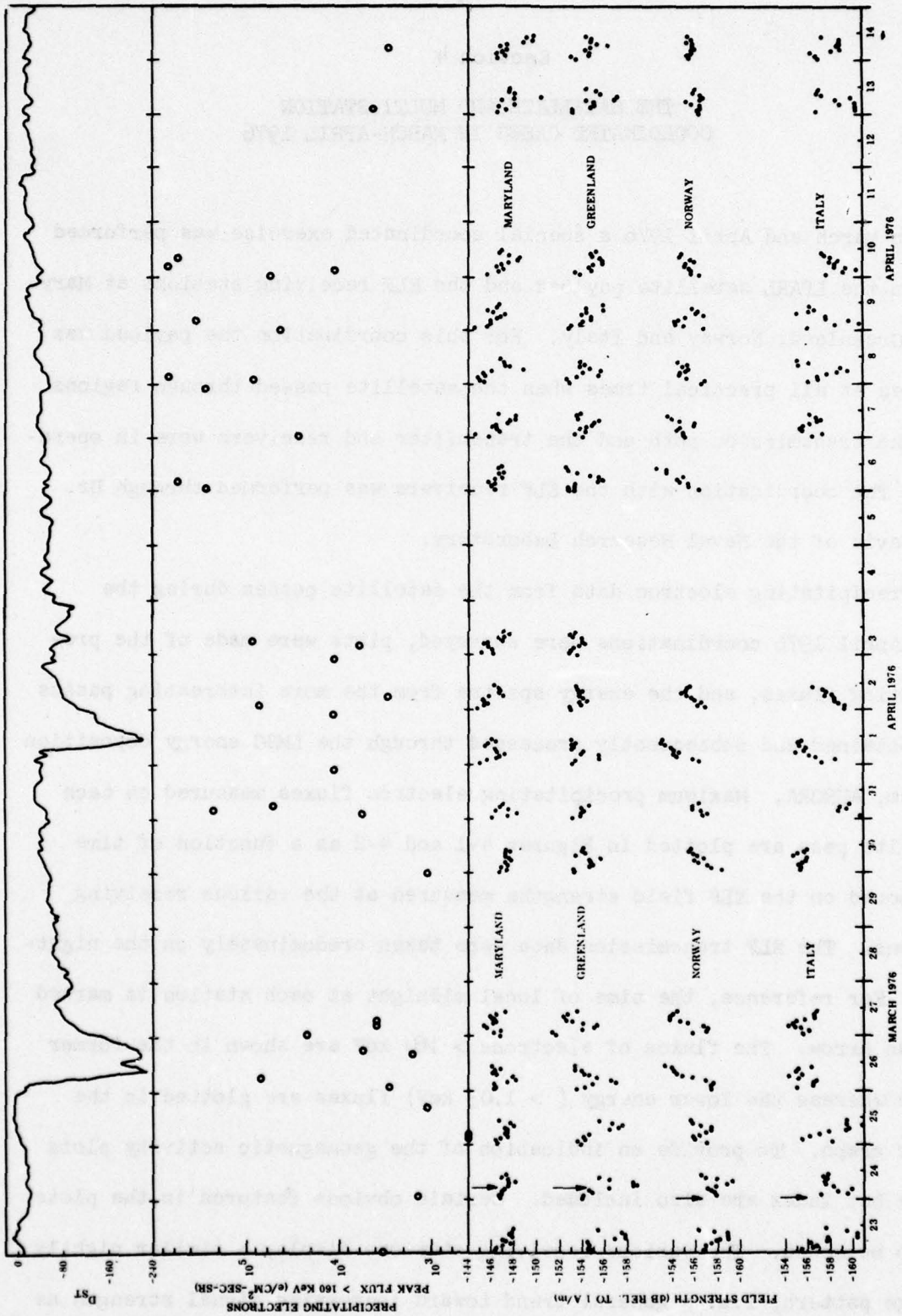

Figure 4-1. Plot of the precipitating electron flux > 160 keV as measured from the satellite on coordinated passes and the ELF signal strengths as received at the various stations. For comparison the D_{st} geomagnetic index is also plotted to indicate the general occurrence of magnetic storms.

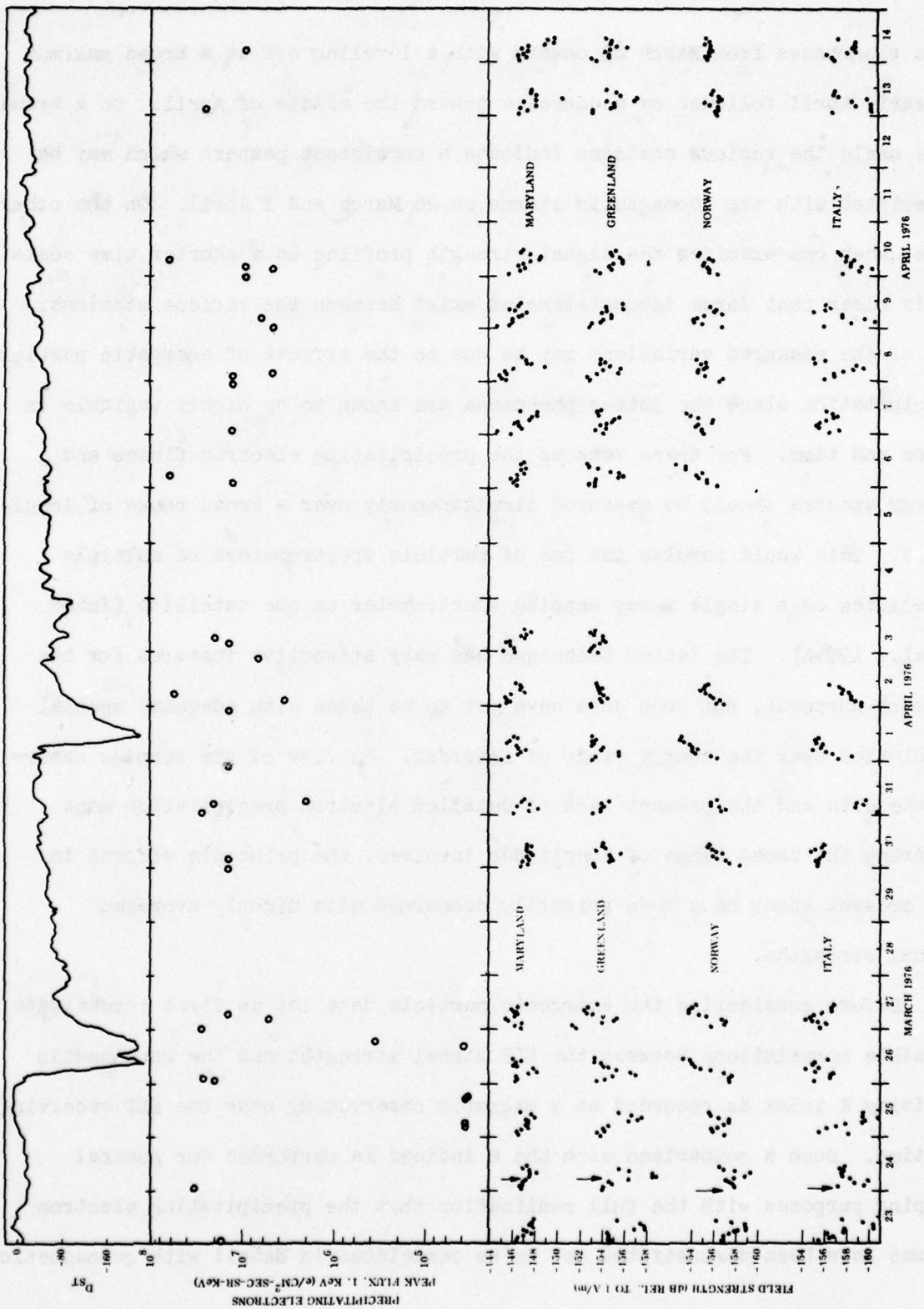

Figure 4-2. Plot of the precipitating electron flux at 1 keV as measured from the satellite on coordinated passes and the ELF signal strengths as received at the various stations. For comparison, the Dst geomagnetic index is also plotted to indicate the general occurrence of magnetic storms.

time progresses from March 23 onward with a leveling off at a broad maximum in early April followed by a decrease toward the middle of April. On a broad time scale the various stations indicate a consistent pattern which may be associated with the geomagnetic storms on 26 March and 1 April. On the other hand, when one examines the signal strength profiles on a shorter time scale it is clear that large inconsistencies exist between the various stations. All of the measured variations may be due to the effects of energetic particle precipitation since the latter phenomena are known to be highly variable in space and time. For these reasons the precipitating electron fluxes and energy spectra should be measured simultaneously over a broad range of longitudes. This would involve the use of particle spectrometers on multiple satellites or a single x-ray mapping spectrometer on one satellite (Imhof et al., 1974A). The latter technique has many attractive features for the present purposes, but such data have yet to be taken with adequate spatial resolution over the energy range of interest. In view of the complex nature of the data and the present lack of detailed electron precipitation maps covering the broad range of longitudes involved, the principle efforts in the present study have been primarily concerned with nightly averaged signal strengths.

Before considering the energetic particle data let us first investigate possible correlations between the ELF signal strengths and the geomagnetic activity K index as recorded at a magnetic observatory near the ELF receiving station. Such a comparison with the K indices is performed for general scoping purposes with the full realization that the precipitating electron fluxes have been demonstrated not to be correlated in detail with geomagnetic

activity. In Figures 4-3 and 4-4, for stations at Tromso and Maryland respectively, these two quantities are plotted with overlapping scales against time during the period March-April 1976. The appropriate data have been averaged over the indicated time intervals to minimize fine time scale variations consistent with restriction to nightime measurements. At each of these stations the variations of the two quantities display many similarities, suggesting some degree of correlation. The indicated similarities are in the direction of acquiring higher signal strengths when more geomagnetic activity occurs and hence when the fluxes of precipitating particles are expected to be greater. The reader should be cautioned, however, that despite the consistency displayed in Figures 4-3 and 4-4, the agreements are less convincing when similar plots are made for other time periods. This is illustrated in Figures 4-5 through 4-6 for the time periods March-April 1975. Some features appear with a similar behavior in both the signal strengths and the K index over the region of the receiver. However, there are also many examples of opposite behavior. For example, the ELF signal strengths at Maryland were below the threshold of detection at times in March 1975 when intense relativistic electron precipitation occurred. Similar plots of the coordinated data taken in July-August 1975 are not presented here because of the daylight nature of many of the observations.

A correlative analysis was performed on the basis of the particle data survey and the ELF data provided by Dr. Davis. For Figure 4-7 the measured ELF signal strengths are plotted against the precipitating electron fluxes for the Maryland, Greenland, and Norway stations in March-April 1976. The

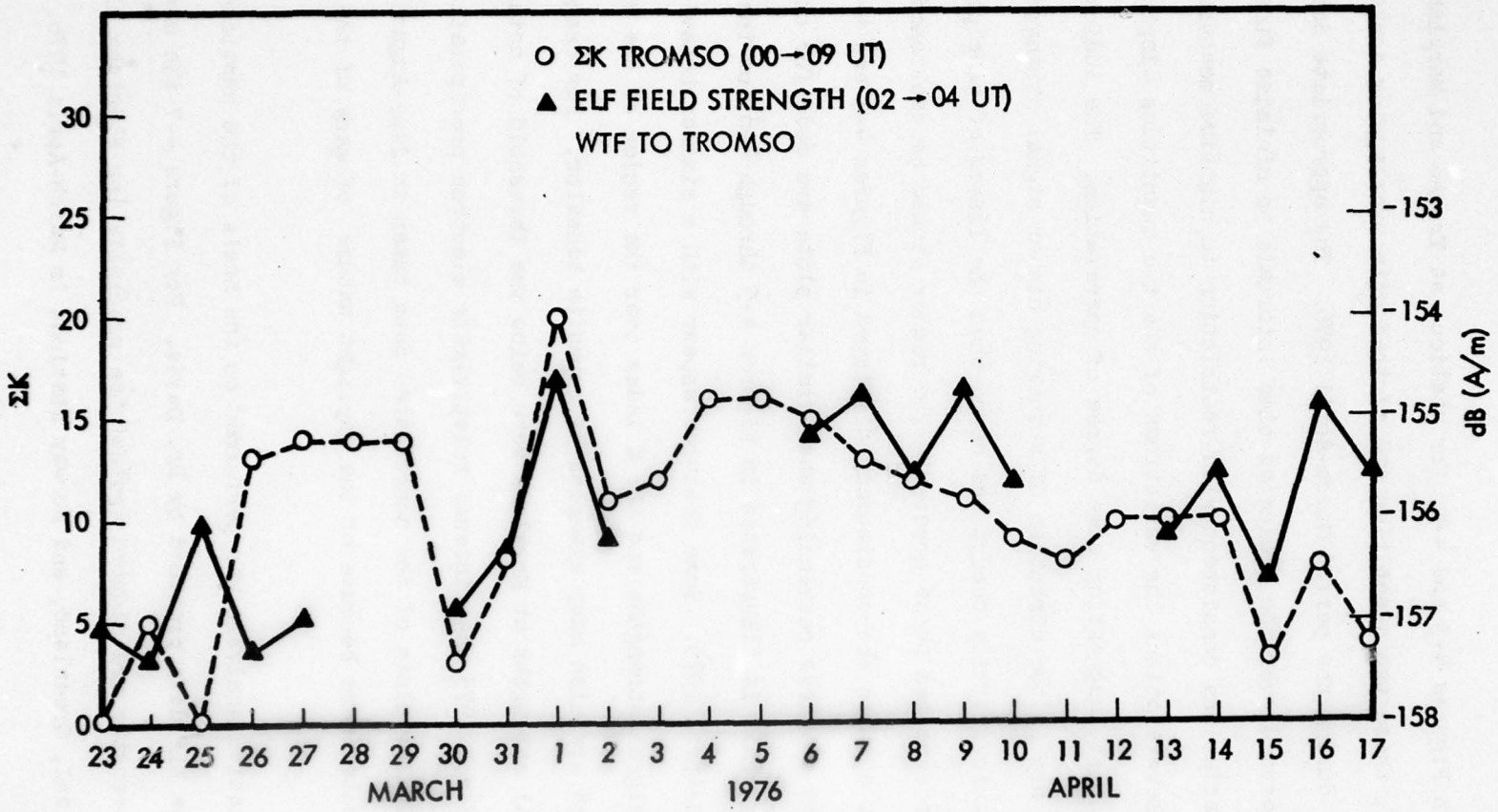

Figure 4-3. Plot of the nightly averaged ELF signal strengths averaged over the indicated time interval March-April 1976 (right hand scale) and the nightly averaged local K index values (left hand scale).

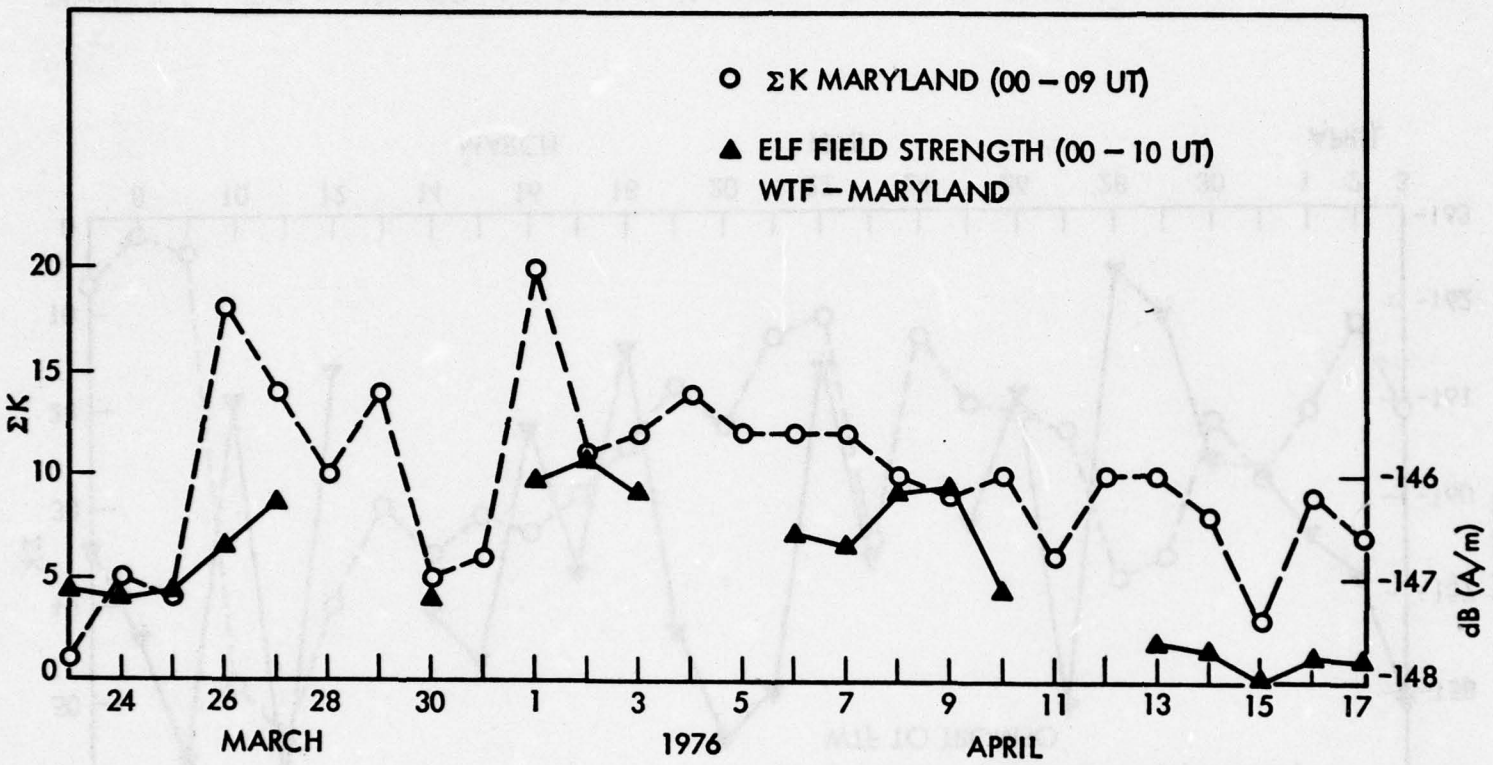

Figure 4-4. Plot of the nightly averaged ELF signal strengths for the station at Maryland, March-April 1976 (right hand scale) and the nightly averaged local K index values (left hand scale).

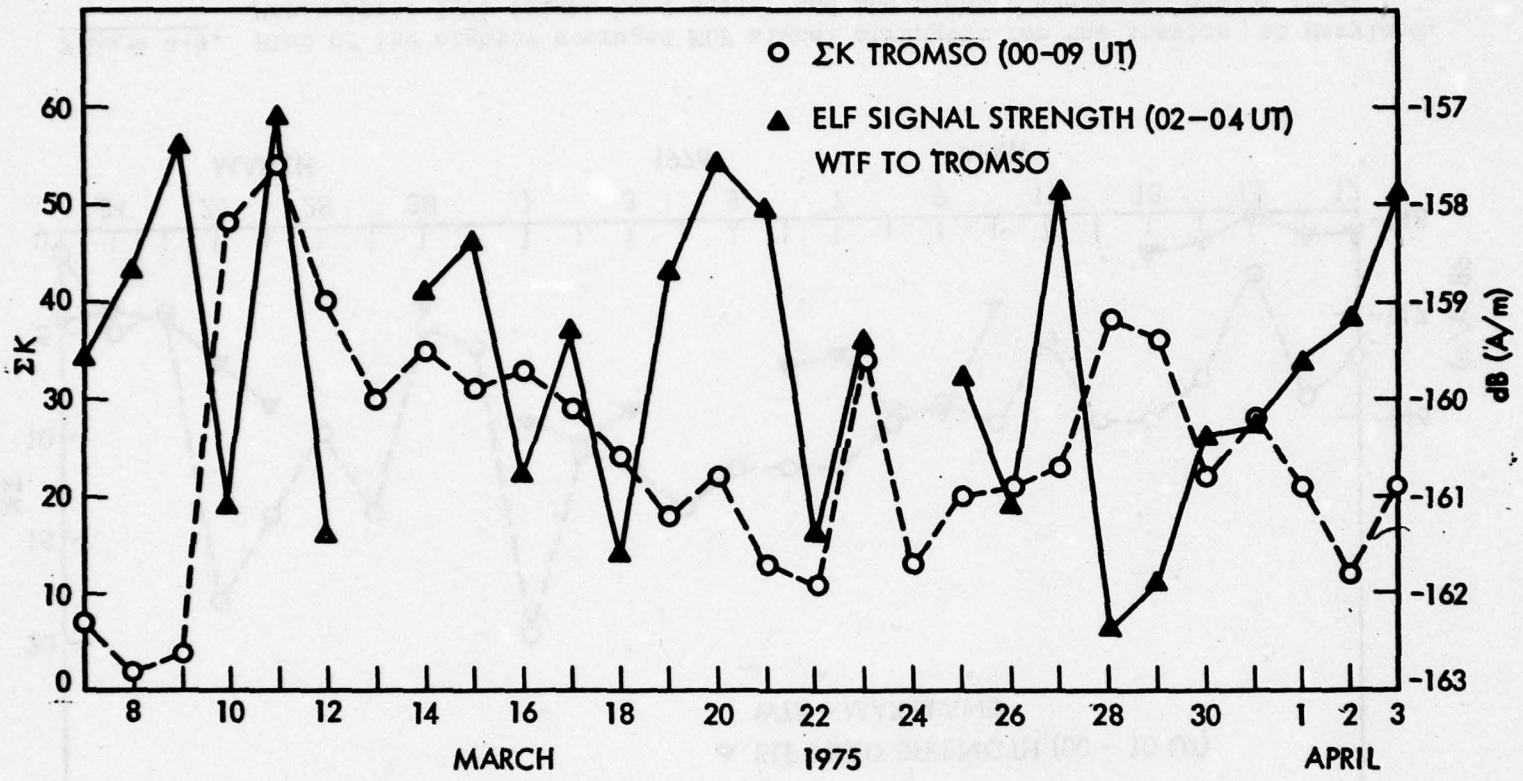

Figure 4-5. Plot of the ELF signal strengths averaged over the indicated time interval for the station at Tromso March-April 1975 (right hand scale) and the nightly averaged local K index values (left hand scale).

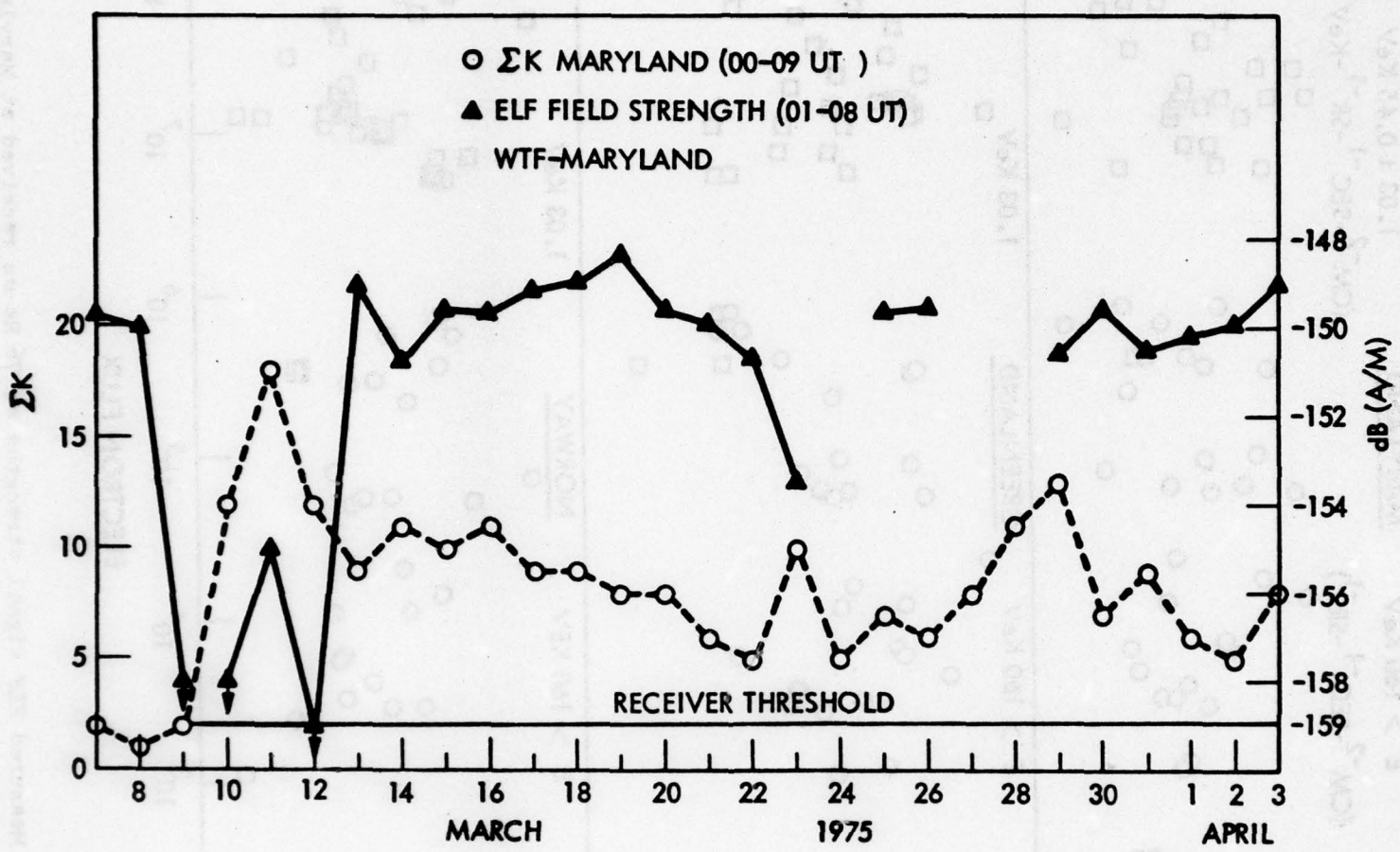

Figure 4-6. Plot of the nightly averaged ELF signal strengths for the station at Maryland March-April 1975 (right hand scale) and the nightly averaged local K index values (left hand scale).

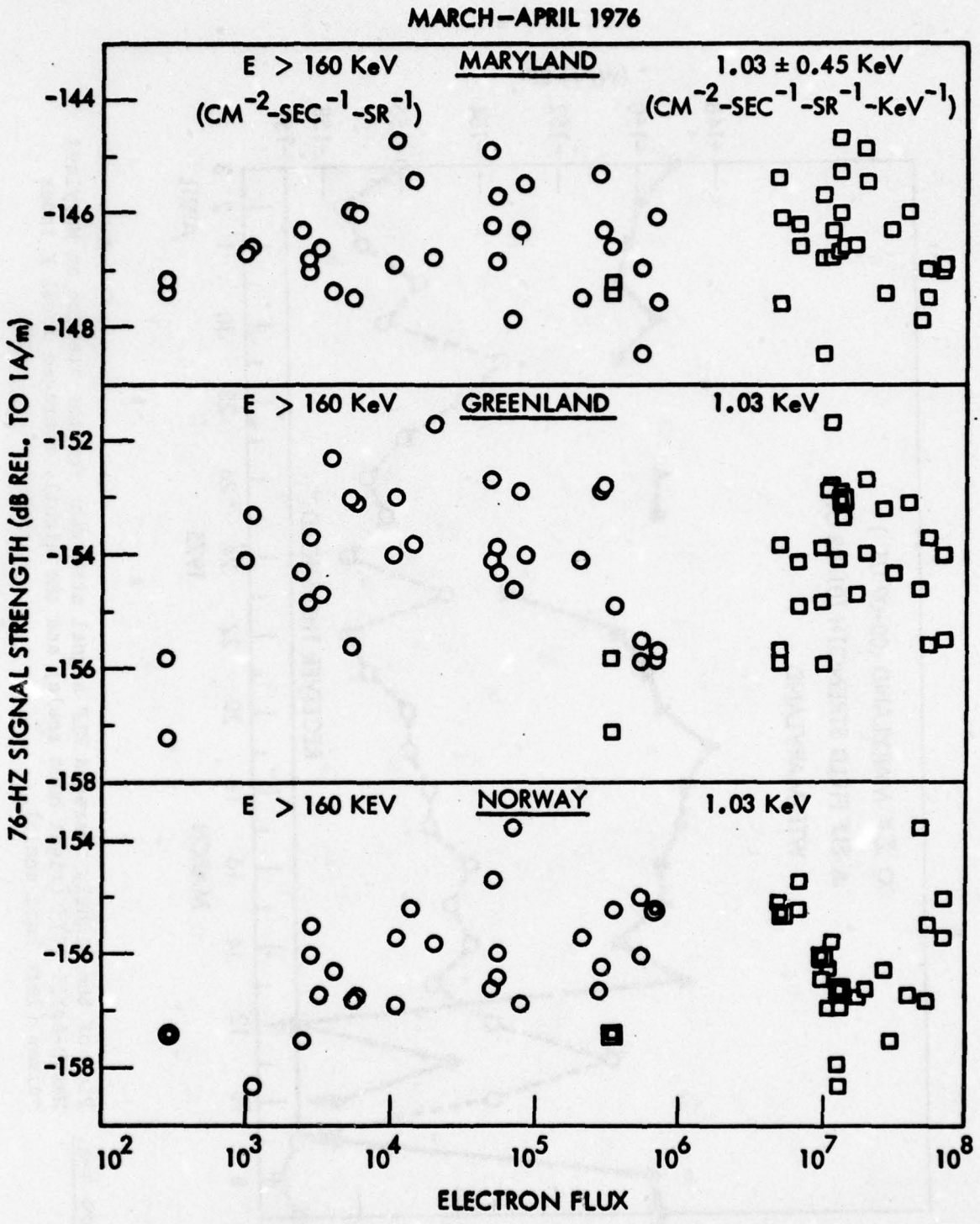

Figure 4-7. Measured ELF signal strengths at 76 Hz as received at Maryland, Greenland and Norway stations plotted as a function of the integral fluxes of precipitating electrons above energies of 160 keV and the differential precipitating electron fluxes at 1.03 keV $\pm$ 0.45 keV.

data points clearly display a large amount of scatter, masking any general trends. The measurements may suggest some tendency toward higher signal strengths at greater electron fluxes, but this is not clearly established with the present data base. In some earlier Connecticut data presented in Figure 4-8 there appears to be a general decrease in signal strength with increasing flux of the precipitating electrons above 160 keV. These trends are not suggested in the fluxes of 1 keV electrons which deposit their energy in the upper portions of the E-region. From these figures one is left with the impression that energetic (> 160 keV) particle precipitation may effect the ELF signal strengths, but that either attenuations or amplifications may occur as a result of increase precipitating flux. Clearly, a more detailed analysis of the data, making use of the intensity profiles and energy spectra is needed to be performed in conjunction with calculations of the expected signal strengths. In line with these objectives the satellite data have been analyzed in detail, as discussed below.

For several coordinated satellite passes during the period March-April 1976 the measured fluxes of precipitating electrons > 160 keV are plotted in Figure 4-9 as a function of invariant latitude. The latter parameter is a geomagnetic coordinate appropriate for study of energetic particle precipitation. For reference the invariant latitude of the WTF transmitter is 59° and the receiving stations at Connecticut, Maryland, Greenland and Norway are 57°, 54°, 86° and 66°, respectively. Since the waveguide program provides for segmenting the propagation path into different regions but does not allow for variation of the guide parameters perpendicular to the propagation path some type of latitude averaging must be invokved, and therefore

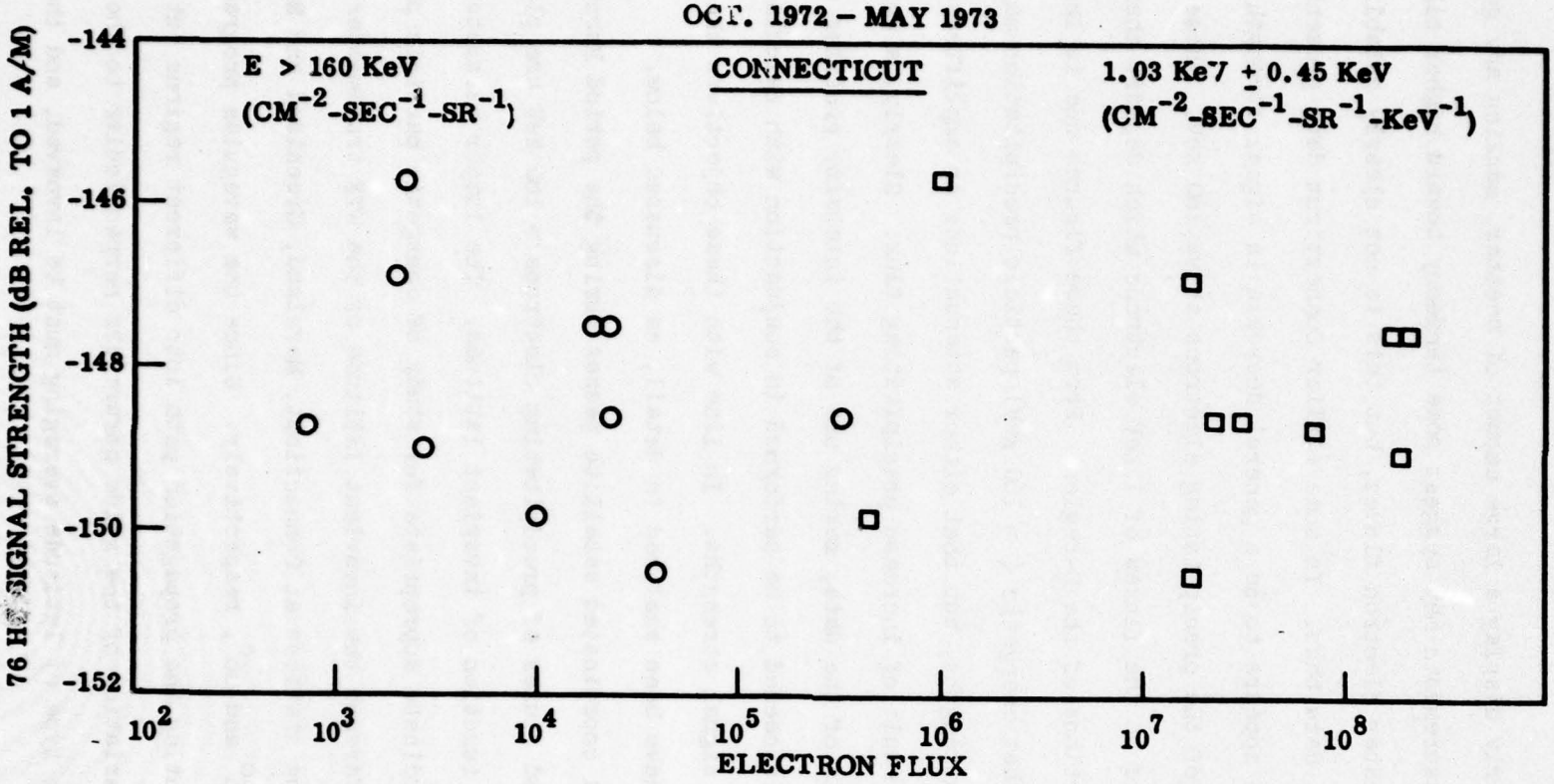

Figure 4-8. Measured ELF signal strengths at 76 Hz as received at the Connecticut station plotted as a function of the integral fluxes of precipitating electrons above energies of 160 keV and the differential precipitating electron fluxes at 1.03 keV ± 0.45 keV.

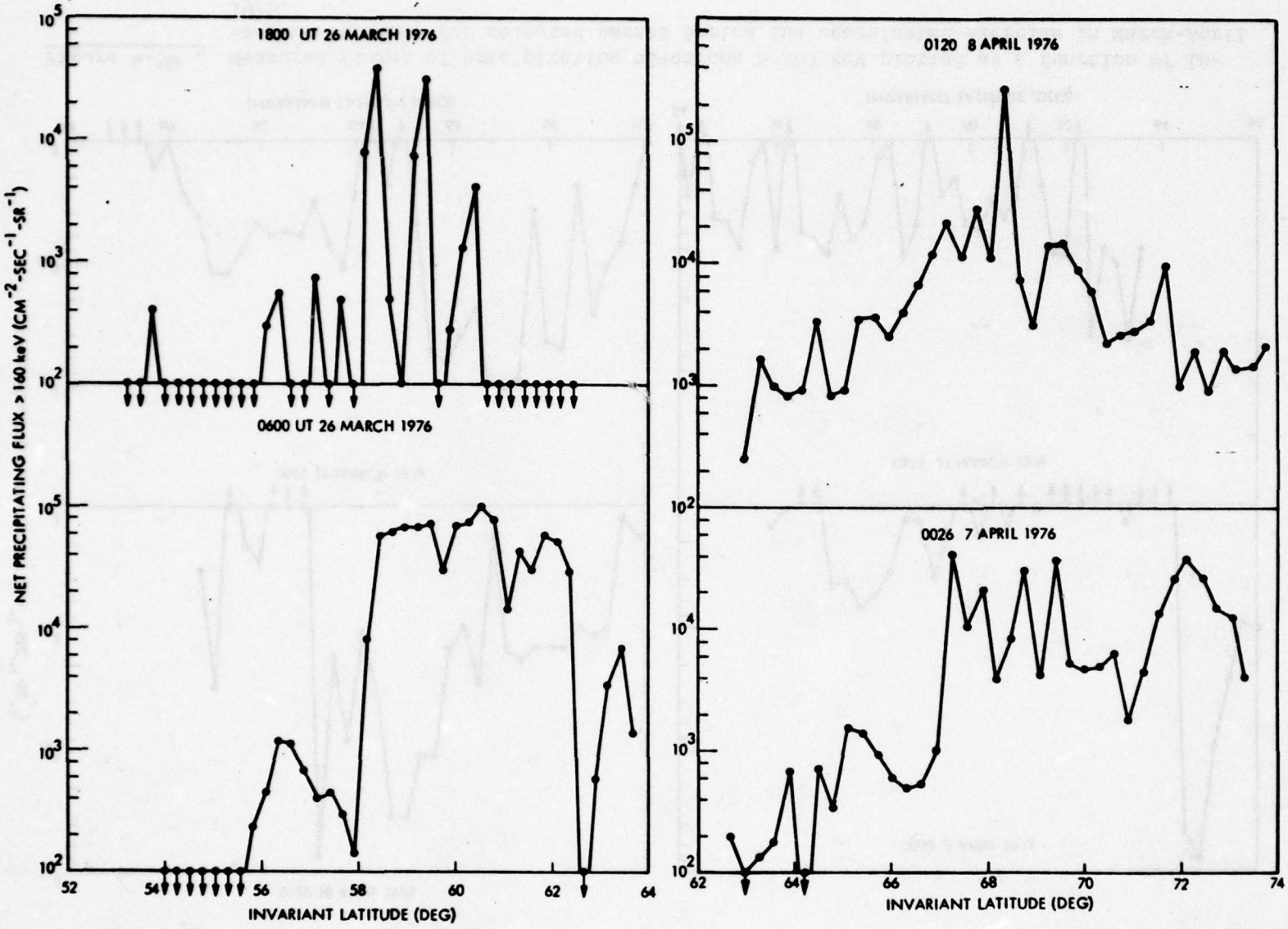

Figure 4-9A. Measured fluxes of precipitating electrons > 160 keV plotted as a function of invariant latitude for selected passes during the coordinated exercise in March-April 1976.

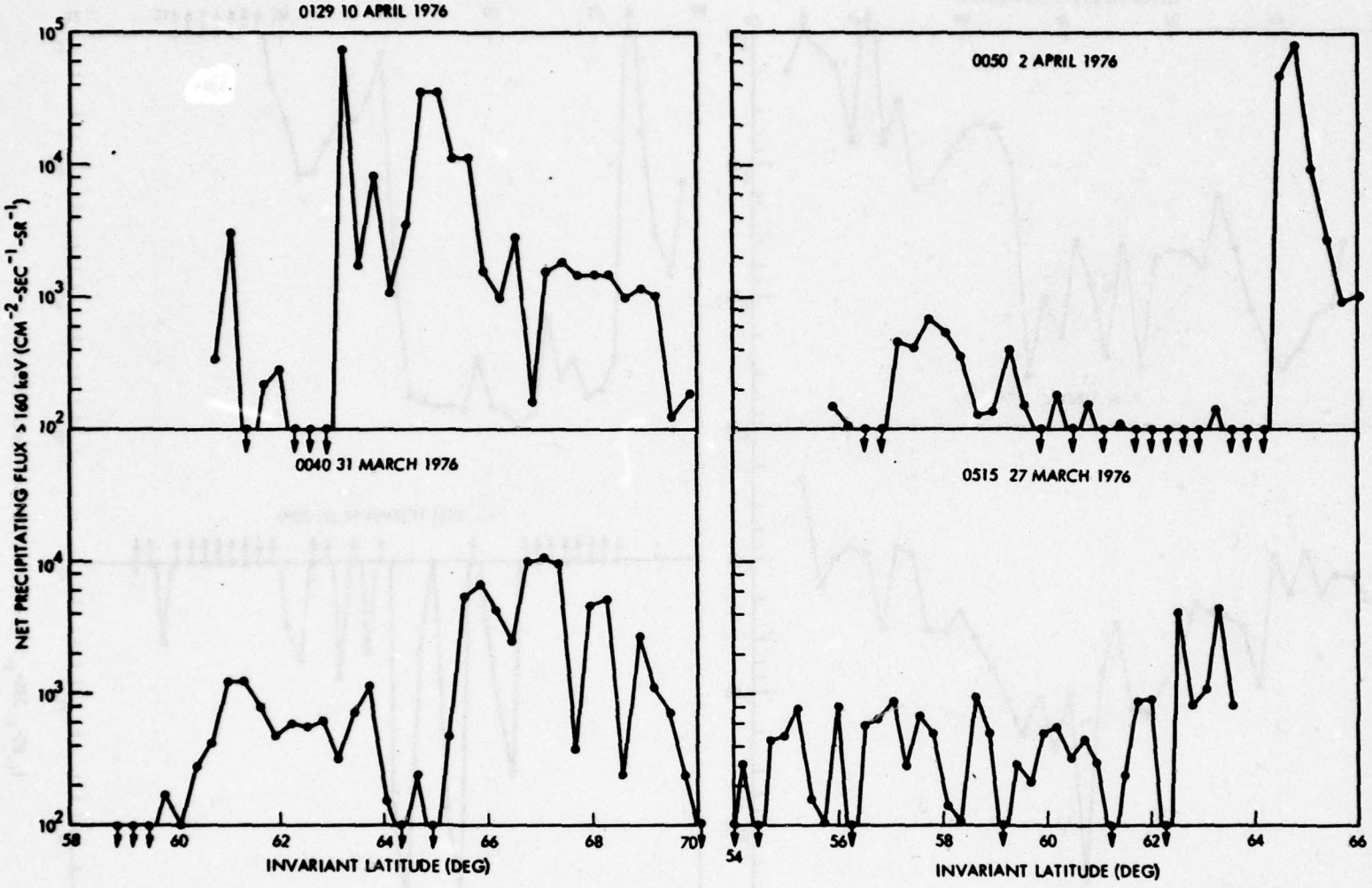

Figure 4-9B . Measured fluxes of precipitating electrons > 160 keV plotted as a function of invariant latitude for selected passes during the coordinated exercise in March-April 1976.

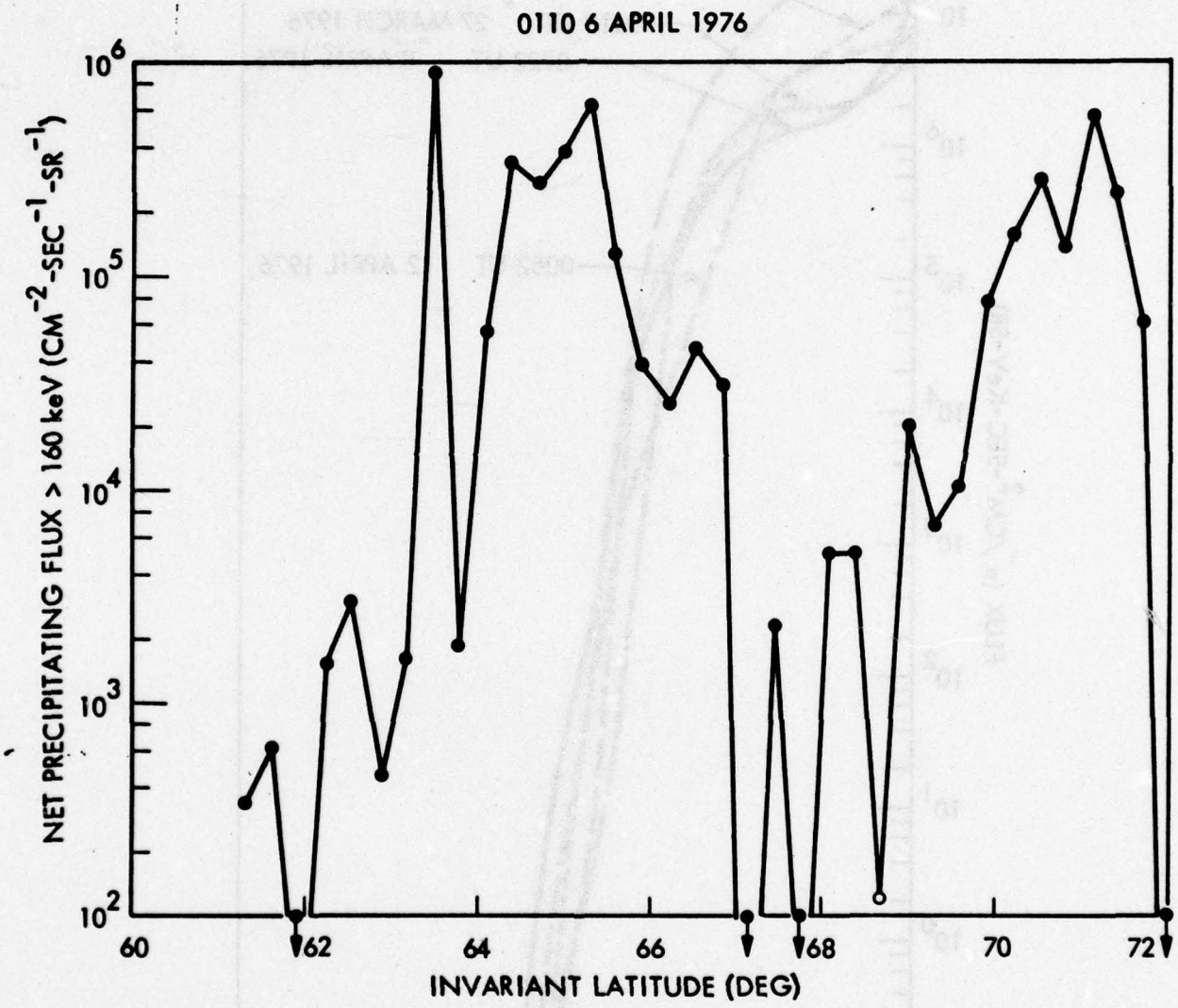

Figure 4-9C. Measured fluxes of precipitating electrons > 160 keV plotted as a function of invariant latitude for a selected pass during the coordinated exercise in March-April 1976.

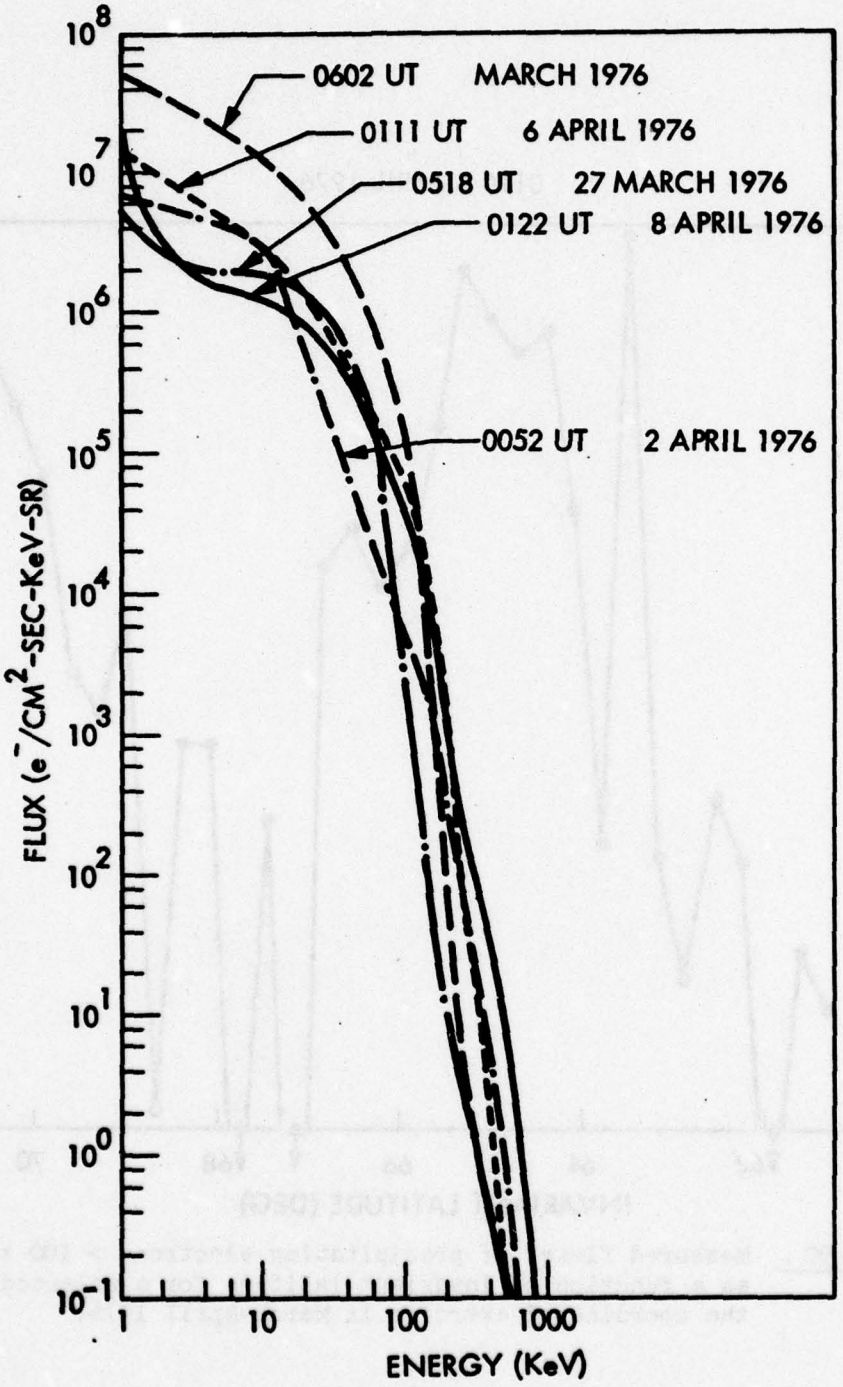

Figure 4-10. Examples of the energy spectra of precipitating electrons measured during the March-April 1976 coordinations.

several empirical approaches were taken. These included a linear averaging of the energy deposition profiles over the complete magnetic latitude interval between the transmitter and the receiving station as well as other procedures such as selecting the highest fluxes within an interval. For many of the analyses presented here maximum fluxes over a latitude interval of at least a few tenths of a degree were used.

Examples of the more intense energy spectra of precipitating electrons measured during the March-April 1976 coordinations are shown in Figure 4-10. These measurements were all performed near local midnight, and in each case all or virtually all of the propagation path of interest was in darkness. Overall the precipitating electron intensities are quite high but somewhat lower than many recorded during the 31 October-1 November 1972 magnetic storm event when high fluxes of precipitating electrons were observed and when pronounced ELF transmission anomalies were recorded. The spectra shown indicate significant intensities at energies > 1 MeV, but spectra with much greater fluxes of relativistic electrons have been observed and are presented in Section 5.

For each of the electron energy spectra processed the ion-electron production rates in the atmosphere were calculated as a function of altitude, using the computer program AURORA (Walt et al., 1968). The method consists of solving the time-independent Fokker-Planck diffusion equation of electrons by use of finite difference techniques. The mirroring effects of the converging magnetic field are included. The program accepts an input electron differential energy spectrum of arbitrary shape along with any pitch angle distribution. Energy-dependent pitch angle distributions may

also be applied. In such a case the program uses the input pitch angle distributions prescribed for selected energies to obtain distributions at other energies through interpolation. In the calculations the electrons are allowed to interact with the atmosphere below 300 km. The program outputs include the electron pitch angle distribution between 0° and 180°, thus including backscattered and reflected electrons, at pre-selected energies and altitudes as well as the total energy deposition within specified altitude regions. Examples of ion-electron production rate profiles are shown in Figure 4-11.

The ion-pair production rates shown in Figure 4-11 are in general quite large compared to the natural ionization rates from cosmic rays. For example, at 70 km the cosmic ray production rates are less than 0.1 ion pair/cm^3-sec. The ion pair production rates encountered in the events of present interest are to be compared with those obtained during the very intense solar particle events in August 1972 (Reagan and Watt, 1976). During the peak of the August 1972 event the production rates over the Chatanika, Alaska radar site were less than 10^5 ion pair/cm^3-sec at all altitudes below 90 km. Of course, due to the high energy protons in the PCA event the ion pair production rates were much higher at the lower altitudes. For example, at 40 km over Chatanika at 1508 UT on 4 August 1972 the production rate was about 3×10^4 ion-pair/cm^3-sec. However, at an altitude of 90 km the production rate was only about 3×10^3 ion-pairs/cm^3-sec which is to be compared with the rates in Figure 4-11 that are higher by one to two orders of magnitude. This difference largely reflects the higher fluxes of electrons in the tens of keV energy range during the events covered in Figure 4-11. Likewise, during

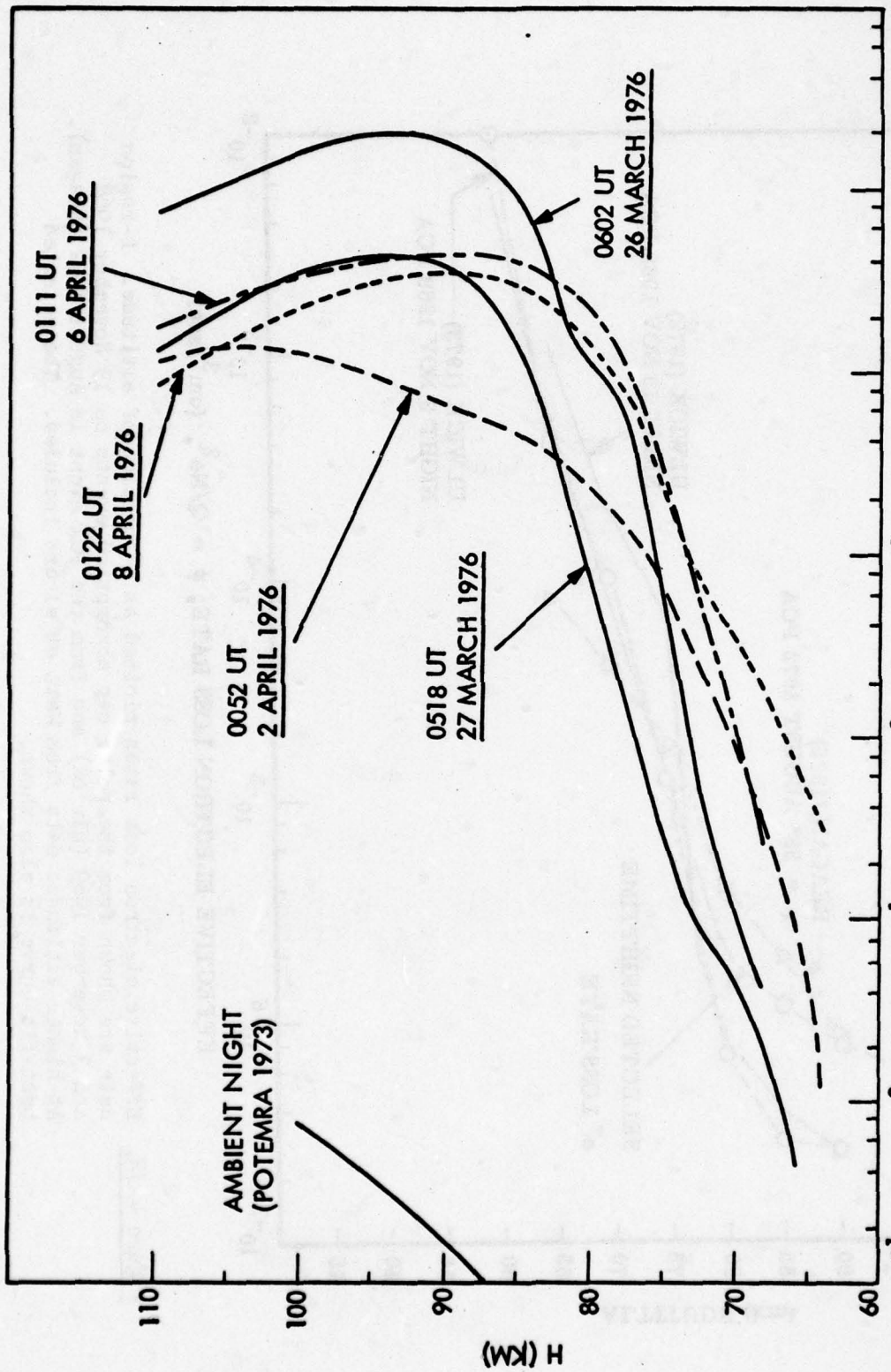

Figure 4-11. Ion-pair production rates obtained from the measurements of precipitating electrons during selected satellite passes in March-April 1976.

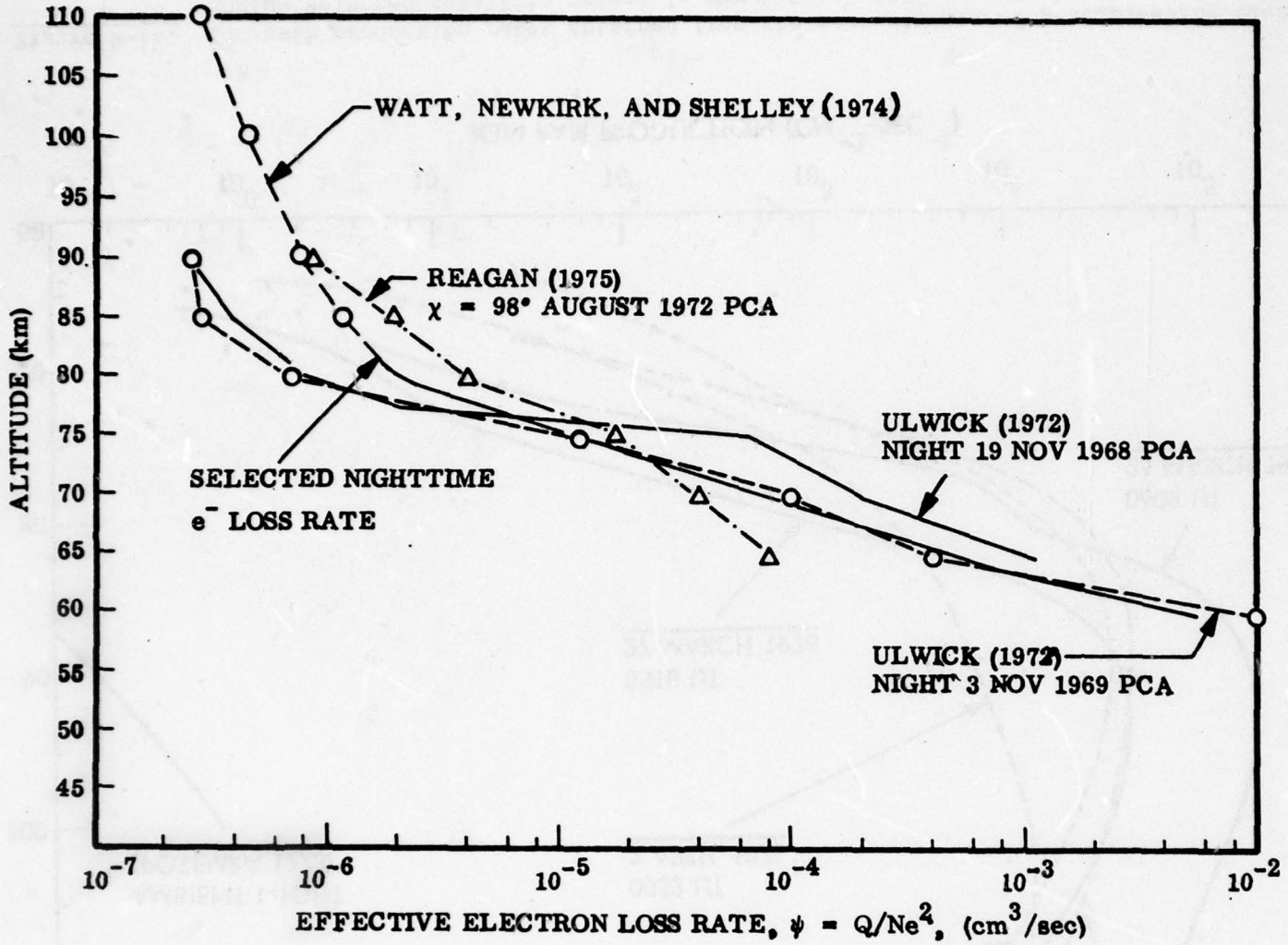

Figure 4-12. Effective electron loss rates plotted as a function of altitude. D-region data are shown from the polar cap absorption events on 19 November 1968 and 3 November 1969 (Ulwick) and from the PCA event in August 1972 (Reagan). At higher altitudes data from Watt et al are included. The selected best-fit curve is also shown.

some other selected solar particle events such as April 13, 1969 Potemra and Zmuda (1972) calculated production rates of $10^3 \rightarrow 10^4$ ion pairs/cm^3-sec in the 70 to 90 km altitude range.

In order to obtain electron densities from the ion pair production rates it is necessary to invoke values for the effective nighttime loss rate coefficients. Various measurements of the loss rate coefficients have been made in the past, but at present there is not a general concurrence on the values. The effective loss rates are known to vary with the production rate at night in contrast to the daytime loss rates (Swider and Keneshea, 1972). At the times of the ELF transmission anomalies of interest here the ion pair production rates are generally comparable to those at the times of PCA events. The loss rates obtained from PCA observations should therefore be applicable. These are shown in Figure 4-12. The loss rate coefficients are for nighttime conditions ($\chi = 98^o$) during the PCA event in August 1972 (Reagan and Watt 1976). At higher altitudes, data from Watt et al., 1974 are also included. Based on the published values a best-fit curve was selected, as shown.

For analysis of these data we have assumed the existence of a steady-state condition in the D-region. Such an assumption simplifies the analysis, but requires that the energy input not change substantially during typical recombination time periods which are of the order of tens of seconds. From the data acquired on a single satellite pass it is difficult to separate temporal and spatial events. The data acquired on subsequent passes (about 100 minutes later) typically indicate substantially different electron precipitation profiles but these differences may largely reflect longitude

variations. From a large body of satellite data acquired by the LPARL group on the rates of precipitation of energetic electrons over a large area using the atmospheric bremsstrahlung technique (Imhof et al., 1974A) it has been found that the total electron influxes typically remain rather constant during the time ($\sim$ 5 minutes) for traversal of the satellite over a given region. The conclusion drawn from the satellite bremsstrahlung measurements should be applicable to the present analyses where we are primarily concerned with the ionization produced over a rather large area. For a steady-state condition in the D-region the relation between production and loss of electrons may be written:

$$Q = \psi N^2$$

where Q = total ion pair production rate, ψ = effective electron loss rate and N = electron density. Based on this relation and the values of Q and ψ discussed above the electron densities were obtained as a function of altitude. Examples of electron density profiles for the March-April 1976 coordinated exercise are shown in Figure 4-13.

At altitudes above $\sim$ 80 km the positive ion density profiles were taken to be equal to the electron densities. This altitude limit was somewhat arbitrarily selected, and may indeed be as high as 85-90 km, but the computer runs indicated a lack of sensitivity to the N^+ densities in this altitude region. At altitudes below $\sim$ 40 km ambient densities for the N^+ profiles were used. In between these altitude limits a smooth curve interpolation was assumed. For the electron precipitation at 0602 HR UT on 26 March 1976 the electron and positive ion density profiles are shown in Figure 4-14.

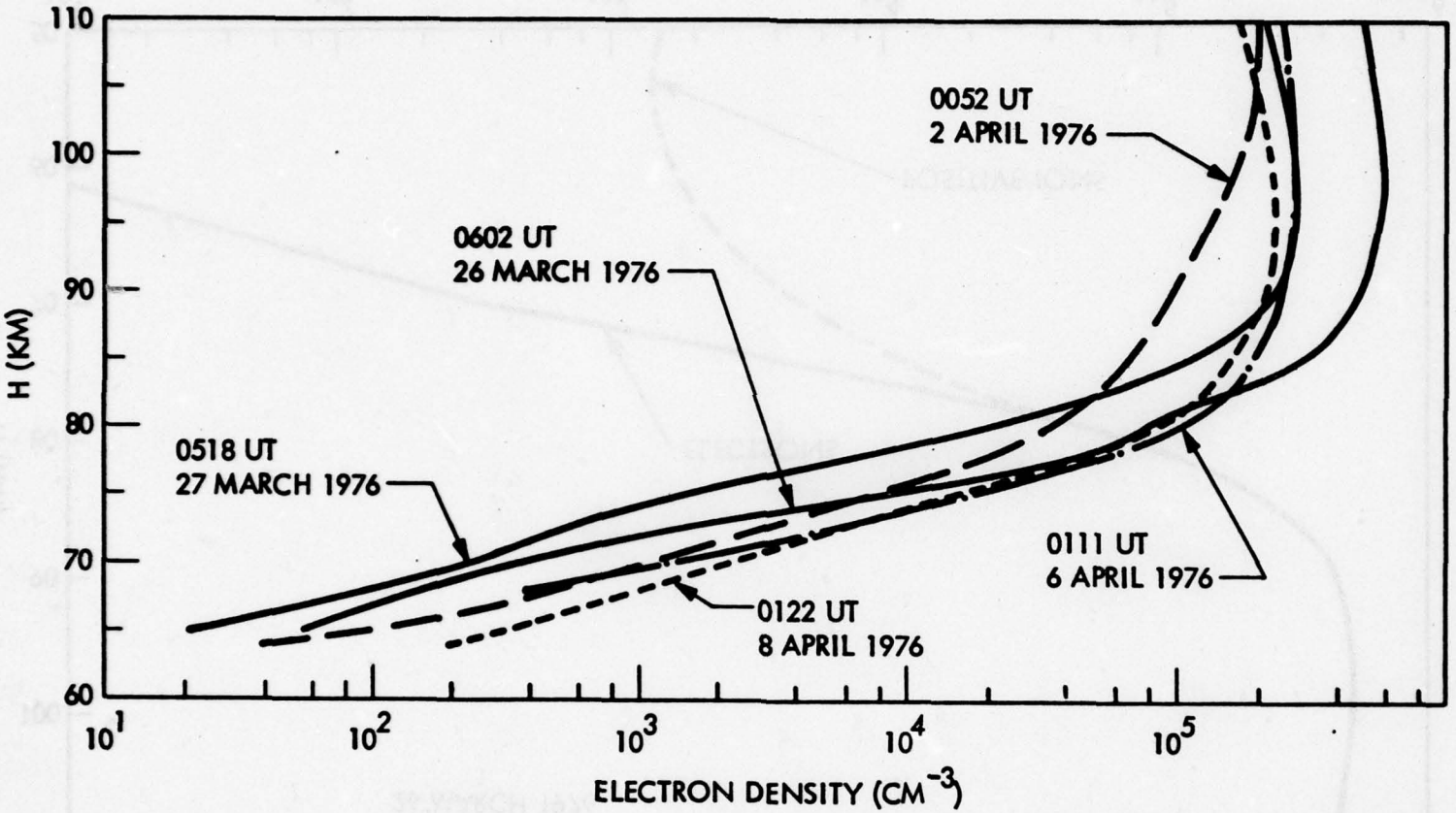

Figure 4-13. Examples of electron density profiles obtained from the March-April 1976 coordinated satellite passes.

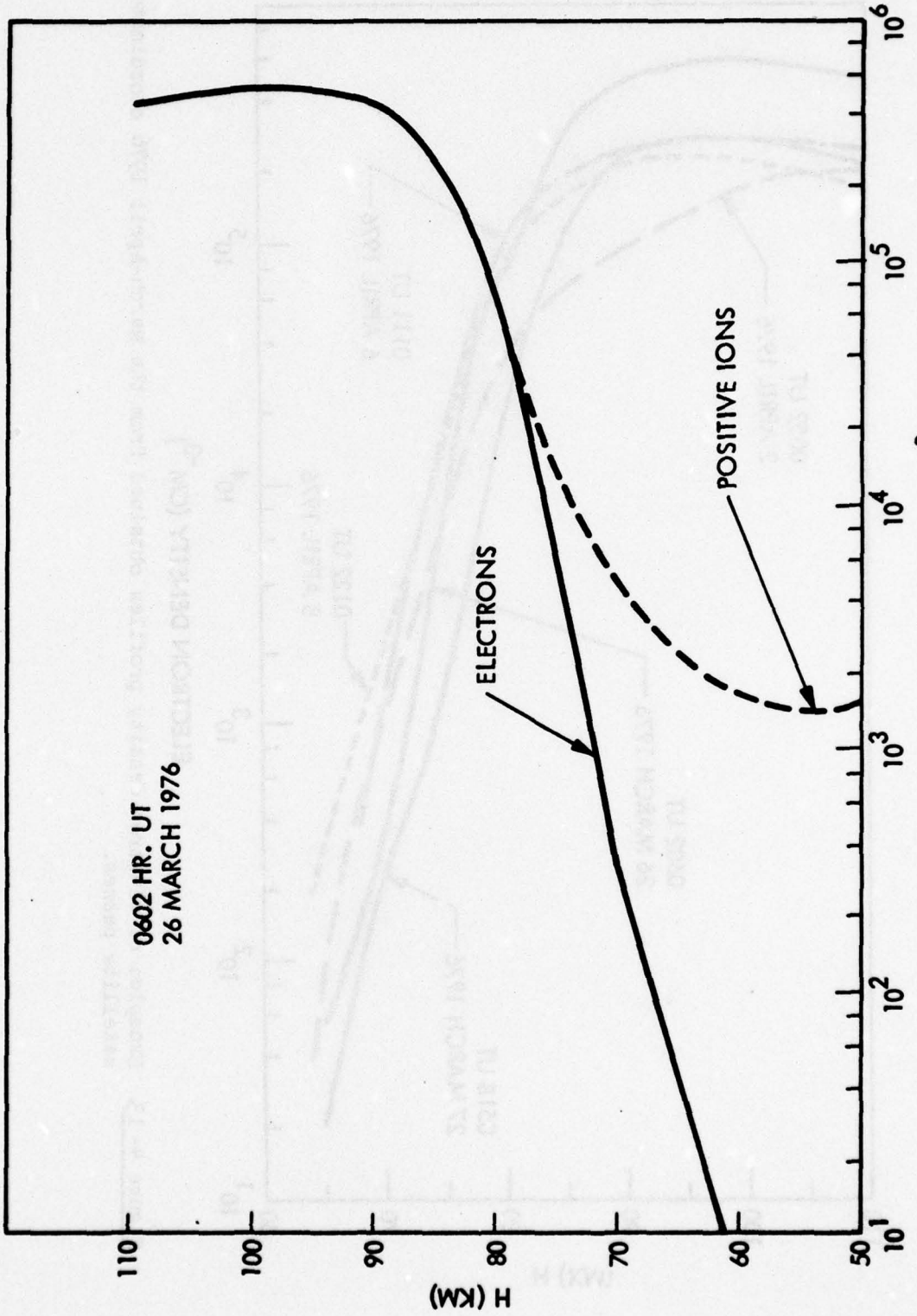

Figure 4-14 Electron and positive ion density profiles for the electron precipitation event at 0602 UT on 26 March 1976.

The electron density profiles obtained by the above procedures were then incorporated into the ELF propagation computer program. Since at any given time the satellite measurements of the precipitating electrons were performed at only one longitude crossing it was necessary to make certain assumptions regarding the spatial extent of the enhanced ionization densities. The geometry of the transmitter, the satellite crossing, the electron precipitation oval and the receiver are illustrated schematically in Figure 2-1. The guidelines used for calculation purposes were to assume that the maximum precipitating electron inputs averaged over a 4^{o} wide latitude band applied over the full longitude interval of concern and over a latitude dimension consistent with the segmentation used in the ELF computer program. Even if available, more detailed electron density profiles could not be used in the present waveguide mode program due to the important limitations of that program in not being able to treat variations of the guide parameters perpendicular to the propagation path. Clearly, for future more quantitative studies this major simplification in the program should be rectified and more detail spatial mappings of the precipitating electrons obtained. The effect of the present simplified analysis is perhaps to set an upper limit to the signal attenuations, although for any given case the effect on the ELF signals might be either underestimated or overestimated due to the possible variations with longitude in the precipitating electron fluxes.

Several runs of the ELF waveguide mode computer program were made to study the effects on the field strength of electron density profiles measured during the March-April 1976 coorindated exercise. The results of these runs for a representative electron spectrum (0602 UT on 26 March 1976) are listed

in Table 4-1 for transmission to each of several receiving stations. One can see that signal enhancements are predicted for the receivers at each of the stations. The trend for obtaining enhanced signal strengths during intense auroral zone precipitation of the type often observed in March-April 1976 is consistent with the measured increase in signal strengths during early April 1976 (see Figures 4-1 and 4-2). These similarities between the measured and calculated signal strengths are compared in the summary section with those obtained for other classes of electron precipitation events.

Table 4-1

Calculated Field Strengths for Electron Precipitation Event
0602 HR UT on 26 March 1976

Receiving Station	Segment for Electron Precipitation	Calculated Field Strengths (at 75 Hz) in dB wrt 1 A/M)			Measured Change in Field Strength (dB wrt 1 A/M)
		Ambient	During Event	Change due to Event	
Tromso, Norway	0-800 KM	-155.6	-154.5	+1.1	+2.0
Thule, Greenland	0-200 KM	-151.1	-148.7	+2.4	+0.5
Pisa, Italy	0-200 KM 2400-6200 KM	-158.5	-157.0	+1.5	+3.2
Connecticut, USA	0-300 KM	-145.2	-144.3	+0.9	-
Maryland, USA	0-100 KM	-144.6	-143.7	+0.9	0.0

Section 5

THE EFFECTS OF RELATIVISTIC ELECTRON PRECIPITATION EVENTS

On several satellite passes during the coordinated exercises in March-April 1975 and July 1975 intense relativistic electron precipitation events (REP's) with very high fluxes of energetic electrons were observed. An example of an REP spectrum measured on 11 March 1975 is shown in Figure 5-1 for comparison with other spectra. During the REP event the intensities at energies of several hundred keV and above are much higher than observed during the 31 October-1 November 1972 solar particle event when high fluxes of precipitating electrons were measured. In the REP one should note the broad peaking near 1 MeV which leads to a high energy deposition rate and hence a high electron concentration at low altitudes.

Other examples of REP spectra measured during the coordinated exercises are shown in Figure 5-2. Spectra of this type, with broad peaks in the several hundred keV to few MeV region, have been observed many times at high latitudes near the radiation belt trapping boundary. These precipitationg spectra cause high ion pair production rates at low altitudes, as shown in Figure 5-3, but their effects on ELF transmission may be somewhat reduced by the rather narrow latitude interval over which they are effective. The REP spectra considered here were all measured near local midnight. So to obtain the electron densities shown in Figure 5-4, use was made of the nighttime effective loss rates discussed in Section 4.

An evaluation of the effects of the measured REP events on the ELF transmission signal strengths has been made with use of the derived electron

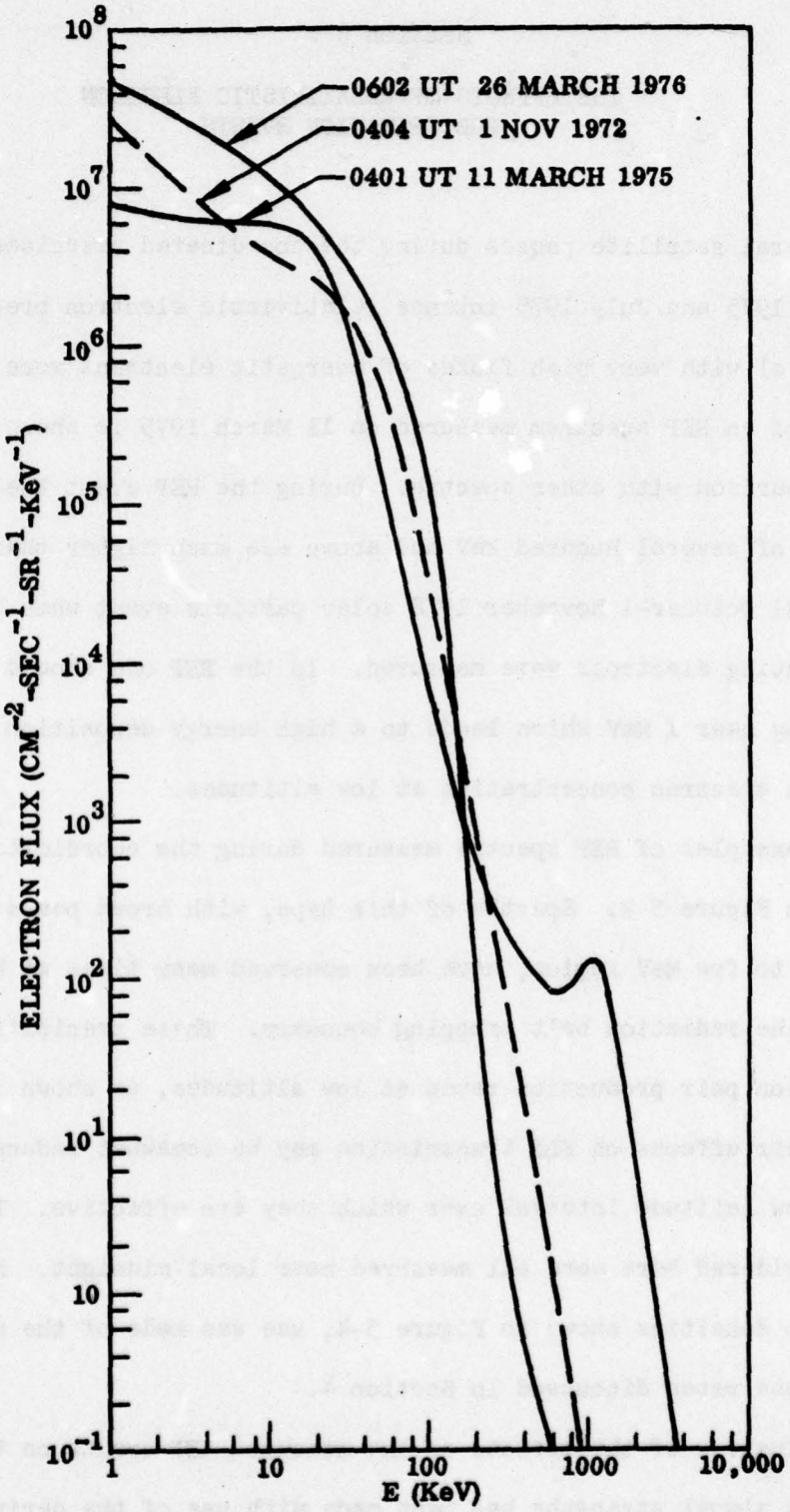

Figure 5-1. Example of an REP energy spectrum measured on 11 March 1975.

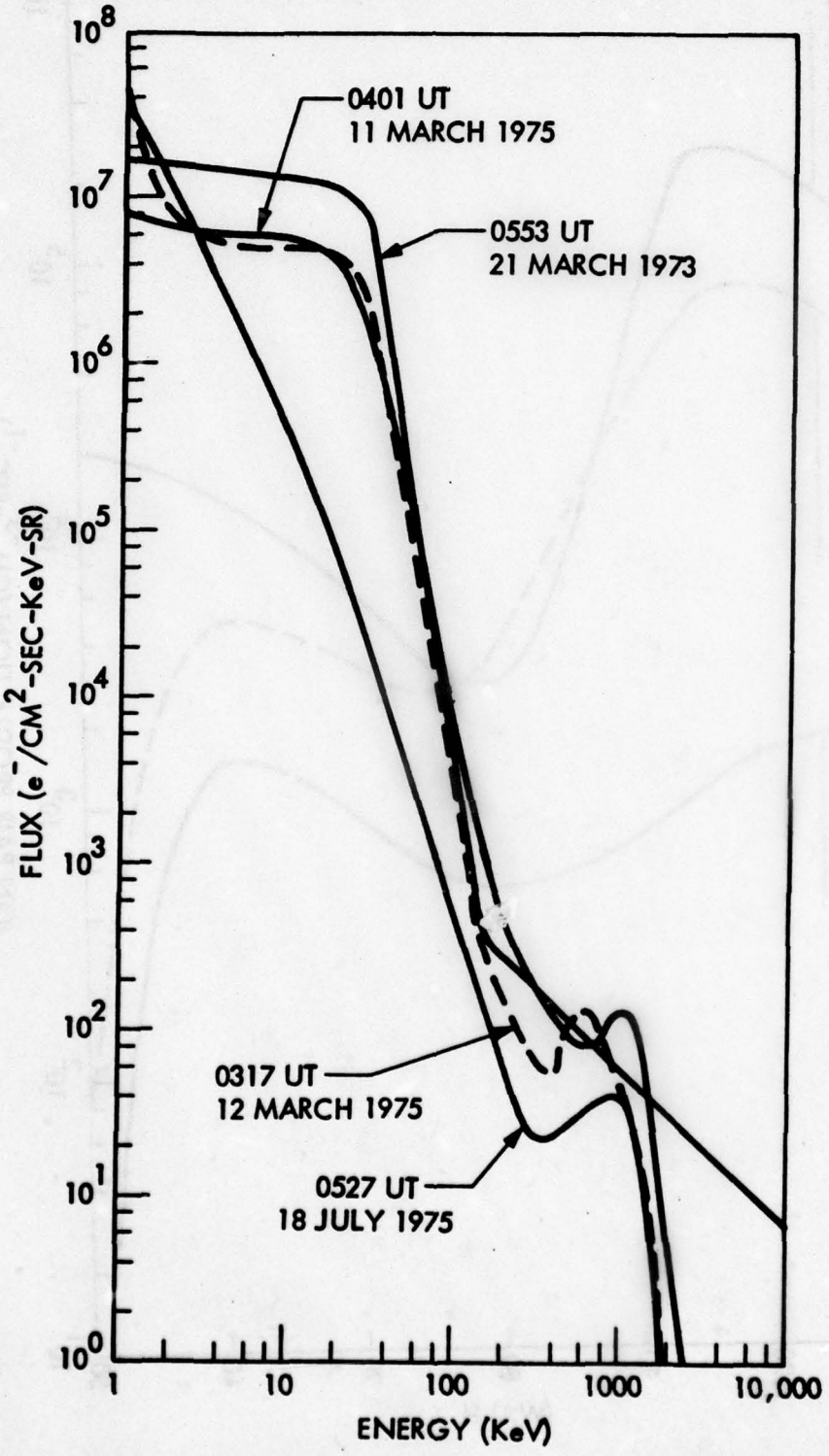

Figure 5-2. Additional examples of REP energy spectra measured during the coordinated exercises.

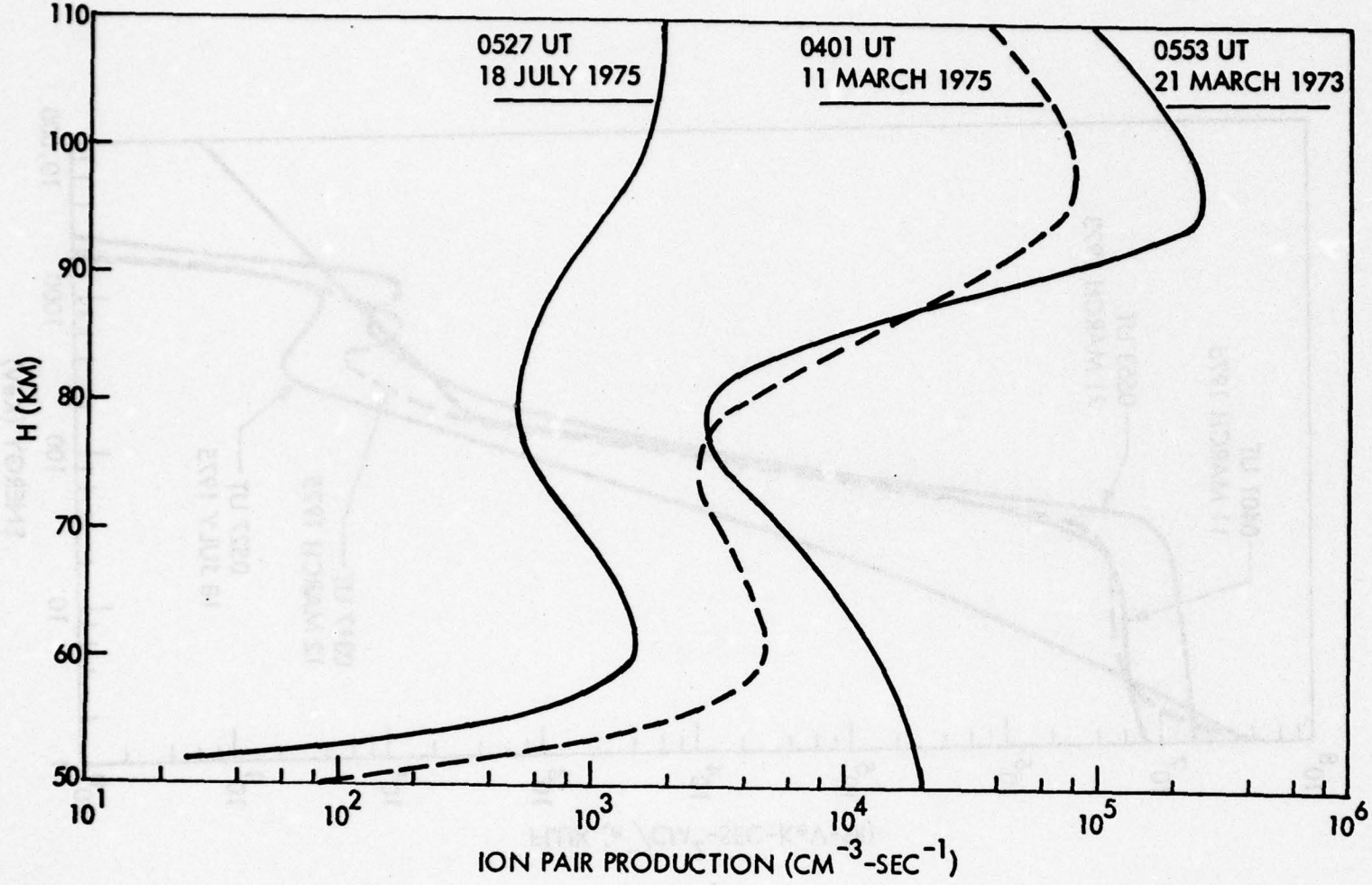

Figure 5-3. Examples of ion-pair production rates from REP events.

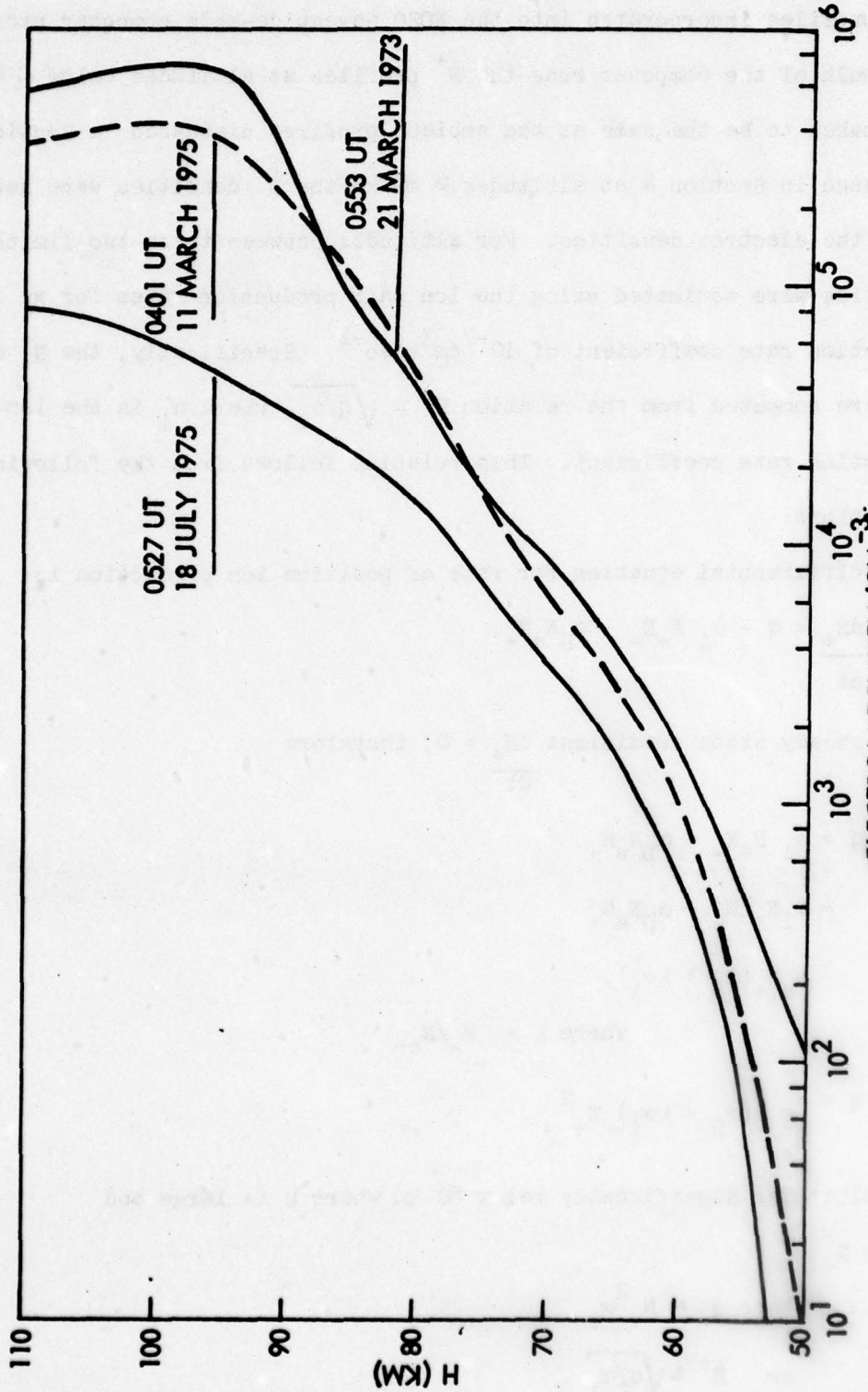

Figure 5-4. Examples of enhanced electron density profiles resulting from REP events.

density profiles incorporated into the NOSC waveguide-mode computer program. For the bulk of the computer runs the N^+ profiles at altitudes below ~ 40 km were taken to be the same as the ambient profiles discussed in Section 3.2. As discussed in Section 4 at altitudes ≥ 80 km the N^+ densities were set equal to the electron densities. For altitudes between these two limits the N^+ densities were estimated using the ion pair production rates for an ion-ion recombination rate coefficient of $10^{-7} cm^3\text{-}sec^{-1}$. Specifically, the N^+ densities were computed from the relation $N^+ = \sqrt{q/\alpha_i}$, where α_i is the ion-ion recombination rate coefficient. This relation follows from the following considerations:

The differential equation for rate of positive ion production is:

$$\frac{dN_+}{dt} = q - \alpha_i N_+ N_- - \alpha_D N_e N_+ \qquad (1)$$

For steady state conditions $\frac{dN_+}{dt} = 0$, therefore

$$q = \alpha_i N_+ N_- + \alpha_D N_e N_+$$

$$= \alpha_i N_+ \lambda N_e + \alpha_D N_e N_+$$

$$= N_e N_+ (\alpha_D + \lambda \alpha_i)$$

where $\lambda = N_-/N_e$

or $q = \frac{N_e}{N_+} (\alpha_D + \lambda \alpha_i) N_+^2$

At altitudes significantly below 80 km where λ is large and $N_- \approx N_+$

then $q \approx N_+^2 \alpha_i$

or $N^+ = \sqrt{q/\alpha_i}$

In order to gain an understanding of the sensitivity of the calculated signal strengths to the N^+ profile, computer runs were also made with a different value of the ion-ion recombination rate coefficient. For a value of $6 \times 10^{-8} cm^3\text{-}sec^{-1}$, shown in Figure 5-5, the signal strengths were not significantly different from those obtained with $10^{-7} cm^3\text{-}sec^{-1}$. From these computer calculations one concludes that over the range of "reasonable" values of the ion-ion recombination rate coefficient the transmitted signal strength is not very sensitive to the N^+ profile.

For the event on 11 March 1975 the calculations were performed for paths from WTF to each of the following receiving stations; Norway, Greenland, Italy, Connecticut and Maryland. Since for a given REP event the measurements were limited to the immediate vicinity of the satellite path certain assumptions were made as to the world-wide extent of the electron precipitation. The high electron fluxes, measured over a latitude extent of $\sim 0.5^\circ$ to $\sim 1.0^\circ$ at one longitude crossing of the satellite, were assumed to extend over a significant portion of the transmission path. Under these assumptions the calculated signal strengths for a relativistic electron precipitation event, on 11 March 1975, are provided in Table 5-1. The calculations were performed at the frequency 42 Hz, in effect at the time of the electron measurements. The computer program predicts signal enhancements for the stations at Maryland, Connecticut, Italy, Greenland and Norway.

ELF transmission calculations were also performed for the intense REP event at 0553 UT on 21 March 1973. The computations were applied to the path from WTF to Tromso, Norway for a variety of assumptions as to the location of electron precipitation consistent with the outer belt/auroral zone region

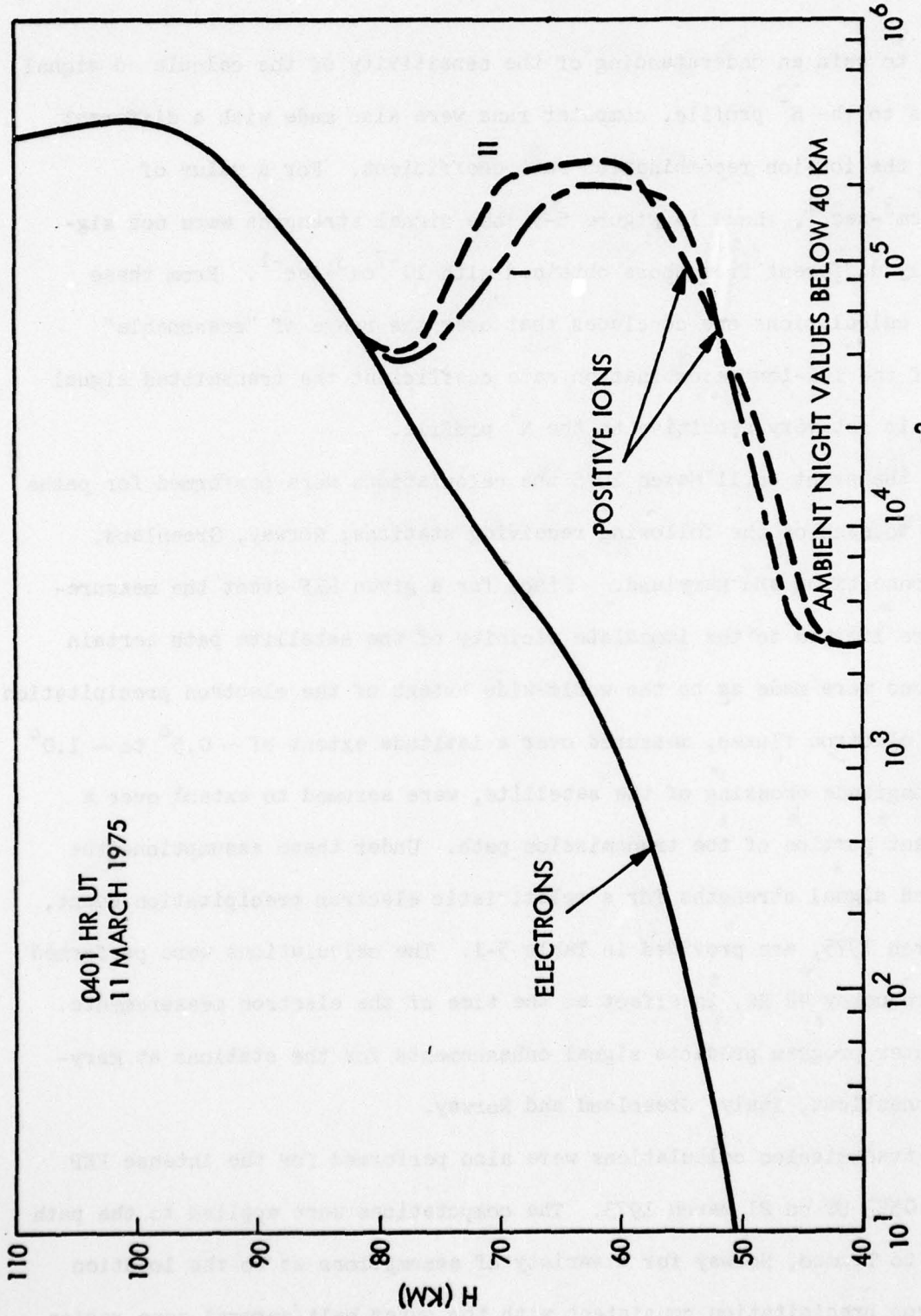

Figure 5-5. Two different positive ion density profiles corresponding to an ion-ion recombination rate coefficient of 10^{-7}cm^3-sec^{-1} (Curve I) and 6×10^{-8}cm^3-sec^{-1} (Curve II).

Table 5-1

Calculated Field Strengths for Electron Precipitation Event
at 0401 UT on 11 March 1975

Receiving Station	Segment for Electron Precipitation	Calculated Field Strengths at 42 Hz (in dB wrt 1 A/M) Ambient	During Event	Change due to Event
Tromso, Norway	0-200 KM	-159.3	-157.5	+1.8
Thule, Greenland	0-200 KM	-155.4	-153.6	+1.8
Pisa, Italy	0-2400 KM	-162.1	-160.0	+2.1
Connecticut, USA	0-300 KM	-149.8	-148.0	+1.8
Maryland, USA	0-100 KM	-149.2	-147.4	+1.8

illustrated in Figure 2-1. Since the precipitation oval comes close to the vicinity of the transmitter and the receiver at Tromso the ELF waveguide program was run for precipitation near the transmitter above, near the receiver alone and at both locations. The results are summarized in Table 5-2. It is clear that either signal increases or decreases may occur, depending upon the spatial extent and location of the ionization. Although insufficient coordinated data are available for verifying the predicted effects of these very intense and hard relativistic electron precipitation events the calculations based on the satellite data indicate that either signal enhancements or degradations may occur. The predicted effects of a single relativistic electron precipitation event are not severe, but due to their frequent occurrence they may provide the opportunity to verify experimentally the predicted effects of more severe and rarely occurring phenomena such as PCA events. For a more precise evaluation of their continual role in regard to ELF propagation, the acquisition and analysis of data on more coordinated passes should be performed.

Electron precipitation events can produce some ionization at altitudes down to $\sim$ 30 km through the production at higher altitudes of bremsstrahlung x-rays which can penetrate deeply into the atmosphere. Examples of the ionization produced by the bremsstrahlung are shown in Figure 5-6, both for an REP event and for softer electron precipitation of the type discussed in Section 4. As one can see the ion pair production rates from the bremsstrahlung x-rays may exceed nighttime ion production rates and hence can modulate mid D-region ionization.

Table 5-2

Calculated Field Strengths for Electron Precipitation Event at 0553 UT on 21 March 1973, Transmissions from WTF to Receiving Station at Tromso, Norway

Segment for Electron Precipitation	Calculated Field Strengths at 75 Hz (in dB wrt 1 A/M)		
	Ambient	During Event	Change due to Event
0-200 KM	-155.6	-153.3	+2.3
0-1000 KM	-155.6	-153.6	+2.0
0-1000, 4400-5800	-155.6	-154.2	+1.4
4400-5800 KM	-155.6	-156.2	-0.6

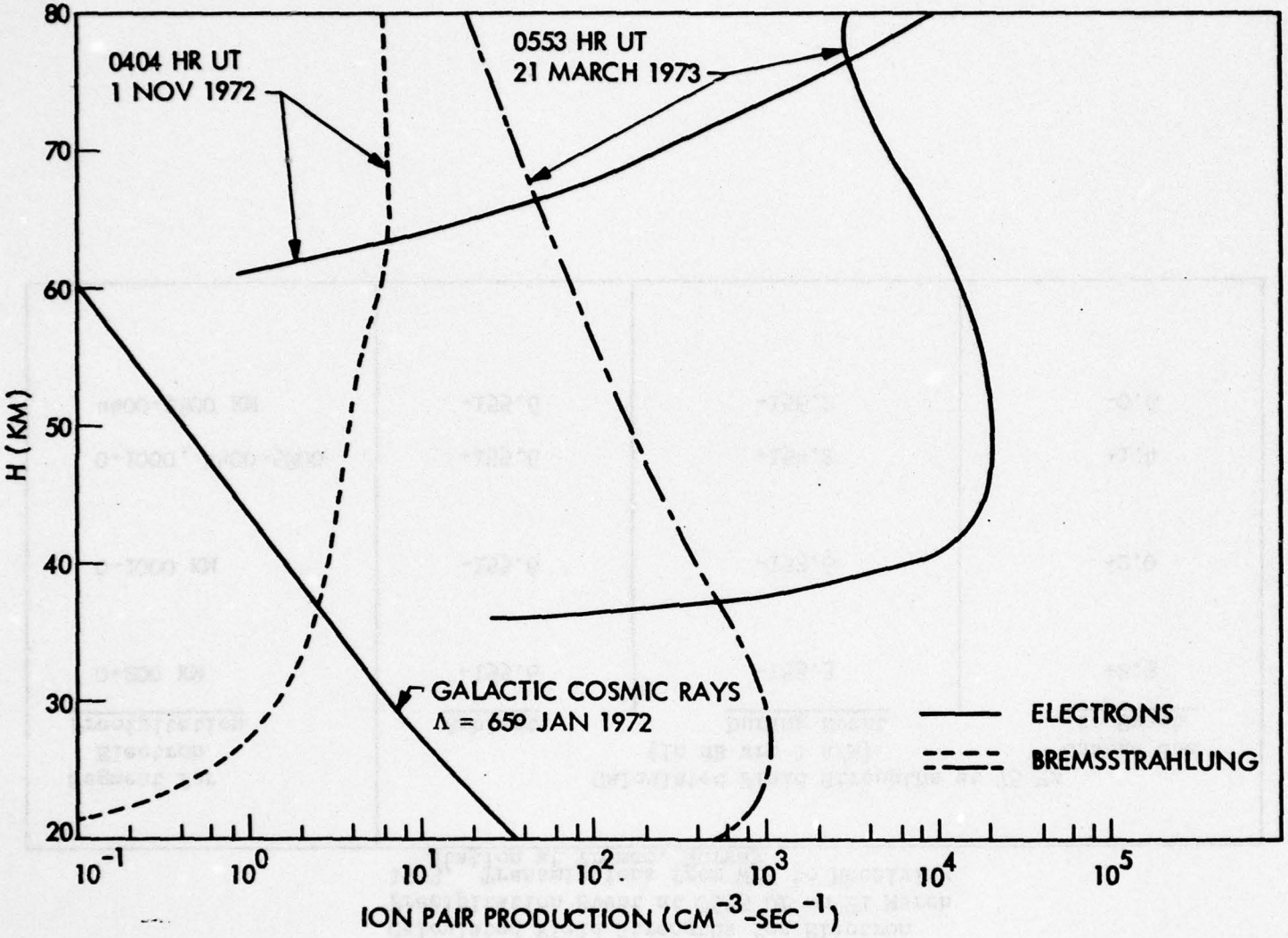

Figure 5-6. Examples of the ion pair production rates associated with bremsstrahlung x-rays produced by precipitating electrons.

For the REP event on 21 March 1973 ELF signal strength calculations were performed with inclusion of the additional ionization produced by the bremsstrahlung generated in the atmosphere by the precipitating electrons. The results for a frequency of 75 Hz are listed in Table 5-3.

Table 5-3

Effect of Bremsstrahlung Produced in Precipitation Event at 0553 UT on 21 March 1973 Transmission from WTF to Receiving Station at Tromso, Norway

Segment for Electron Precipitation	Field Strength in dB wrt 1 A/M at 75 Hz		
	During Event Bremss. Excluded	During Event Bremss. Incl.	Change due to Bremsstrahlung
0-200 KM	-153.3	-152.9	+ 0.4
0-1000 KM	-153.6	-153.4	+ 0.2
0-1000, 4400-5800	-154.2	-154.1	+ 0.1
4400-5800 KM	-156.2	-156.3	- 0.1

Section 6

WAVEGUIDE MODE CALCULATIONS FOR POLAR CAP ABSORPTION EVENTS

6.1 Calculations for Particle Inputs Measured during the 4 August 1972 PCA Event

No ELF propagation data from WTF have been obtained at Tromso, Norway during polar cap absorption (PCA) events (up to March 1977). In order to estimate the effects of PCA events, calculations were performed with the NOSC waveguide computer program on the basis of actual electron density and energetic particle precipitation data. Nighttime PCA conditions for this path were simulated using nighttime ionospheric data from the great event of 4 August 1972. This PCA event was the most intense in regard to proton precipitation with energies between 20-100 MeV during the present solar cycle. The data were obtained during a coordinated experiment with LPARL and Stanford Research Institute using the ground-based Chatanika incoherent scatter facility and the 1972-076B satellite (Reagan, 1975; Reagan and Watt, 1976).

In Figure 6-1 is shown the electron density profile as measured by the Chatanika radar between 59 and 100 km at 4 August 1972 1144 UT (0144 LT) for a solar zenith angle of $\chi = 95.3^{\circ}$. For the ELF calculations it is important also to know the N(h) densities below 59 km. For this purpose the production rates (q) of ion pairs have been combined with typical daytime and nighttime electron loss rates (Ψ) to yield electron densities by the following relation:

$$N \simeq q/\Psi$$

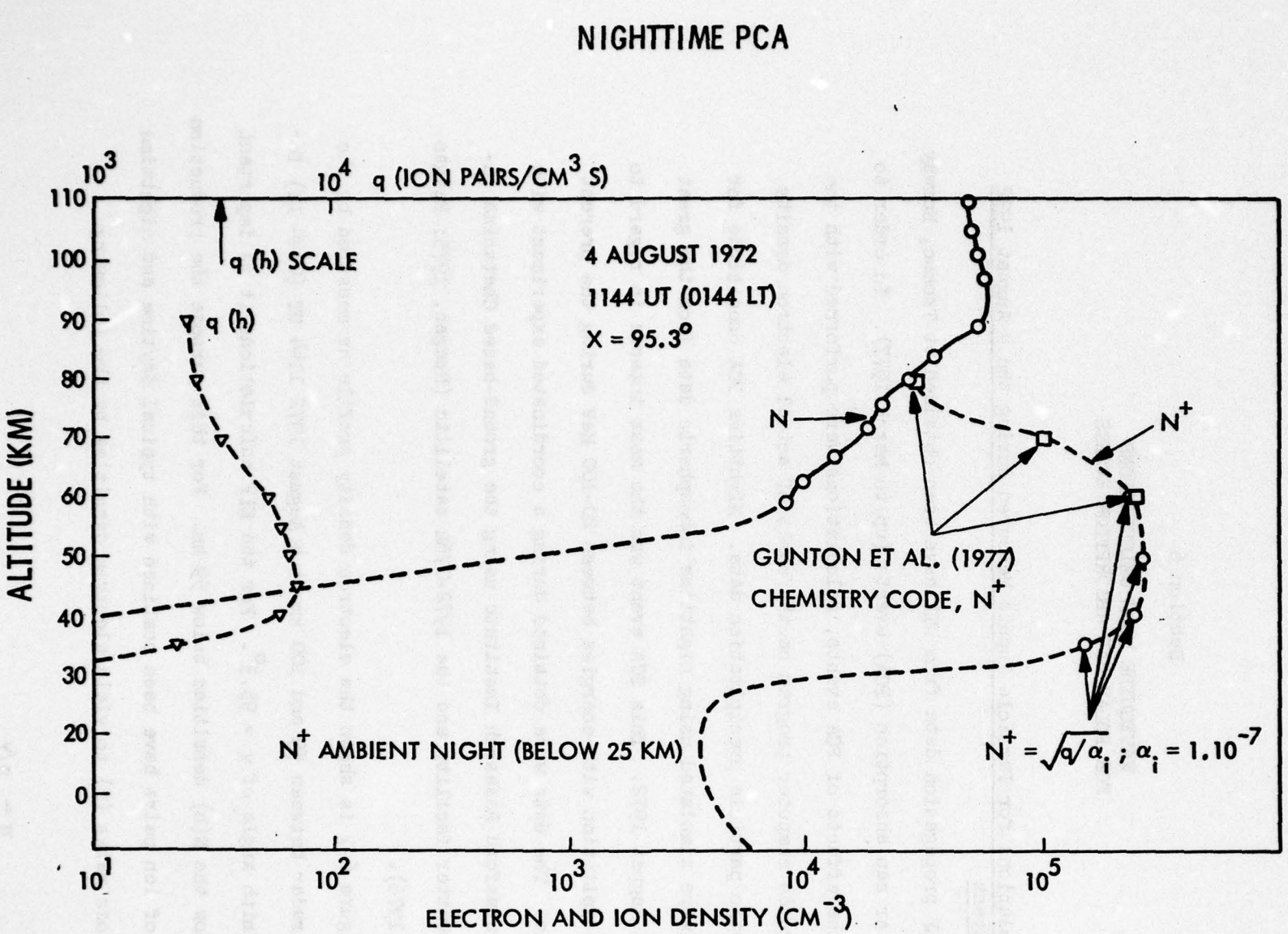

Figure 6-1. Electron density profiles as measured by the Chatanika radar at 1144 UT on 4 August 1972. The ion-pair production rates obtained from coordinated satellite measurements of the precipitating particles are also shown. The N^+ densities computed by Gunton et al (1977) are shown as open squares. At lower altitudes the N^+ densities, plotted as open circles, were obtained from the ion-pair production rates and an ion-ion recombination rate coefficient of 10^{-7}cm^3-sec^{-1}.

It is surmised that these values will serve as upper and lower limits to the electron densities present at $\chi = 95.3^{\circ}$.

The electron loss rates for daytime conditions (4.0×10^{-5} and $4.0 \times 10^{-4} cm^3\text{-}s^{-1}$ at 55 and 50 km, respectively) were taken from Reagan (1975); the value at 50 km being obtained by extrapolation. The nighttime loss rates were obtained by extrapolation to lower altitudes the values deduced by Sellers and Stroscio (1975) for the November 69 PCA (1.0×10^{-2} and $1.0 \times 10^{-1} cm^{-3} s^{-1}$ at 55 and 50 km, respectively).

The N(h) profile below 59 km used in the ELF calculations is a "best guess" between the established upper and lower limits with preference given to the lower, nighttime values. Below 40 km the N(h) profile joins smoothly with the ambient nighttime profile. The positive ion density for this case is derived as follows: above 83 km N^+ is taken to be equal to N_e the N^+ densities at 80, 70 and 60 have been computed for the total duration of this PCA event by Gunton et al. (1977), and the values marked by open squares represent the computed densities at $\simeq$ 1144 UT on the day in question. At 35 to 50 km the values were approximated by

$$N^+ \simeq q/\alpha_i$$

where α_i is the ion-ion recombination rate coefficient. This approximation is valid at low altitudes where

$$\alpha_d N^+ N < \alpha_i N^+ N^-$$

and steady state conditions are assumed ($dN^+/dt = 0$). The factor α_d is the electron-ion recombination rate coefficient. Since at these altitudes the electron densities $N << N^-$, we have $N^+ \simeq N^-$ and $q \simeq \alpha_i (N^+)^2$. When a constant value of $\alpha_i = 1.10^{-7} cm^3\text{-}sec^{-1}$ with height is assumed, the N^+ values

marked by open circles are obtained. Below 25 km ambient densities for N^+ are assumed. The N^+ values marked with asterisks at 50, 40 and 35 km were obtained using the "selected" $\alpha_i(h)$ values listed by Cole and Pierce (1965). It may be concluded that for our computations the assumption of a constant α_i with height is sufficiently accurate.

The propagation characteristics using these N and N^+ profiles for the various segments for the WTF path to Tromso, Norway are listed in Tables 6-1 and 6-2 for 42 and 75 Hz, respectively. It may be noted that the attenuation rates are up significantly over the ambient nighttime values. Simultaneously, the excitation factor has increased by 5-6 dB.

Using these propagation constants the calculated field strength at Tromso for 75 Hz is:

-158.9 dB wrt 1 A/M (uncorrected for antenna phasing)

which is -3.3 dB lower than calculated for ambient conditions.

It may happen, however, as in the present case, that the region disturbed by the solar protons will not cover the complete WTF-Tromso path. At ~ 1200 UT on 4 August 1972 the latitude cutoff for 20-100 MeV proton precipitation was occurring at approximately $L \approx 3.8$ or an invariant latitude of 59°. In fact, had this been a real coordinated case the WTF transmitter region would have been outside the PCA disturbed area.

If we make the assumption that the WTF segment is outside the PCA disturbance and has ambient nighttime ionospheric conditions, while the PCA is occurring over the rest of the path, the calculated field-strength at Tromso for 75 Hz is

-161.5 dB wrt 1 A/M (uncorrected for antenna phasing)

Table 6-1

Propagation characteristics @ 42Hz for the segmented path WTF to Tromso

Segment No.	Segment Length (km)	Path Segment	Att. Rate (dB/Mm)	v/c	Wait's Mag (dB)
1	200	WTF	1.34	0.73	+ 2.56
2	800	Canada	1.26	0.73	+ 2.45
3	800	Hudson Bay	1.17	0.74	+ 2.33
4	1100	North Canada	1.26	0.73	+ 2.45
5.	400	Davis Straight	1.16	0.74	+ 2.33
6	1100	Greenland	2.04	0.68	+ 3.56
7	1400	Norwegian Sea	1.16	0.74	+ 2.33
8	200	Tromso Area	1.25	0.73	+ 2.45

PCA - simulation (profile Chatanika 4 August 1972,1144 UT ; 0144LT, χ = 95.3°)

Table 6-2

Propagation characteristics @ 75Hz for the segmented path
WTF to Tromso, Norway

Segment No.	Segment Length (km)	Path Segment	Att. rate (dB/Mm)	v/c	Wait's Mag. (dB)
1	200	WTF	2.21	0.76	+ 1.47
2	800	Canada	2.11	0.76	+ 1.39
3	800	Hudson Bay	1.99	0.77	+ 1.30
4	1100	North Canada	2.11	0.76	+ 1.39
5	400	Davis Straight	1.98	0.77	+ 1.30
6	1100	Greenland	3.16	0.72	+ 2.26
7	1400	Norwegian Sea	1.97	0.77	+ 1.30
8	200	Tromso Area	2.10	0.76	+ 1.39

PCA - simulation (profile Chatanika 4 August 1972, 1144UT ; 0144LT, χ = 95.3°)

AD-A045 606 LOCKHEED MISSILES AND SPACE CO INC PALO ALTO CALIF PA--ETC F/G 20/14
ANALYSIS OF SATELLITE DATA ON PRECIPITATING PARTICLES IN COORDI--ETC(U)
JUN 77 W L IMHOF, T R LARSEN, J B REAGAN N00014-75-C-0954

UNCLASSIFIED LMSC-D560323 NL

2 OF 2
AD
A045606

END
DATE
FILMED
11-77
DDC

This is a 5.9 dB signal strength reduction over ambient conditions.

6.2 Calculations for Hypothesized PCA Profiles

Using the waveguide computer program an investigation was made of the effects on the ELF signal strengths of varying electron density profiles over a range of values expected for PCA events. These studies were performed with variations of the density profile based on measurements during the 1254 UT 5 August 1972 event (Reagan et al., 1973). Since the computer runs indicated that for the densities of concern the calculated signal strengths were dependent on the positive ion profile, for each of the electron density profiles the positive ion profile was adjusted so that both are consistent with the same ion-pair production profile. At all altitudes the ion-ion recombination rate coefficient was taken to be 10^{-7} cm^3-sec. To check the sensitivity of the calculated signal strengths to the positive ion densities in the altitude regions of enhancement during PCA events, a series of runs was made for vastly differing N^+ density profiles with a given electron density profile. These are shown in Figure 6-2. Each of the N^+ curves is labelled with the calculated signal strength. Although an exhaustive study of the sensitivity of the ELF transmission to the ion densities in each of several altitude regions was not performed, these runs suggest that the signal strengths are most sensitive to the N^+ densities at altitudes of $\sim$ 45 km or lower. To check the sensitivity of the calculated signal strengths to the ion ion recombination rate coefficient, one of the runs was made with a coefficient of 6×10^{-8} cm^3-sec. For that run the N^+ densities at altitudes of $\sim$ 50 km were increased by 29%, but no changes, within 0.1 dB, occurred in

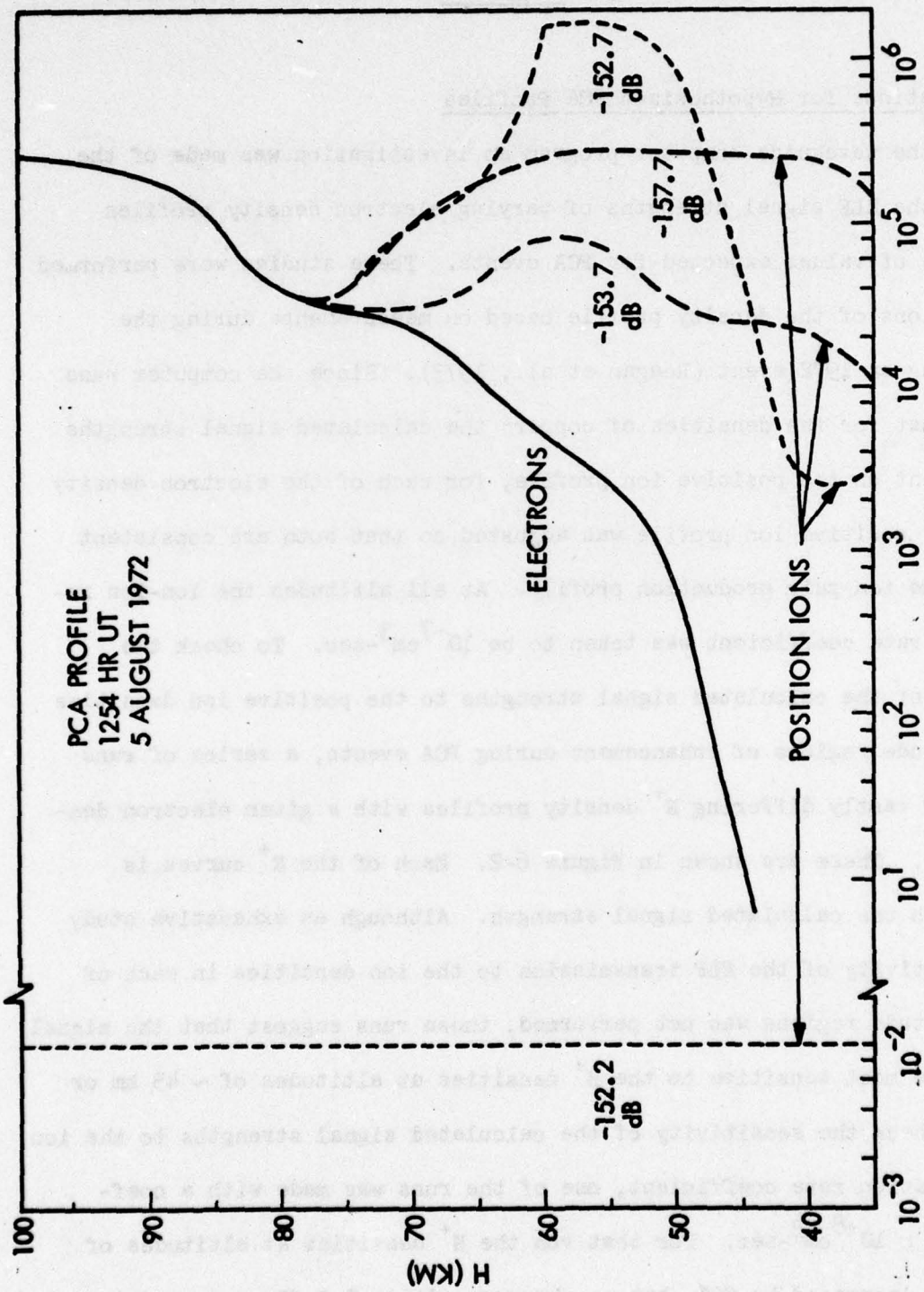

Figure 6-2. Various positive ion density profiles used in the waveguide mode calculation along the electron density profile shown.

the signal levels.

The various electron and ion density profiles used in the field strength calculations are shown in Figure 6-3. The electron density profiles differ mainly in regard to the lower altitude to which significant densities extend. The signal strengths calculated for each of the profiles are listed in Table 6-3. The full set of calculations was performed for a) the WTF transmitter inside of the PCA ionization region and b) the transmitter outside of the region. The signal strengths were 1.1 to 2.1 dB lower when the transmitter was not in the region of enhanced ionization. In order to gain some insight as to the importance of certain features of the density profiles the calculated signal strengths are plotted in Figure 6-4 as a function of the electron density at 60 km and also as a function of the height of the $10^3 cm^{-3}$ density value. The calculations clearly indicate a decrease in signal strength with an increasing electron density or with a lowering in altitude of a given density. But all of the signal strengths are higher than ambient.

It appears that a major PCA event with large fluxes of high energy protons penetrating to low altitudes, as on 4 August 1972, can cause significant attenuations in the ELF signal strengths. However, during weaker PCA events with lower fluxes of high energy protons the ELF signal strengths may be either attenuated or enhanced, depending upon the details of the resulting electron and positive ion density profiles. The variability of the ELF transmission in response to the shape and magnitude of the density profiles is illustrated in Table (s) 6-4, 6-5, and 6-6. Here the attenuation rates and Wait excitation factors, over each of several segments on the path

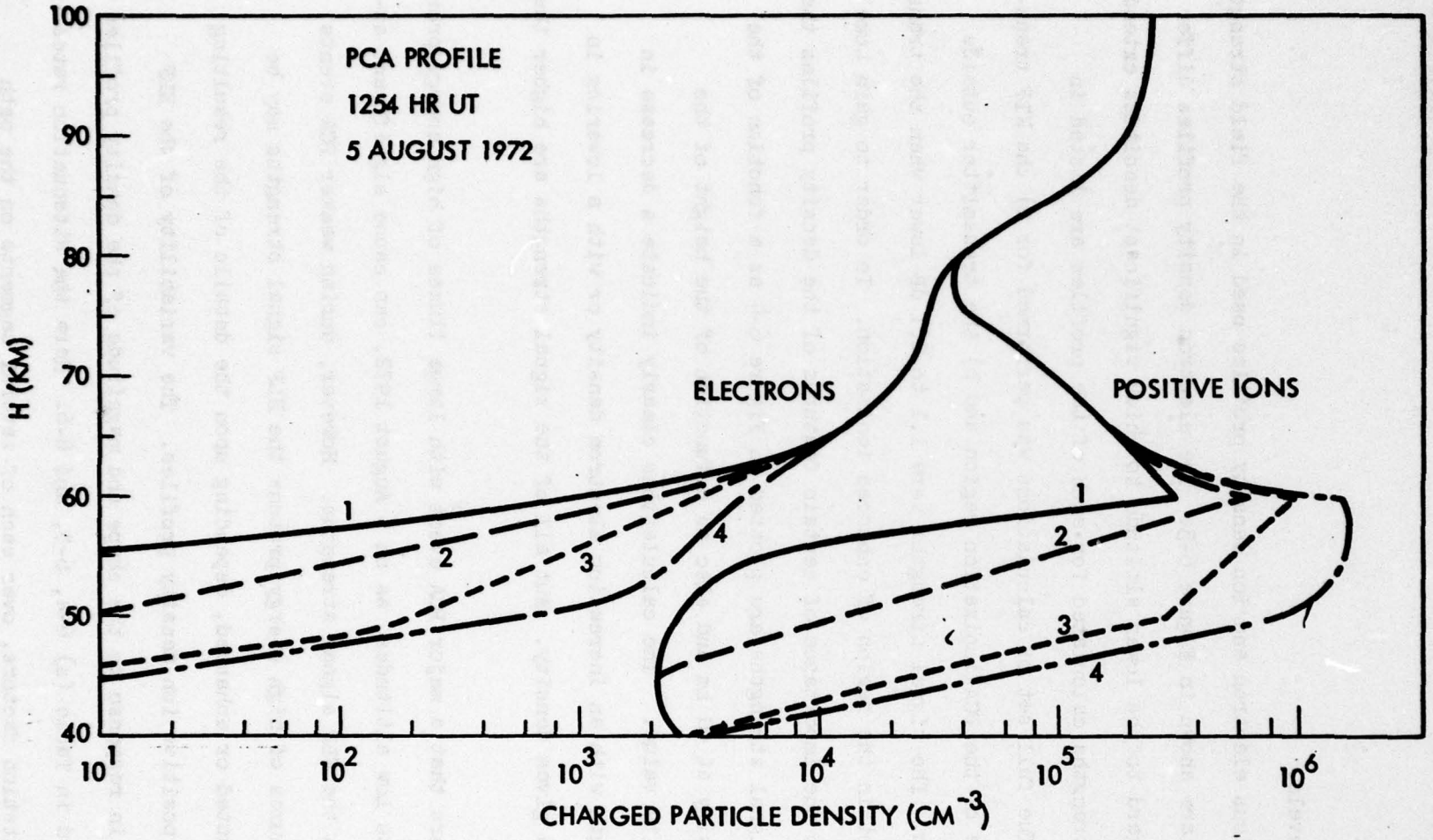

Figure 6-3. Various electron and ion density profiles, for hypothesized PCA events based on measurements during the 1254 UT 5 August 1972 event (Reagan et al., 1973), used in the field strength calculations.

Table 6-3

Calculated Field Strengths for the Various Density Profiles based on the PCA Event at 1254 UT on 5 August 1972. Transmission from WTF to Tromso, Norway at 75 Hz.

Profile	Signal Strength in dB Relative to 1 A/M	
	Profile over Entire Path	Ambient Night at WTF Profile over Remainder of Path
1	-152.0	-153.1
2	-152.6	-154.1
3	-152.6	-154.6
4	-152.7	-154.8

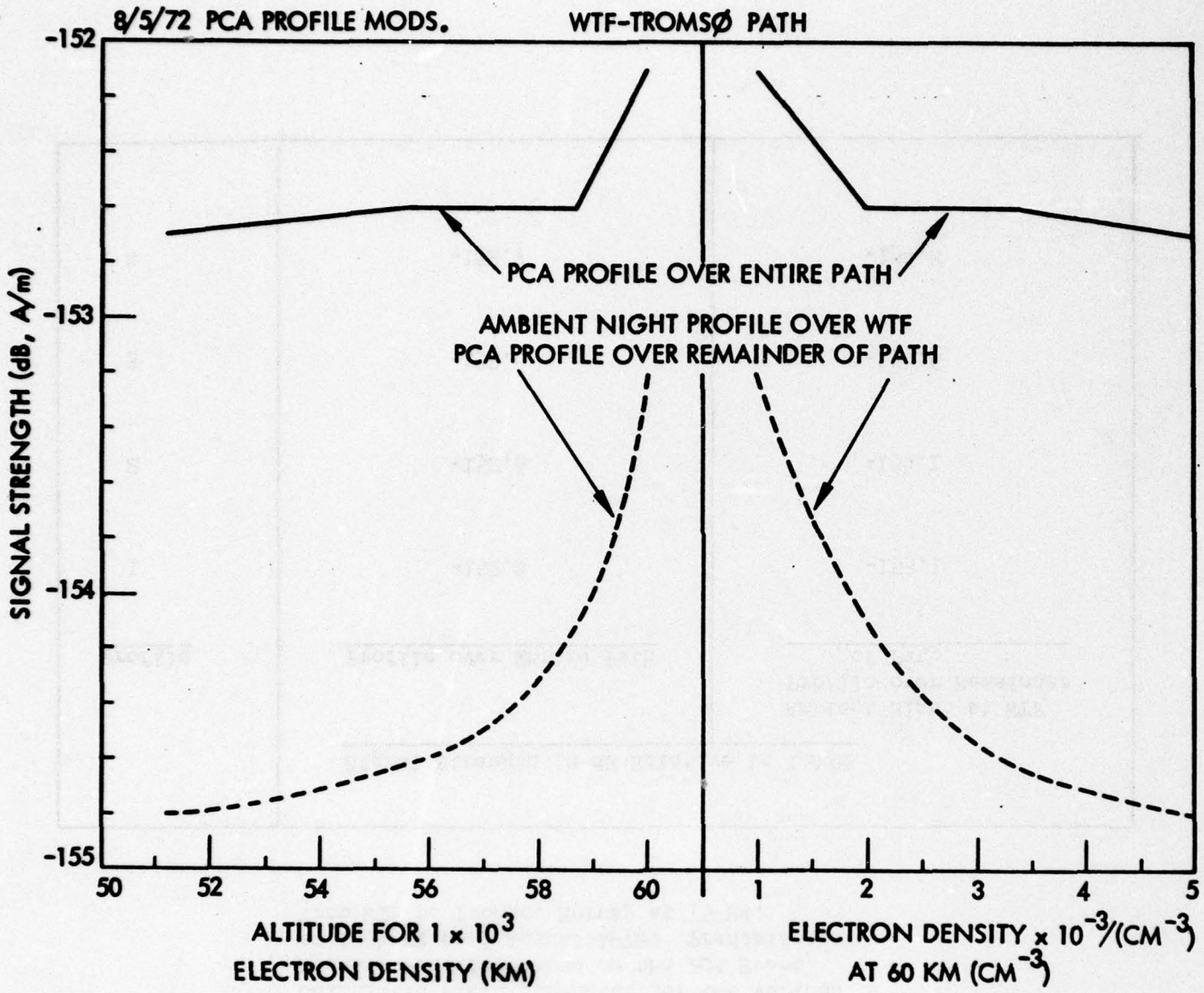

Figure 6-4. For the various PCA density profiles shown in Figure 6-2, the calculated ELF signal strengths are plotted as a function of the altitude for an electron density of $10^3 cm^{-3}$ (left hand section) and as a function of the electron density at 60 km (right hand section).

from WTF to Norway, vary in either direction from ambient conditions and can result in an overall signal attenuation or amplification depending upon the details of the propagation path. For comparison these propagation characteristics are also listed for various REP profiles, discussed in Section 5, and for sporadic E layers, discussed in Section 7.

6.3 Comparison of Effects from PCA and REP Events

The PCA event on 4 August 1972 contained large fluxes of high energy penetrating protons which produced intense ionization at altitudes below 40 km. Softer PCA events with insignificant fluxes of high energy protons, such as observed on 5 August 1972, may produce enhanced ionization only down to altitudes of 50-60 km. In comparison, electron precipitation events can exhibit much higher ion pair production rates at altitudes above $\sim$ 60 km, but even the most energetic REP events observed to date do not produce large ionization at altitudes much below 50 km. The bremsstrahlung produced by the electrons interacting with the atmosphere can penetrate much deeper into the atmosphere and can produce significant ionization down to altitudes below 30 km. Comparisons between PCA and REP events in regard to energy deposition are illustrated in Figure 6-5. The resulting electron densities are shown in Figure 6-6.

We have just seen that the energy deposition profiles for PCA and REP events may be similar but the PCA enhancements typically extend to lower altitudes. Pronounced differences between these classes of events are generally associated with the geographic distribution and hence in the contributions along the various segments of the transmission paths. Polar cap absorption

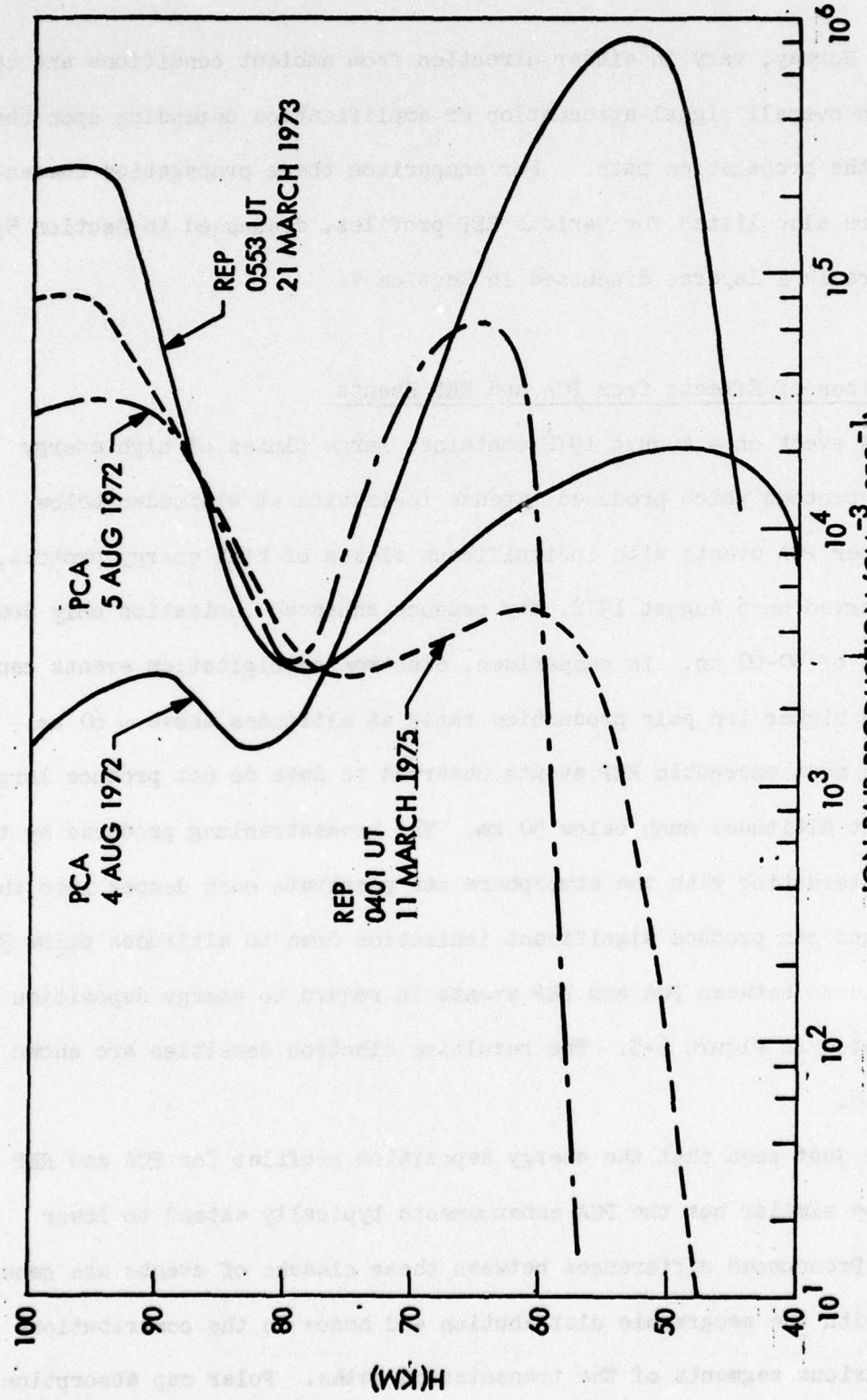

Figure 6-5. Ion-pair production rates versus altitude for selected PCA and REP events.

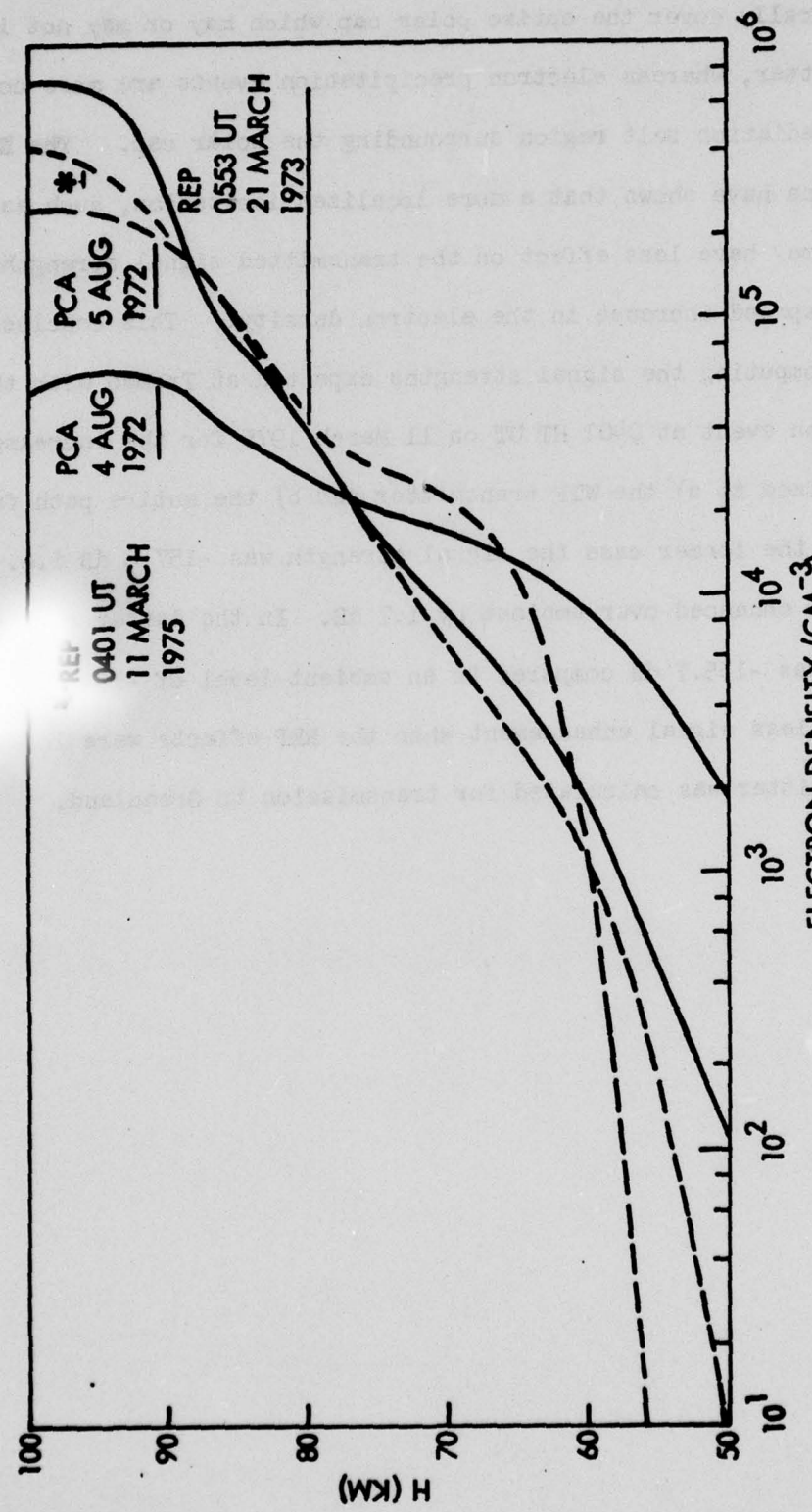

Figure 6-6. Electron density profiles resulting from the PCA and REP ion-pair production rate profiles shown in Figure 6-5.

events typically cover the entire polar cap which may or may not include the WTF transmitter, whereas electron precipitation events are more confined to the outer radiation belt region surrounding the polar cap. The ELF waveguide computer runs have shown that a more localized ionization, such as occurs in REP events may have less effect on the transmitted signal strengths than does a widespread increase in the electron density. This conclusion was confirmed by computing the signal strengths expected at Tromso with the electron precipitation event at 0401 HT UT on 11 March 1975 for the increased ionization being localized to a) the WTF transmitter and b) the entire path from WTF to Tromso. In the former case the signal strength was -157.6 dB i.e. the signal strength was enhanced over ambient by 1.7 dB. In the latter case the signal strength was -155.7 dB compared to an ambient level of -159.3 dB. A similar trend for less signal enhancement when the REP effects were localized to the transmitter was calculated for transmission to Greenland.

Section 7

WAVEGUIDE MODE CALCULATIONS FOR SPORADIC E-LAYER PROFILES

In the previous study (Imhof et al., 1976) calculations with the NOSC waveguide computer program were made to test the sensitivity of the wave propagation to sporadic E layers, E_s. For this purpose an E_s layer at heights of 120-125 km was superimposed on the ambient nighttime conditions. The maximum electron density in the layer was chosen rather arbitrarily as was the detailed variation of electron density with height. The computer attenuation rates displayed a strong frequency dependence, reaching a very high value of 10.347 dB/Mm at 80 Hz. This very high figure and the rather narrow resonance absorption peak between 60 and 85 Hz gave indications that the results should be treated with caution. Accordingly, it was concluded that more computer calculations should be made to test the sensitivity of the results to peculiarities in the electron density profile, the thickness of the E_s layer as well as its height and maximum electron density.

Based on the aforementioned conclusions we have made a series of computer runs with various hypothesized sporadic E-layer profiles. Specifically, the height and thickness of the E_s layer were varied. The attenuation versus frequency profile was found to depend very strongly on the altitude of the E_s layer. For a sporadic E layer at $\sim$ 105 km, as measured over Wallops Island by Smith and Voss (1977), an attenuation versus frequency curve was computed at the following frequencies; 45, 75, 80, 85, 90, 95, 100, 110, 120, 130, 140, 150, 170, 190 and 200 Hz. The runs revealed no peaks in attenuation, perhaps indicating their presence beyond the range of frequencies at which

the ELF transmitters are operating.

Instead of pursuing further the computer calculations with a sporadic layer at altitudes of ~ 105 km we made a run with the same E_s profile displaced upward to 118 km and found that the attenuation increased from 0.65 dB/Mm to 1.6 dB/Mm at 75 Hz. The sensitivity to the earth's magnetic field strength was investigated by changing B from 0.594 gauss to 0.41 gauss, whereupon the attenuation increased from 1.6 dB/Mm to 4.02 dB/Mm. Subsequently a series of runs was made with an E_s layer at an altitude of ~ 122 km, where the original runs were performed, and with a variety of layer thicknesses, as illustrated in Figure 7-1 and Table 7-1. For these runs the earth's conductivity at the WTF antenna was taken to be 3.2×10^{-4} MHO/meter which was the value used in the original runs. The attenuation rates are plotted in Figure 7-2 as a function of frequency for the various sporadic E-layer profiles shown in Figure 7-1. Clearly large attenuations are predicted, even for sporadic E-layers as thin as ~ 2 km. The computer runs have shown that the calculated signal strengths are very sensitive-to certain parameters such as altitude of the E_s layer and the magnetic field strengths. Since this aspect of the effort is not directly in line with the primary objectives of investigating the correlation between ELF propagation anomalies and energetic particle precipitation as measured from satellites the effects of E_s layers were not pursued further.

Table 7-1

E_s Layer Superposed Ambient Nighttime Densities (cm^{-3})

Altitude (km)	Profile I Ambient	II Ambient	III Ambient	IV Ambient	V Ambient	VI Ambient
130	3.70×10^2					
125	3.00×10^4	1.30×10^3	1.30×10^3	1.30×10^3	1.30×10^3	
123		3.00×10^4	3.00×10^4	3.00×10^4	1.50×10^3	1.50×10^3
122	4.00×10^4	4.00×10^4	4.00×10^4	4.00×10^4	4.00×10^4	4.00×10^4
121.5						3.00×10^4
121				3.00×10^4	3.00×10^4	1.20×10^3
120	3.00×10^4	3.00×10^4	3.00×10^4	1.20×10^3	1.20×10^3	
119			1.20×10^3			
115	1.00×10^3	1.00×10^3				
	Ambient	Ambient	Ambient	Ambient	Ambient	Ambient

Approximate thickness of E_s layer

$\Delta h \simeq 14$ km $\Delta h \simeq 10$ km $\Delta h \simeq 6$ km $\Delta h \simeq 5$ km $\Delta h \simeq 3$ km

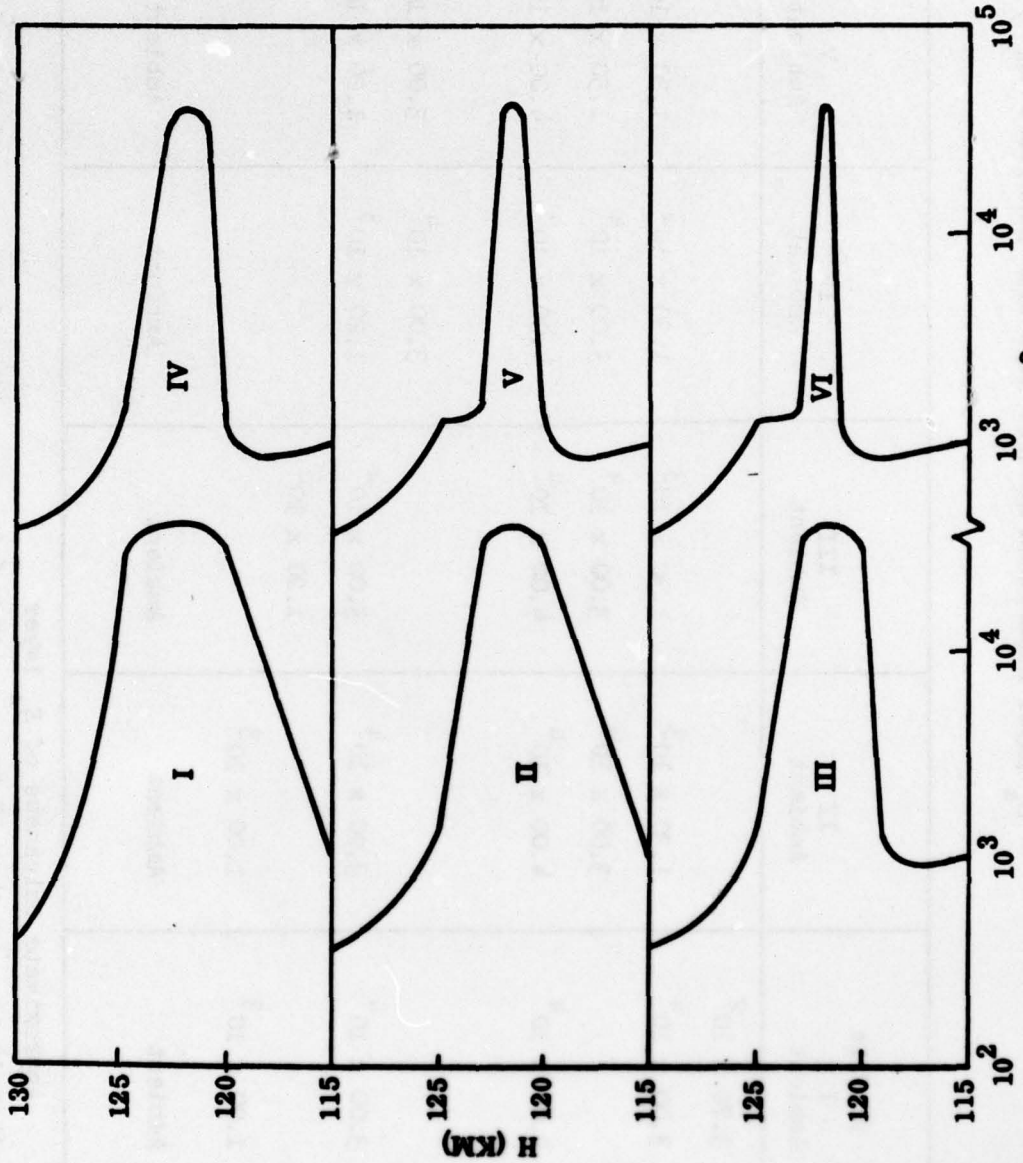

Figure 7-1. Electron density profiles hypothesized for a variety of E_s layers and used in the waveguide calculations.

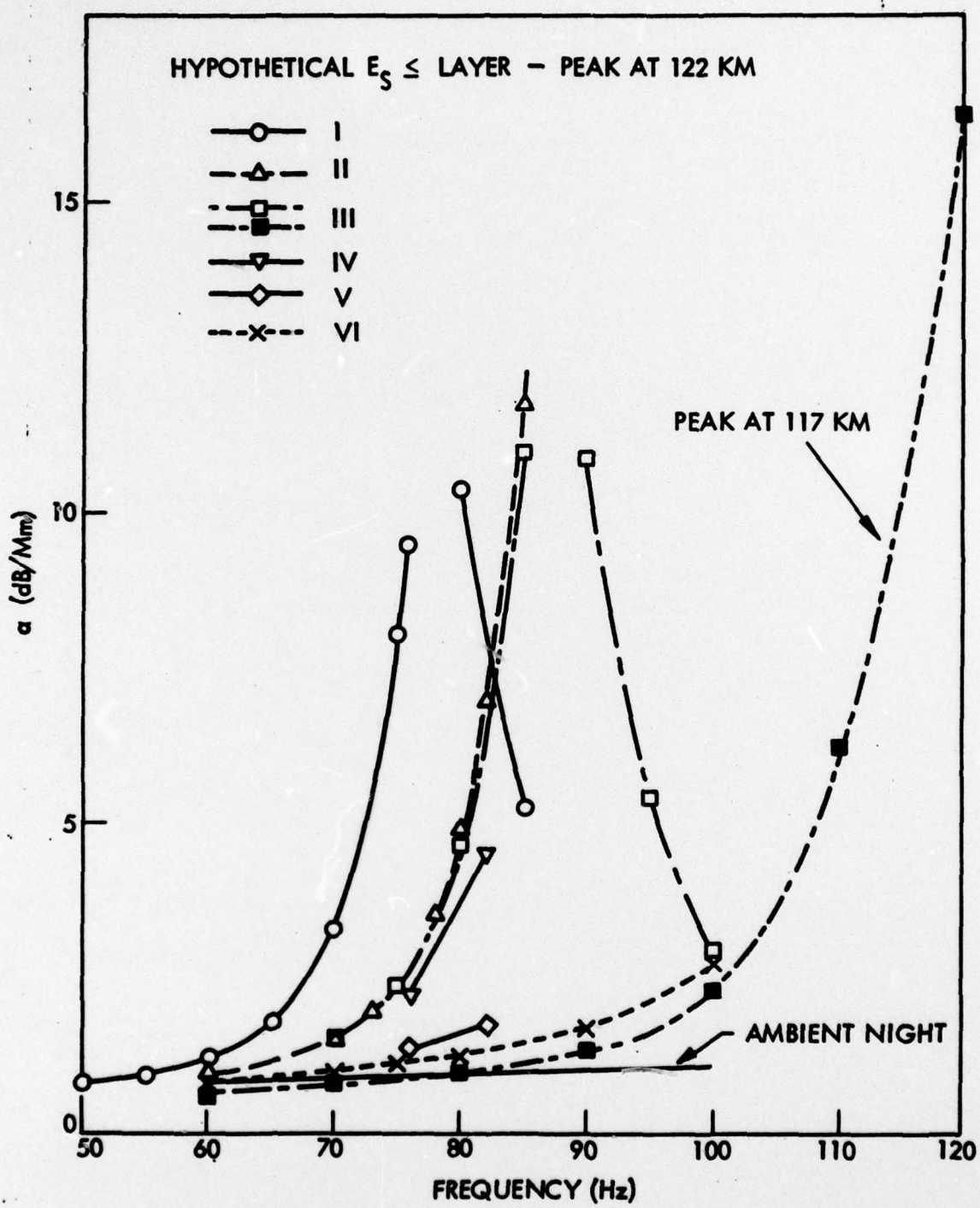

Figure 7-2. Calculated attenuation rates for the sporadic E layers shown in Figure 7-1, plotted as a function of frequency.

Section 8

SUMMARY

Past efforts to account for the frequent absorption anomalies encountered in the nighttime propagation of ELF radiowaves have not been conclusive. It is realized that at least some of the variations encountered in the absence of sunlight are due to anomalous ionospheric ionization caused by the precipitation of energetic electrons and protons into the earth's atmosphere. Recently under the present contract, a successful correlation was made for the first time between direct particle precipitation and anomalous nighttime ELF signal strengths. However, a detailed quantitative correlation between the particle inputs and the ELF signal levels remained to be demonstrated. This report describes the results of an effort to perform quantitative correlations between ELF anomalies observed at various stations around the world and precipitating energetic particle inputs as measured from a satellite.

Calculations have been made of the predicted signal strengths for transmissions from the Wisconsin Test Facility (WTF) to each of the receiving stations at Maryland, Connecticut, Greenland, Norway and Italy. The greatest emphasis in these calculations has been on the path from WTF to Tromso, Norway. This path encompasses high latitude regions of operational importance where significant transmission anomalies may often result from energetic particle precipitation into the atmosphere during geomagnetic storms and polar cap absorption events. Computations of the ELF transmission from WTF to Tromso were performed using an 8-segmented propagation path. For nighttime ambient

conditions the calculated values at 42 and 75 Hz were found to be in good agreement with the values measured in 1975 and 1976. If the predicted values are corrected for the dipole moment of the N-S WTF antenna using values supplied by Dr. P. R. Bannister then the predicted values are slightly above the measured averages. For the other stations varying degrees of agreement were achieved, but since an evaluation of the NOSC computer program for ambient conditions is not a primary objective of the present effort the matter was not pursued further. For the present purposes it is sufficient to have demonstrated a general consistency between the measurements and calculations as a baseline for evaluating the effects of energetic particle precipitation.

For strong PCA events with large fluxes of high energy penetrating protons pronounced ELF signal strength attenuations of the order of 2 to 6 dB are predicted for the path WTF to Tromso. However, during weaker PCA events with lower fluxes of high energy protons the ELF signal strengths may be either attenuated or enhanced, depending upon the ion pair production profiles and the resulting electron and positive ion density profiles. The signal strengths were found to be 1.1 to 2.1 dB lower when the transmitter was not in the region of enhanced ionization.

The effects of energetic electron precipitation on nighttime signal transmission have been studied with several different approaches, making full use of the satellite data and the waveguide computer program. An initial correlative survey was performed with the geomagnetic K index as a general indicator of particle precipitation. For the March-April 1976 period the variations in the signal strengths at Norway and Maryland displayed

many similarities to variations in the K indices, with greater signal strengths generally occurring at times of geomagnetic disturbance. However, this consistency may have been misleading since the agreements for a time period in 1975 are much less satisfactory and at times lower signal strengths were observed when the geomagnetic activity was high. For example, the ELF signal strengths at Maryland were below the threshold of detection at times in March 1975 when intense relativistic electron precipitation occurred.

During the coordinated exercises in March-April 1976 the nightly averaged signal strengths were found to generally increase during periods when the fluxes of precipitating electrons > 130 keV were higher on the average. On a broad time scale the various ELF receiving stations indicated a fairly consistent pattern which may be associated with the energetic electron precipitation. On a finer time scale, however, large inconsistencies exist between the various stations, suggesting the possible importance of other effects.

An evaluation of the effects of REP events on the ELF transmission signal strengths was made on the basis of the electron density profiles derived from the measured spectra of precipitating electrons. Due to the limited spatial coverage in the satellite measurements and to the limitations of the waveguide computer program in regard to its inability to treat variations of the guide parameters perpendicular to the propagation path, certain assumptions had to be made regarding the spatial extent of the electron precipitation measured on a given satellite crossing. Positive ion density profiles were obtained from the ion pair production rates with an assumed ion-ion recombination rate coefficient of $10^{-7} cm^3 sec^{-1}$. For the densities and altitudes of

concern the calculated signal strengths were found to be significantly dependent upon the value of the ion-ion recombination rate coefficient over the range from 6×10^{-8} to $10^{-7} cm^3\text{-}sec^{-1}$. The waveguide computer calculations were performed for paths from WTF to each of the receiving stations at Norway, Greenland, Italy, Connecticut and Maryland. The results indicate that hard electron precipitation events may cause a signal enhancement, due mainly to changes in the excitation factor. The consistent occurrence of anomalies in the ELF signal strengths during REP events, seems to be supported by the coordinated satellite ELF station measurements. During the intense events of October-November 1972 lower ELF signal strengths were recorded. Low signal strengths were also associated with the REP events on March 11-12, 1975. However, during the weaker electron precipitation events in March-April 1976 there was a trend toward higher signal levels.

In summary, the following major conclusions have followed from this study effort:

- From both the satellite and ELF station measurements it has been found that direct particle precipitation into the atmosphere can cause ELF transmission anomalies. The signal strengths may be either attenuated or enhanced depending upon the geometry and details of the ion pair production profiles.

- Sensitivity studies have been made to assess the dependence of the ELF signal strengths on such parameters as the electron and ion density profiles and their distribution along the propagation path. The following effects were discovered:

- The signal strengths tend to decrease with increasing electron density at altitudes of ~ 60 km or lower.

- The effect of a given ionization profile depends strongly on its location along the propagation path.

- The ELF signal strengths are most sensitive to positive ion density profiles at altitudes of ~ 45 km or lower.

- The ELF signal strengths are very sensitive to sporadic E-layers with the altitude of the ledge being a very critical parameter.

- The measured and predicted effects of energetic electron precipitation events can provide a readily available verification of the effects of ELF transmission of more rarely occurring and possibly more severe phenomena such as polar cap absorption (PCA) events.

- Variations in the nighttime ELF signal strengths on a fine time scale are observed which may be due entirely to electron precipitation but cannot be accounted for quantitatively due to present limitations in the measurements and computational techniques.

- The geometry for the effect of electron precipitation on nighttime ELF transmission is very complex and as a result the following recommendations are made for future investigations:

- New techniques for mapping electron precipitation profiles simultaneously over a broad spatial region should be used in a coordinated measurement program.

- Existing ELF waveguide-mode computer programs should be modified to include treatment of variations in the electron and ion density profiles along a direction perpendicular to the propagation path.

Section 9

REFERENCES

Bannister, P. R., private communication, 1976.

Budden, K. G., "Radiowaves in the Ionosphere," Cambridge University Press, 1961.

Budden, K. G., and G. J. Daniell, "Rays in Magnetoionic Theory," J. Atmos. Terr. Phys., Vol. 27, No. 3, 395-415, March 1965.

Cole, R. K., Jr., and E. T. Pierce, "Electrification in the Earth's Atmosphere for Altitudes between 0 and 100 Kilometers," J. Geophys. Res., 70, 2735-2749, 1965.

Davis, J. R., "ELF Propagation Irregularities on Norther and Mid-Latitude Paths," in ELF-VLF Radio Wave Propagation, J. Holtet, Editor, D. Reidel Publ. Company, Dordrecht-Holland, pp. 263-277, 1974.

Davis, J. R., and W. O. Meyers, NRL Report 7923, Naval Research Laboratory, Washington, D. C., 1975.

Gunton, R. C., R. E. Meyerott, and J. B. Reagan, "Ion and Neutral Chemistry of the D-Region during the Intense Solar Particle Event of August 1972," Lockheed Report No. LMSC/D556351, 1977.

Imhof, W. L., E. E. Gaines, and J. B. Reagan, "Dynamic Variations in Intensity and Energy Spectra of Electrons in the Inner Radiation Belt," J. Geophys. Res., 78, 4568, 1973.

Imhof, W. L., G. H. Nakano, R. G. Johnson, and J. B. Reagan, "Satellite Observations of Bremsstrahlung from Widespread Energetic Electron Precipitation Events," J. Geophys. Res., 79, 565, 1974a.

Imhof, W. L., E. E. Gaines, and J. B. Reagan, "Evidence for the Resonance Precipitation of Energetic Electrons from the Slot Region of the Radiation Belts," J. Geophys. Res., 79, 3141, 1974b.

Imhof, W. L., E. E. Gaines, and J. B. Reagan, "L-Dependent Peaks in the Energy Spectra of Electrons Precipitating from the Inner Belt," in Magnetospheric Physics, B. M. McCormac, Editor, D. Reidel Publ. Co., Dordrecht-Holland, pp. 129-133, 1974c.

Imhof, W. L., and R. V. Smith, "Longitudinal Variations of Higher Energy Electrons at Lower Altitudes," J. Geophys. Res., 70, 569, 1965.

Imhof, W. L., "Electron Precipitation in the Radiation Belts," J. Geophys. Res., 73, 4167, 1968.

Imhof. W. L., T. R. Larsen, J. B. Reagan, and E. E. Gaines, "Analysis of Satellite Data on Precipitating Particles in Coordination with ELF Propagation Anomalies," Annual Report on Contract N00014-75-C-0954 covering the period ending 14 March 1976, Lockheed Report No. LMSC/D502063, April 1976.

Larsen, T. R., "Preliminary Discussion of ELF/VLF Propagation Data," in ELF-VLF Radio Wave Propagation, J. Holtet, Editor, D. Reidel Publ. Co., Dordrecht-Holland, pp. 263-277, 1974.

Larsen, T. R., J. B. Reagan, W. L. Imhof, L. E. Montbriand, and J. S. Belrose, "A Coordinated Study of Energetic Electron Precipitation and D-Region Electron Densities over Ottawa during Disturbed Conditions," J. Geophys. Res., 81, 2200, 1976a.

Larsen, T. R., W. L. Imhof, and J. B. Reagan, "L-Dependent Energetic Electron Precipitation and Mid-Latitude D-Region Ion Pair Production Profiles," J. Geophys. Res., 81, 3444, 1976b.

Pappert, R. A., "Effects of Elevation and Ground Conductivity on Horizontal Dipole Excitation of the Earth-Ionosphere Waveguide," Radio Science, 5, 579-590, March 1970.

Pappert, R. A., and W. F. Moler, "Propagation Theory and Calculations at Lower (ELF) Extremely Low Frequencies," IEEE Trans. Comm., Vol. COM-22, No. 4, 438-451, April 1974.

Potemra, T. A., and A. J. Zmuda, "Solar Electrons and Alpha Particles during Polar Cap Absorption Events," J. Geophys. Res., 77, 6916, 1972.

Potemra, T. A., in Physics and Chemistry of Upper Atmospheres, B. M. McCormac, Editor, D. Reidel Publ. Co., Dordrecht-Holland, p. 67, 1973.

Reagan, J. B., "A Study of the D-Region Ionosphere during the Intense Solar Particle Events of August 1972," Lockheed Report No. LMSC/D454290, May 1975.

Reagan, J. B., and T. M. Watt, "Simultaneous Satellite and Radar Studies of the D-Region Ionosphere during the Intense Solar Particle Events of August 1972," J. Geophys. Res., 81, 4579, 1976.

Reagan, J. B., W. L. Imhof, and V. F. Moughan, "Characteristics of the August 1972 Solar Particle Events as Observed over the Earth's Polar Caps," Report UAG-23, Part 3, edited by H. F. Coffey, p. 676, World Data Center A for Solar Terrestrial Physics, Boulder, Colorado, 1973.

Sellers, B., and M. A. Stroseio, "Rocket-Measured Effective Recombination Coefficients in the Disturbed D-Region," J. Geophys. Res., 80, 2241, 1975.

Sheddy, C. H., "A General Analytic Solution for Reflection from a Sharply Bounded Anisotropic Ionosphere," Radio Science, 3, 792-795, August 1968.

Smith, L. G., and H. D. Voss, "Ionization of Energetic Electrons in the Mid-Latitude Nighttime E-Region," presented at COSPAR, Philadelphia, Pa., June 1976.

Swider, W., and T. J. Keneshea, "Diurnal Variations in the D-Region during PCA Events," AFCRL-72-0474 Special Reports, No. 144, Proceedings of COSPAR Symposium on Solar Particle Event of November 1969, 1972.

Ulwick, J. C., AFCRL-72-0474 Special Reports, No. 144, Proceedings of COSPAR Symposium on Solar Particle Event of November 1969, 1972.

Walt, M., W. M. McDonald, and W. E. Francis, "Penetration of Auroral Electrons into the Atmosphere," in Physics of the Magnetosphere, R. Carovillano and J. F. McClay, Editors, Reinhold, New York, New York, p. 534, 1968.

Watt, T. M., L. L. Newkirk, and E. G. Shelley, "Joint Radar-Satellite Determination of the Effective Recombination Coefficient in the Auroral E-Region," J. Geophys. Res., 79, 4725, 1974.

Distribution List
for Lockheed Report
LMSC/D560323

30 June 1977

Director
Defense Advanced Research Projects Agency
Architect Building
1400 Wilson Boulevard
Arlington, VA 22209
1 cy Attn: TIO Fred A. Koethe
1 cy Attn: STO James C. Goodwyn

Defense Documentation Center
Cameron Station
Alexandria, VA 22314
12 cy Attn: TC

Director
Defense Nuclear Agency
Washington, D. C. 20305
1 cy Attn: STTL Tech Library
1 cy Attn: DDST Peter Haas
1 cy Attn: DDST David Oakley
1 cy Attn: RAAE Carl Fitz
1 cy Attn: RAAE Dow Evelyn
1 cy Attn: Charles Blank
1 cy Attn: RAAE Maj. John Clark
1 cy Attn: RAAE Paul Fleming
1 cy Attn: RAEV

Director of Defense Research and Engineering
Department of Defense
Washington, D. C. 20301
1 cy Attn: DDS & SS R. S. Ruffine

U. S. Army Communications Command
C. E. Services Division
Pentagon Room 1B269
Washington, D. C. 20310
1 cy Attn: CEAO

Chief
U. S. Army Research Office (Durham)
P. O. Box 12211
Triangle Park, N. C. 27709
1 cy Attn: CRDARD-P Robert Mace

Chief of Naval Operations
Navy Department
Washington, D. C. 20350
1 cy Attn: NOP 985

Chief of Naval Research
Navy Department
Arlington, VA 22217
1 cy Attn: Code 461 R. Gracen Joiner
1 cy Attn: Code 427 Henry Mullaney

Commander
Naval Electronics Laboratory Center
San Diego, CA 92152
1 cy Attn: Code 2200 Ilan Rothmuller
1 cy Attn: Code 2200 W. F. Moler

Director
Naval Research Laboratory
Washington, D. C. 20375
2 cy Attn: Code 7750 John Davis
1 cy Attn: Code 7700 Timothy Coffey
1 cy Attn: Code 7701 Jack Brown
1 cy Attn: Code 7727 Charles Johnson

Commander
Naval Surface Weapons Center
White Oak, Silver Spring, Md. 20910
1 cy Attn: Lee Rodlin

Commander
Naval Electronics Systems Command
Navy Department
Washington, D. C. 20360
2 cy Attn: PME 117 Capt. W. Cobb
1 cy Attn: PME 117T John Doncarlos
1 cy Attn: PME 117-21
2 cy Attn: PME 117-21A Bodo Kruger

AF Geophysics Laboratory, AFSC
Hanscom Air Force Base
Bedford, Ma 01730
1 cy Attn: OPR James Ulwick
1 cy Attn: LKB William Swider
1 cy Attn: LKB Kenneth Champion

AFTAC
Patrick AFB, Florida 32925
1 cy Attn: TN

Headquarters
Air Force Systems Command
Andrews AFB
Washington, D. C. 20331
1 cy Attn: SDR

Department of Commerce
Office of Telecommunications
Institute for Telecommunications Science
Boulder, Colorado 80302
1 cy Attn: L. A. Berry
1 cy Attn: William F. Utlant

Lockheed Missiles and Space Company
3251 Hanover Street
Palo Alto, Ca. 94304
3 cy Attn: J. B. Reagan
3 cy Attn: W. L. Imhof
1 cy Attn: Martin Walt

General Electric Company
TEMPO-Center for Advanced Studies
816 State Street
Santa Barbara, Ca. 93102
2 cy Attn: Warren S. Knapp
1 cy Attn: DASIAC

Pacific-Sierra Research Corporation
1456 Cloverfield Boulevard
Santa Monica, Ca. 90404
1 cy Attn: E. C. Field

Pennsylvania State University
Ionospheric Research Laboratory
University Park, Pa 16802
2 cy Attn: John S. Nisbet
1 cy Attn: Les Hale
1 cy Attn: A. J. Ferraro
1 cy Attn: H. S. Lee

The Rand Corporation
1700 Main Street
Santa Monica, Ca. 90406
1 cy Attn: Cullen Crain

Professor Chalmers F. Sechrist
155 Electrical Engineering Building
University of Illinois
Urbana, Illinois 61801
1 cy Attn: C. Sechrist

Stanford Research Institute
333 Ravenswood Avenue
Menlo Park, Ca. 94025
2 cy Attn: Allen M. Peterson
2 cy Attn: Ray L. Leadabrand